University of BIRMINGHAM

Research at Birmingham

Characterization and Source Apportionment of Carbonaceous PM2.5 Particles in China - A Review

Wu, Xuefang; VU, Van Tuan; Shi, Zongbo; Harrison, Roy; Cen, Kuang

Link to publication on Research at Birmingham portal

Review article

Characterization and source apportionment of carbonaceous PM$_{2.5}$ particles in China - A review

Xuefang Wu[a,b], Tuan V. Vu[b], Zongbo Shi[b,1], Roy M. Harrison[b,*,2], Di Liu[b], Kuang Cen[a]

[a] *School of Earth Sciences and Resources, China University of Geosciences, Xueyuan Road 29, 100083, Beijing, China*
[b] *Division of Environmental Health & Risk Management, School of Geography, Earth & Environmental Sciences, University of Birmingham, Edgbaston, Birmingham, B15 2TT, United Kingdom*

ABSTRACT

Organic aerosols (OAs) account typically for 20–90% of fine particles (PM$_{2.5}$) in the lower troposphere. They contribute to a wide range of environmental problems, from local issues (e.g., urban haze) to global problems (e.g., climate change). Huge efforts have been dedicated to studying the composition, abundance, spatial and temporal distribution and sources of organic aerosols in China. This review aims to summarize recent studies on characteristics and sources of OAs and assesses the current state of understanding of the organic aerosol pollution in China. The OA constitutes ~20–45% of the PM$_{2.5}$ with an annual mean value of 5.2–44.5 μg/m^3 at sites across China, which is about five times higher than that reported in North America and Europe. There are thousands of different organic compounds in atmospheric aerosols, but only about 5–10% of them have been identified and quantified. OAs show pronounced spatial variations with much higher concentrations in Northern than Southern China. Seasonally, the highest OA concentrations are observed in the winter, whereas the lowest are in the summer. This is due to higher emission rates from anthropogenic sources (e.g., biomass and coal combustion) and poorer dispersion conditions in the winter. Approximately 60–80% of total OA is apportioned by receptor modeling (such as Chemical Mass Balance, CMB) and tracer-yield method, based on the source profiles of primary organic aerosols (POA) and secondary OA (SOA) derived from local emission sources. A number of OA sources are identified, including motor vehicles, industrial emissions, biomass combustion, food cooking, and coal combustion for POA and anthropogenic and biogenic emissions for SOA. Industrial emissions and motor vehicular exhaust are the dominant sources of organic aerosols in the industrialized areas of Northern China, as well as the Pearl River Delta and Eastern China, whereas in other urban areas, residential coal combustion and motor vehicular exhaust are the dominant sources in winter and summer respectively.

1. Introduction

Atmospheric aerosols have been well-known as a major air pollutant in China's megacities during the last decades (Chan and Yao, 2008; Yang et al., 2016). Organic aerosol (OA) can make up a significant fraction of atmospheric particles, accounting for 20–90% of fine particulate matter (PM$_{2.5}$) mass in the lower troposphere (Jimenez et al., 2009; Kanakidou et al., 2005; Murphy et al., 2006; Zhang et al., 2007a). Over the last decade, a number of field observation and lab studies of organic aerosols have been carried out in China, which have reported that organic matter constitutes a substantial fraction (30–50%) of PM$_{2.5}$ in Beijing, Shanghai, Guangzhou and Xi'an (He et al., 2011; Huang et al., 2014; Zheng et al., 2005). Cao et al. (2003a) has reported that in

the Pearl River Delta Region (PRDR), carbonaceous aerosols (those that include organic carbon (OC) and elemental carbon (EC)), accounted for 40.2% of PM$_{2.5}$ and 35.9% of coarse particles (PM$_{2.5-10}$), while organic aerosols were the most abundant components contained in PM$_1$ (39.7%) (He et al., 2011). OC can be directly emitted from combustion sources or formed through gas to particle conversion processes. While organic carbon is always bound to other elements (H, O, N etc) in organic compounds, elemental carbon is that not bound to other elements. The latter can be measured by thermal-optical techniques which differentiate it from organic carbon, but it is often measured optically as black carbon which is an ideally light-absorbing substance composed of carbon. Recommended definitions are given by Petzold et al. (2013). Because organic carbon is associated with oxygen, hydrogen and

---

Table 1
Statistics for carbonaceous aerosol (OC, OA and EC) mass concentrations in $PM_{2.5}$ measured in the major cities of China from the literature (µg/m^3) during 2008–2015.

Location	Type	Site type	Sampling time	OC[a]	OA[b]	EC[a]	Protocol	PM$_{2.5}$	Reference
Shanghai	urban	residential	Jun 2010–May 2011	8.6	13.8	2.4	IMPROVE-TOR	59.7	Zhang et al. (2014b)
Shanghai	urban	residential	2014	7.8	12.5	2.1	NIOSH-TOT		Chang et al. (2017)
Shanghai	urban	Traffic, commercial and residential	Jan. 2010–Jan.2011	11.2	16.8	2.8	IMPROVE-TOR		Feng et al. (2013)
Shanghai	suburban	Residential, industry	Jan. 2010–Jan.2011	11.9	18.3	2.9	IMPROVE-TOR		
Hong Kong	suburban	coastal	2011/2012	4.5	8.6	1.3	IMPROVE_A-TOR	46.8	Gao et al. (2016)
Guangzhou	urban	residential	2014	8.2	13.1	4.0	IMPROVE_A-TOR	48	Tao et al. (2017b)
Zhuhai	suburban	residential	2014	9.4	15.0	2.6	IMPROVE_A-TOR	45	
Mt. Lu	mount		Aug.–Sep. 2011	3.8	6.0	1.3	IMPROVE_A-TOR	58.8	Li et al. (2015b)
Lhasa	urban	Tibetan plateau	May 2013–Mar.2014	3.3	5.3	2.2	IMPROVE_A-TOR	26.7	Li et al. (2016a)
Nanjing	urban	Residential, road	2013	18	28.8	6.8	IMPROVE_A-TOR	129	Li et al. (2016b)
Nanjing	suburban	Industry zones	2013	27.8	44.5	9.3	IMPROVE_A-TOR	135.5	
Xiamen	urban	Residential, traffic, commercial	2009	19.3	30.9	3.3	NIOSH-TOT	72.1	Zhang et al. (2011a)
Xiamen	Suburb	Residential, road	2009	15.8	25.3	2.7	NIOSH-TOT	63.9	
Xiamen	Suburb	Industry	2009	19.7	31.6	3.5	NIOSH-TOT	74.8	
Xiamen	Urban	Residential, road	Aug.–Sep. 2012	4.8	7.7	1.1	NIOSH-TOT	43.4	Zhao et al. (2015a)
Fuzhou	urban	Residential, road	2007/2008	8.5	13.6	2.2	IMPROVE-TOR	44.3	Xu et al. (2012)
Xiamen	Urban	Resident	2011–2013	8.7	13.8	1.3	NIOSH-TOT	51.5	Wu et al. (2015)
Quanzhou	Urban	Road	2011–2013	10.1	16.1	1.5	NIOSH-TOT	53.9	
Putian	Suburban	Scattered residence	2011–2013	8.1	12.9	1.2	NIOSH-TOT	50.3	
Fuzhou	Urban	Road, residential	2011–2013	12.0	19.1	1.8	NIOSH-TOT	58.7	
Chengdu	Urban	Road	2009/2010	22.3	35.7	9	IMPROVE-TOR	165	Tao et al. (2013)
Chengdu	Urban	Road, residential	2012/2013	19	30.4	4.6	NIOSH-TOT		Chen et al. (2014)
Chongqing	Urban	Road, residential	2012/2013	15.2	24.3	4	NIOSH-TOT		
Sanya	suburb	residential	Jan.–Feb.2012	3.4	5.4	1.3	IMPROVE_A-TOR	20.4	Wang et al. (2015b)
Sanya	suburb	residential	Jun.–Jul. 2013	3.2	5.1	0.9	IMPROVE_A-TOR	3.2	
Wanzhou (Chongqing)	urban	residential	2013	23.6	37.8	8.7	NIOSH-TOT	125.3	Zhang et al. (2015b)
Tianjin	urban	Residential, commercial, road	Dec.2013–Jan.2014	26.4	42.2	2.3	IMPROVE_A-TOR	105.9	Wang et al. (2016a)
Tianjin	urban	residential	2009–2010	18.8	30.1	6.9	IMPROVE_A-TOR		Zhao et al. (2013)
Beijing	urban	Residential and commercial	Oct.2010–Nov. 2011	15.7	22	5.2	IMPROVE-TOT		Du et al. (2014)
Beijing	urban	road	Sep. 2009–Aug. 2011	22.5	31.5	2.7	IMPROVE-TOR		Xu et al. (2015)
Beijing	urban	residential	April.2009–Jan. 2010	16.9	23.7	5	IMPROVE-TOR	135	Zhang et al. (2013a)
Beijing	urban	road	Nov. 2012	19.8	27.7	2.8	NIOSH-TOT	106.9	Sun et al. (2014)
Beijing	urban	road	Mar. 2013–Feb. 2014	14	19.6	4.1	NIOSH-TOT	93.8	Ji et al. (2016)
Beijing	urban	road	Jul 2012–Apr 2013	13.3	18.6	3.3	IMPROVE_A-TOR	95.6	Wang et al. (2015a)
Beijing	urban	road	Jun.–Jul. 2011	12.0	19.3	2.5	IMPROVE_A-TOR		Cheng et al. (2013b)
Beijing	urban	road	Dec.2011–Jan. 2012	24.6	39.4	8.1	IMPROVE_A-TOR		
Beijing	Urban	Road	Jul.–Aug. 2008	10.4	14.6	2.9	NIOSH-TOT		Guo et al. (2012)
Beijing	Rural	residential, farm-land	Jul.–Aug. 2008	9.4	13.2	2.4	NIOSH-TOT		
Beijing	Urban	Residential, road	2015	12.5	17.5	3	IMPROVE-TOR		Lang et al. (2017)
Beijing	Suburban	Residential, road, biomass burning	Nov.–Dec. 2013	10.6	14.8	1.3	NIOSH-TOT	24.2	Jiang et al. (2016)
Xi'an	Urban	Residential, commercial, road	2010	21.8	34.9	7.6	IMPROVE_A-TOR	167.2	Wang et al. (2015d)
Jinan	Urban	Residential	2010	18	28.7	5.5	IMPROVE-TOR	168.9	Gu et al. (2014)
Zhengzhou	urban	Industry	2010	20.1	32.2	3.9	NIOSH-TOT	175	Geng et al. (2013)
Dunhuang	Urban	Desert region	Mar.–May 2012	21.8	34.9	6.2	IMPROVE_A-TOR		
Tangshan	urban	Regional pollutants	Jul 2012–Apr 2013	22.7	31.8	6.9	IMPROVE_A-TOR	146.5	Wang et al. (2015a)
Shijiazhuang	urban	Residential, road	Apr. 2009–Feb. 2010	26.4	42.2	9.7	IMPROVE_A-TOR	191.2	Zhao et al. (2013)
Chengdu	urban	Northern mountainous	Apr. 2009–Feb. 2010	19	30.4	7.3	IMPROVE_A-TOR	92.4	
Shangdianzi	rural	Background station	Apr. 2009–Feb. 2010	10.8	17.28	3.9	IMPROVE_A-TOR	71.8	

[a] OC and EC were measured from field samples.

[b] OA concentration was derived from OC. Beijing: OA = OC*1.4 (Song et al., 2007); Hongkong: OA = OC*1.9 (Gao et al., 2016); other sites: OA = OC*1.6 (Cao et al., 2007).

nitrogen, the organic carbon (OC) can be converted to OA by multiplying its concentration by factors of 1.6 ± 0.2 in urban areas (Duan et al., 2007; Turpin and Lim, 2001), although a wide range of values has been used from 1.2 close to traffic emissions to > 2.0 for a large secondary component.

Evidence from a large number of studies shows that OAs adversely affect not only human health, but also influence climate. In addition, OAs cause visibility reduction, material and ecosystem damage, and affect cloud condensation nuclei (CCN) (Cao et al., 2006; Dentener and Crutzen, 1993; Mauderly and Chow, 2008; Seinfeld and Pandis, 2016). For example, epidemiological studies have found strong relationships between the level of OA in the ambient particulate matter and cardiovascular health outcomes and adverse respiratory health (Bi et al., 2002, 2005; Janssen et al., 2011). Considering effects on climate, more attention has been paid to polar organic aerosols owing to their hygroscopic character and their ability to reduce visibility by causing uptake of water into the aerosol (Cao et al., 2012; Huang et al., 2014;

Watson, 2002). In addition, OA can modify the earth's climate through scattering and absorption of solar radiation, altering cloud properties and lifetimes (Jimenez et al., 2009; Kanakidou et al., 2005; Penner et al., 2003). OAs in different size ranges may have different physicochemical properties, such as water solubility, due to different sources and composition.

In the ambient air, OA occurs as primary organic aerosol (POA) which is directly emitted from numerous anthropogenic and biogenic sources, or secondary organic aerosols (SOA) which are formed through chemical oxidation of high vapour pressure compounds (Fuzzi et al., 2006; Han et al., 2016b; Kanakidou et al., 2005). Han et al. (2016b) investigated the composition and distribution of OA over eastern China, finding that POA and SOA contributed 52% and 48% of total OA, respectively. Huang et al. (2014) reported that the SOA contributes 44–71% of OA (averages for all four cities of Beijing, Shanghai, Guangzhou, and Xi'an). Numerous source apportionment studies of OA have been conducted in China. For example, Lu et al. (2011) have
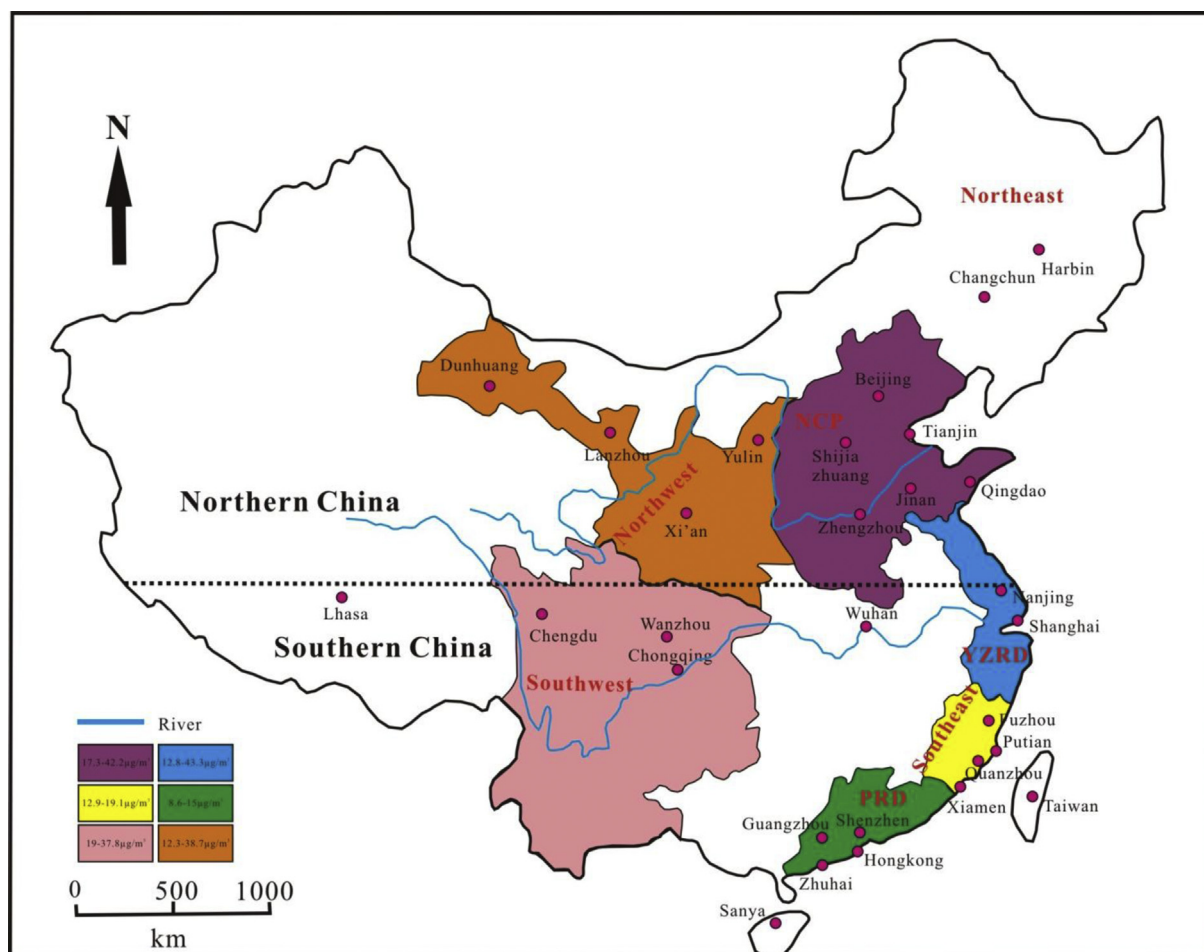
Fig. 1. Map of major research sites for carbonaceous aerosol characterisation in China.

studied the inventory of primary organic aerosol from 1996 to 2010 and reported that the dominant contributor to anthropogenic emissions is residential emissions (69%), in which residential biofuel (56%) is combusted in the home for cooking and heating. Biomass burning, industrial and traffic emissions, and coal combustion are also considered as major sources of OA in Beijing (Dan, 2004; Duan et al., 2004; Song et al., 2006a, 2006b, 2007). Similar results were observed in the south of China (Cao et al., 2006; Feng et al., 2016; He et al., 2011; Zhang et al., 2008c), and the organic species were more enriched in the accumulation mode (particularly, in the size range of 0.43–0.65 μm) (Xu et al., 2015). In order to devise effective policies for the control of the particulate pollution, it is very important to quantify the fractions of POA and SOA.

Several literature reviews on aspects of OA have been published, Hahn (1980) summarized knowledge of the organic constituents of natural aerosols and described a cycle of tropospheric organic matter. Given the availability of quantitative molecular data, Jacobson et al. (2000) presented an extensive and comprehensive description of characteristics and analysis method of OA. Based on earlier reviews, Kanakidou et al. (2005) reviewed knowledge of OA of importance for global climate modelling and identified significant gaps to reduce the uncertainties. De Gouw and Jimenez (2009) reviewed the sources of OA in the global atmosphere. Iavorivska et al. (2016) summarized the deposition of organic carbon by precipitation. Wang et al. (2016b) provided insights into the characteristics of OC and EC pollution in China on a national scale on the basis of published data.

Despite numerous published literature studies on organic aerosols in China, few systematic attempts have been made to analyze spatial and temporal variations. Different protocols were used for OA analysis,

leading to uncertainties in OA characterization. In this review, we will (1) present the general sampling and analysis methods used for OA; (2) summarize the sources of POA and SOA; (3) examine spatial and seasonal variations of OA concentrations and (4) review source apportionment of OA using receptor models. In this paper, unless otherwise stated, the term OA refers to the OA contained in fine particles (particulate matter with an aerodynamic diameter smaller than 2.5 μm). For this reason, the rapidly increasing volume of data collected by Aerosol Mass Spectrometry which is approximately PM_1 is not reviewed in detail. This is included in a recent review by Li et al. (2017).

2. Sampling and analysis of OA

Traditionally, aerosols are collected on filters and analyzed by chemical and optical methods. More recently, online instruments such as the AMS (Aerosol Mass Spectrometer) or online OC/EC analyzer have been developed to measure the concentration of OAs with high time resolution. This section will review the analytical methods used for OA between 2000 and 2017 (Table S1 and Table 1).

2.1. Aerosol sampling

Aerosol sampling for OA analysis needs to consider two key aspects. One is the choice of sampler considering cost, commercial availability, ease of usage and quality of operation. Different instruments have been used for distinct studies (Table S2). For example, high volume samplers are often used to collect organic compounds in the particulate phase at a typical flow of 1.13 m^3/min (Du et al., 2014; Feng et al., 2009; Hart et al., 1992). In some studies, medium volume samplers (TH-150C,

URG-3000K) giving a flow of 30–100 L/min (Li et al., 2015b), or mini volume samplers (Airmetrics, USA) at a flow of 5 L/min have been used for OA collection (Cao et al., 2003b; Zhang et al., 2013a).

The second issue to consider during sampling is the choice of suitable filters, which depends on the type of chemical analysis, the capture efficiency and resistance of filters. The filters, usually of glass fibre or quartz, are weighted before and after sampling to determine the mass of particulate matter and are usually baked at 500–850 °C for several hours before use to remove all residual organic compounds and to drive off water (Zhang et al., 2008a). After sampling, the exposed filters are stored in a freezer at about −20 °C until analysis. However, a number of studies have suggested that it would be better to store filters at −80 °C to prevent organic compounds from evaporating and to avoid oxidation of semi-volatile organic compounds and to prohibit microbial growth, thus ensuring minimization of organic compound losses (Harrison et al., 1996; Zheng et al., 2000). This paper synthesizes data relating to organic aerosols from many sites in China, whose locations appear in Fig. 1.

2.2. OA analysis

Quantification of OA employs a range of instruments depending upon the information sought. Thermal-optical analysis (TOA) quantifies carbon and seeks to differentiate organically bound carbon from elemental carbon. The AMS is able to differentiate source-related components of organic carbon in real time, while carbon isotope analysis can differentiate modern and fossil carbon. Chromatographic separation by gas chromatography (GC) or liquid chromatography (LC) allows analysis of individual compounds by GC/MS and LC/MS when coupled with mass spectrometric detection. Techniques and appropriate applications of these methods are listed in Table 2.

Different protocols for heating temperature and gas flows are available for TOA. The most popular TOA protocols include IMPROVE (Interagency Monitoring of Protected Visual Environments) (Chow et al., 1993, 2001), IMPROVE_A (a modification of the IMPROVE protocol), NIOSH (National Institute of Occupational Safety and Health) (Birch and Cary, 1996; Birch, 1998) and EUSAAR_2 (European Supersites for Atmospheric Aerosol Research). Different protocols yield a varying OC/EC split, resulting in uncertainty in concentrations of OC and EC that are operationally defined (as Table S3). NIOSH exhibits negative EC bias relative to IMPROVE due to premature EC evolution in pure helium (OC4 step), whereas, IMPROVE shows an opposite EC preference owing to the lower temperature of OC4 (580 °C). Lower temperature leads to a fraction of OC being carried into the oxidative condition (Cavalli et al., 2010; Cheng et al., 2011). EUSAAR_2 extends time steps at lower temperature (OC1, OC2) to promote volatilization of OC over pyrolysis, and the highest temperature of 650 °C is reported to be the best for OC yield without premature creation of pyrolysis OC (POC) (which is OC evolved in the EC phase of the analysis). Laser reflectance and laser transmittance are used for correction of POC. The former is mainly affected by near surface char and the latter is more influenced by within filter char leading to longer times to return to initial value of the laser signal and thus more delay in the split point (Bautista et al., 2015; Cao et al., 2013; Chow et al., 2004; Han et al., 2016a). This is consistent with previous observations where the EC estimated from reflectance was 1.57 times as high as that from transmittance in samples from Lhasa (Li et al., 2016a).

GC/MS can be used to isolate a wide range of compounds on a single GC column according to each compound's retention time, and to make compound identification relatively straightforward through mass spectrometry (MS). Major analytical procedures are listed in Table S4 (Chauhan et al., 2014; Fu et al., 2008; Yin et al., 2015). Both thermal desorption (TD) GC/MS and solvent extraction (SE)-based GC/MS have been used in the literature. Although TD-GC/MS does not need sample extraction and requires less filter for detecting molecular organics than that based on SE-GC/MS, polar compounds are lost to the GC column

(Ho et al., 2008). In order to increase the fraction of OAs to be analyzed, a number of previous studies used high-resolution GC and high-resolution MS to measure individual compounds (Hildemann et al., 1994). Recently, two dimensional (2D) GC-time of flight MS (GC × GC-TOFMS) was developed to enhance the GC resolution and sensitivity by separating unresolved complex matter (UCM) with two comprehensively coupled columns (Alam and Harrison, 2016). Welthagen et al. (2003) reported that the UCM fraction account for 70% of the semi-volatile organic materials, and cannot be resolved by 1-D GC. Meanwhile, the TOFMS provides mass spectral data of all separated compounds (Alam et al., 2016).

There are limitations to the analysis of polar organic compounds by GC/MS due to low volatility. Thus different methods of chemical analysis, such as LC/MS, are used to quantify more polar fractions in OA and to fill in the gaps for quantitation of carbonaceous mass. The LC/MS method employs various types of columns to separate the compounds within a narrow compound class (Sato et al., 2012; Fairbaugh, 2015).

Traditional methods of OA analysis such as GC/MS and LC/MS typically identify a limited number of compounds accounting for 10–30% of OA mass due to inadequate separation capability and the requirement for authentic standards to provide the retention time in chromatograms. In recent years, two dimensional gas chromatography coupled with time-of-flight mass spectrometry (GCxGC-ToFMS) has greatly enhanced separation capability (Alam and Harrison, 2016), and when combined with variable energy ionisation offers great power to distinguish between isomeric compounds (Alam et al., 2016). High-resolution mass spectrometry techniques (HRMS), such as Orbitrap MS and Fourier transform ion cyclotron resonance mass spectrometry (FT-ICR MS) (Jiang et al., 2016), coupled with a soft ionization technique such as electrospray ionization (ESI) (Wang et al., 2017; Roach et al., 2010; Gautier et al., 2014) can identify the molecular formulae and elemental composition of organic compounds without authentic standards, especially for determination of secondary organic aerosols (Liu et al., 2017b; Tong et al., 2016). For example, Reinhardt et al. (2007) quantified approximately 60% of organic compounds using FT-ICR MS. However, this gives information on the molecular formulae without defining the structure of a molecule.

Recently, online AMS has been widely used for chemical analysis of OA in real time with high time resolution (seconds to minutes). It is a quantitative instrument, with some models offering unit mass resolution (UMR) (Q-AMS, C-TOF-AMS and ACSM). The Aerodyne high resolution time-of-flight mass spectrometer (HR-TOF-AMS) is commonly used to characterize the size-resolved chemical composition of submicron particles with high mass resolution (Canagaratna et al., 2007; Drewnick et al., 2005; Jayne et al., 2000; Zhang et al., 2015a). A brief description of AMS is given in Table 2 (Aiken et al., 2008; DeCarlo et al., 2006; Zhang et al., 2011b). Normally, the Positive Matrix Factorization (PMF) algorithm is applied to AMS datasets to study sources of OA (Zhang et al., 2011c), and reports the temporal variations of the composition and concentration of the OA in the form of factors with mass spectra and temporal variation characteristics of specific source types and secondary aerosol types.

The ratios of $^{13}C/^{12}C$ ($\delta^{13}C$) and $^{14}C/^{12}C$ ($\delta^{14}C$) can be measured by accelerator mass spectrometry, and can be used to quantify the source of carbonaceous aerosol (Cao et al., 2017). The variation of $\delta^{13}C$ is affected by chemical fractionation processes, like photosynthesis. $\delta^{14}C$ is a function of the age of the carbon, and is an effective isotopic tracer to distinguish contemporary from fossil origin (Heal et al., 2011; Xu et al., 2016; Zhang et al., 2012), because ^{14}C is completely absent in fossil fuel OA owing to its short half-life (5726 years) and can only be found in modern non-fossil carbon sources (biogenic and biomass burning). Comparing $\delta^{13}C$ ratios in samples with values in known sources can be useful for source apportionment. For instance, Chesselet et al. (1981) inferred that fine particles collected over the Tropical North Atlantic and Pacific mainly come from continental sources with

Table 2
Measurement methods for studying organic aerosols.

| Methods	Principle of Operation	Application	Advantages	Disadvantage
TOA	Heated under pure helium and oxidizing atmosphere to volatilize OC and EC with different protocols	TC, OC and EC; OC/EC ratios	Extraction of materials in the filters	Varying OC/EC split; providing very little insight into the types of organic compounds
GC/MS	Extracting samples with 2–30 ml aliquots of DCM and Methanol under mild shaking and separation with GC/MS. Internal standards are used to quantify the organic markers and derivation procedures were performed for polar compounds prior to the GC/MS analysis	Determining the concentrations of individual organic marker species	High efficiency for analysis of the organic matters containing lots of different chemical composition and determination of purity for compounds)	Prohibiting the comprehensive analysis for organic matters if it is used alone. And it prevents most of polar components from entering the extract. Low atmospheric lifetime of organic markers
LC/MS	Extracting samples with 5 ml of methanol by sonicating for collecting organic compounds. The analytes were ionized by electrospray ionization in negative polarity mode and were then analyzed by MS instrument	Analysis of organic acids in extract solution; Separate compounds with wide ranges of polarity for eventual injection into a GC system	Extract solution can be injected into various columns; Determine and identify the polar compounds without derivatization	Besides the targeting of specific composition, it is difficult to couple to MS system.
ESI-HRMS	Extracting twice with 6 ml of acetonitrile and agitated for 20mins. The extract analytes were separated by column. The FTICR-MS and Orbitrap-MS was equipped with a heated ESI source, using a spray voltage of −2.6 and 3.2 kV for ESI- and ESI+, respectively	Identify high molecular weight organic compounds and oligomers; determine the elemental composition of organic compounds	Identify elemental composition of unknown OA without authentic standards; High mass resolution and high mass accuracy for determination of OA	There is no mature protocol, like the choice of ionization source and the solvent. ESI only can ionize polar compounds, but not for the nonpolar materials. This method is often qualitative analysis but not quantitative detection due to varying ionization efficiency in OA
UMR-AMS	AMS is operated in a cycle of two ion optical modes "V" and "W" every 7.5 or 10min. The V mode is more sensitive, which is to receive the mass concentrations of the non-refractory species for processing UMR data. The	Quantifying the mass of OA and providing information on size and composition of single aerosol	has high completeness of mass analysis about 100% of OA	unable to determine the refractory species, EC and oxidation states of OA (O/C ratio)
HR-ToF-AMS	W mode could obtain higher mass resolution to make the elemental composition in the mass spectrum to be quantitatively estimated and evaluate the elemental ratios (O/C, H/C, and OM/OC)	Employed to analyze the chemical characterization of submicronmetre aerosol (PM$_1$) and size distribution	Improving chemical resolution and sensitivity; be able to determine the elemental composition and oxidation states of OA	Accuracy of quantitative components is limited
Carbon Isotope Analysis	WSOC in filter is extracted by ultra-pure water. After freeze-dried, the residue (WINSOC or EC) is combusted in a stream of pure oxygen and quantified by an OC/EC analyzer. Finally, the corresponding evolved CO$_2$ is reduced to graphite for accelerator mass spectrometry target preparation	The ratios of the ^{13}C/^{12}C and ^{14}C/^{12}C are used to demonstrate the sources of carbonaceous aerosols	Facilitating the direct differentiation of non-fossil fuel carbon sources from fossil fuel sources	Difficulty in the estimation of SOA, ambiguous boundary of OC/EC separation, higher cost and bulk samples required
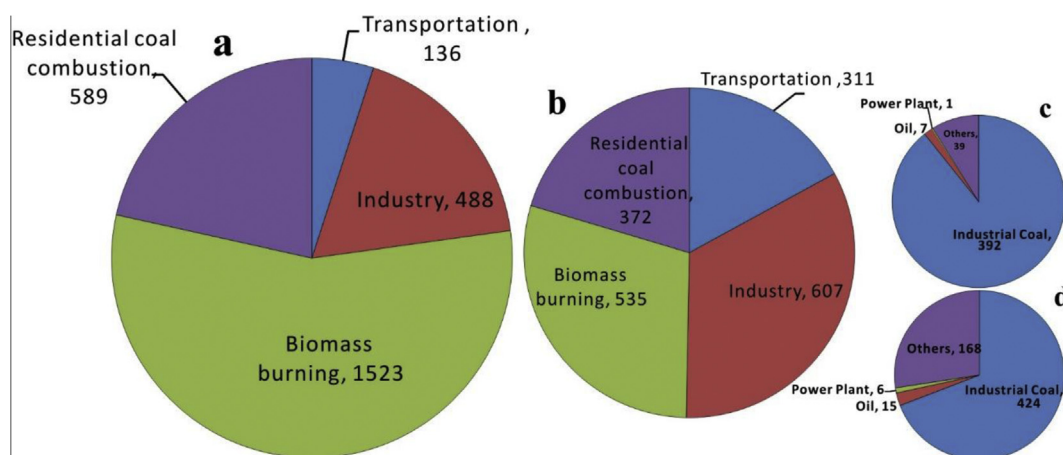
Fig. 2. Pie charts of the OC (a) and EC (b) emissions from distinct sources over China in 2012, and the OC (c) and EC (d) emissions by industrial sector (Gg) (Cui et al., 2015; Lu et al., 2011).

Table 3
Emission factors of OC and EC emitted from vehicles.

Vehicle type/Standard	Fuel type	Test method	Year Measured	Sampling site	Emission Factor (mg.veh^{-1}.km^{-1})			References
					PM$_{2.5}$	OC	EC	
China III, IV	61%LD- 12%HD-27%LPG	TN	2014	Zhujiang Tunnel, Guangzhou	82.70	19.30	13.30	Zhang et al. (2015c)
China III, IV	60%LD- 14%HD-26%LPG	TN	2013	Zhujiang Tunnel, Guangzhou	92.40	16.70	16.40	Dai et al. (2015)
China I	LDV	TN	2004	Zhujiang Tunnel, Guangzhou	52 ± 15	13.6 ± 2.6	16 ± 5.4	He et al. (2008)
China I	HDV				267.3 ± 56	54.3 ± 10	141 ± 21	
China IV	Gasoline	TN	2014	Yantai	7.36 ± 6.51	0.97 ± 5.19	ND	Cui et al. (2016)
China III	Diesel				415 ± 52.0	113 ± 41.4	164 ± 25.4	
–	GS (91–98%)	TN	2011–2012	Yan'an Tunnel, Shanghai	56.7 ± 69.4 (for PM$_{10}$)	18.3 ± 14.9	1.53 ± 1.98	Liu et al. (2015)
–	Gasoline	TN	2003	Hongkong	16.6 ± 28.5	8.5 ± 9.3	3.2 ± 13.3	Cheng et al. (2010)
–	Diesel				225 ± 31.3	67.9 ± 10.2	131.0 ± 14.1	
China II, III, IV Trucks	Diesel	ORM	2015	Shandong	99.13 (for TSP)	9.80	26.67	Cui et al. (2017)
China III, IV-LDDT, MDDT, HDDT	Diesel	ORM	2014	Beijing	85.00	27.00	47.00	Wu et al. (2016c)
pre-EURO-HDDT	Diesel	ORM		Hubei	1100 ± 80	305	677	Zhang et al. (2015c)
EURO II-HDDT					820 ± 120	243	502	

Note: HDV: Heavy duty vehicle; LDV: Light duty vehicle; LDDT: Light duty diesel truck; MDDT: Medium duty diesel truck; HDDT: Heavy duty diesel truck; TN: Tunnel measurement; ORM: On-road measurement.

δ^{13}C of −26‰ ± 2‰, based on the measurements of aerosols collected in urban areas of France. Many ^{14}C studies have measured ^{14}C in both OC and EC rather than in total carbon (TC), which enhances OA source apportionment even for non-fossil sources (Liu et al., 2013; Szidat et al., 2009; Zhang et al., 2012). The analytical procedures for ^{14}C in Water Soluble Organic Carbon (WSOC), Water Insoluble Organic Carbon (WINSOC) and EC have been reported previously (Liu et al., 2016, 2017a).

3. Sources and emissions of OA

In this section, the four main sources of primary organic aerosols (traffic emissions, industrial emissions, residential coal combustion and biomass burning) and their emission rates in China are discussed. This is illustrated by Fig. 2a and b which presents OC and EC emissions from generic sources over China in 2012. The main sources of secondary organic aerosols (biogenic and anthropogenic SOAs) are also considered. Furthermore, the source profiles for source apportionment of POA by receptor modelling and SOA tracers are reviewed in this section.

3.1. POA

3.1.1. Traffic emissions

Road traffic is a major source of carbonaceous aerosols in Chinese cites (Lu et al., 2011). For example, Zhao et al. (2012) estimated that OC and EC from traffic emissions accounted for about 10.3% and 15.0% of total OC and EC in Northern China, respectively. Organic aerosols from road traffic can be released directly in the exhaust due to incomplete combustion of fuels and lubricating oil or can be formed in the atmosphere by the oxidation of traffic generated-VOCs such as aromatics (Kanakidou et al., 2005). Lang et al. (2017) found a very high correlation (r^2) between annual average OC concentration with vehicular OC emissions ($r^2 = 0.95$) and VOC emissions ($r^2 = 0.9$) in Beijing over a 10 year period (2004–2014), suggesting a high contribution of traffic emission to the atmospheric OC level. This section will summarize the emission factors (EFs) of POA released from vehicles in China and factors affecting the measurement of EFs. The contribution of traffic emission to SOA will be discussed later in Section 5.

3.1.1.1. Emission factors of traffic generated primary organic aerosols. The emission factor of primary organic aerosol from vehicles depends strongly upon the type of engine (Cui et al., 2017), the properties of the fuel (Lu et al., 2012), the vehicle use, and the test method (Zhang

et al., 2015c). Because of high bias in the measurement of EFs by chassis dynamometer tests, measurements of on-road vehicles and in traffic tunnels are commonly conducted in China as shown in Table 3. The estimated EFs of OC are quite variable, ranging from 0.96 mg km^{-1} (Cui et al., 2016) for a China IV gasoline vehicle to 305 mg km^{-1} for a pre-EURO heavy duty diesel truck (Zhang et al., 2015c). According to the National Bureau of Statistics of China (NBSC), diesel and gasoline are the dominant vehicle fuels in China, with consumption of around 97.76 and 171.65 million tons in 2014, respectively. Cao et al. (2006) reported that the emissions were 60 Gg/year of organic aerosols from diesel vehicles and 5.1 Gg/year from gasoline vehicles.

3.1.1.2. Effects of fuel types and properties. The type of fuel (e.g. gasoline, diesel, or biofuel) has a significant effect on the EF of organic aerosol. Cheng et al. (2010) measured the EFs of aerosols in a traffic tunnel in Hong Kong and found that the EF of OC emitted from a diesel vehicle (67.9 mg km^{-1}) is 8 times higher than that from gasoline vehicles. This is consistent with the later observation by Cui et al. (2016). In another study, Zhang and Balasubramanian (2016) investigated the impacts of alternative fuels such as biodiesels on EFs. This study found that the blending n-butanol and n-pentanol with biodiesel could reduce significantly the emissions of PM and EC, but increased the proportion of organic aerosol. Similarly, Yang et al. (2017) reported that the blended biodiesel show a higher fraction of OC at low and medium engine loads. In addition, Xu et al. (2013) characterized the exhaust diesel particles from different oxygenated fuels (soybean-based biodiesel blend, dimethyl carbonate blend, and dimethoxy methane blend) and found that the oxygenated fuels could increase the fuel density and viscosity, leading to degradation of combustion efficiency, therefore enhancing the emission rate of OC.

3.1.1.3. Effects of vehicle operating modes. The operating modes (speed, acceleration and load) have a significant influence on the emission factor of traffic-generated organic aerosols. Cui et al. (2017) reported that poor driving conditions (low average and highly variable speeds) could result in a higher emission of OC. This concurs with Wu et al. (2016a) who conducted the measurement of OC under highway and non-highway driving conditions. The lower speeds under non-highway driving conditions lead to a lower combustion temperature, causing higher OC emissions due to less pyrolysis of fuel and lubricant oil. Furthermore, the effect of fuel injection pressure, and the application of exhaust gas recirculation (EGR) was investigated by Li et al. (2014a,b). Those studies found that a high level of EGR could enhance the soot formation from a diesel engine, leading to increased emission of carbonaceous aerosols.

3.1.2. Industrial emissions

Industry is one of major contributors of organic aerosols in China. Cui et al. (2015) estimated that the emissions from the industrial sector account for 17–21% and 30–34% of the total OC and EC emissions, respectively. This section will summarize the emission factors and emissions of OA from coal fired combustion, oil combustion and power plants based on different fuels and industrial processes. Fig. 2c and d present the OC and EC emissions from different industrial sectors.

3.1.2.1. Industrial coal combustion. The emission factor (EF) of industrial boilers is highly affected by the coal maturity. For examples, Zhang et al. (2008c) found that emission factors for industrial bituminous coal combustion are 0.3 and 0.062 mg kg^{-1} coal for OC and EC, respectively, which is much lower than that emitted from industrial brown coal (17.1 mg kg^{-1} for OC and 2.8 mg kg^{-1} for EC). Mixed coal combustion produced moderate levels of organic aerosols (1.9 and 0.7 mg kg^{-1} coal for OC and EC, respectively). Bond et al. (2002) indicated that the types of coal with low maturity have a relative high volatile content that is the precursor component for particle formation, leading to increase of emission factors for OA.

Coal combustion in industry generates carbonaceous aerosols with a range from 394 to 993 Gg/yr for OC and from 430 to 591 Gg/yr for EC from investigations in the field and calculation using models (Cao et al., 2006; Cui et al., 2015; Lu et al., 2011). The estimate of OC and EC emissions in previous studies shows different trends. Cui et al. (2015) estimated that the annual trends of OC and EC emissions from industrial coal combustion showed steady growth during 2000–2005 (387–510 Gg OC per year) and then levelled off for 2005–2012 (455–494 Gg OC per year). However, their estimates are higher than those from Lu et al. (2011) and Zhao et al. (2011). The differences can be attributed to two aspects. First, some studies have omitted some emissions from certain non-combustion industrial processes. Second, Cui et al. (2015) added wood combustion in industry and used larger emission factors for small coal and biofuel stoves. Cao et al. (2006) estimated the highest annual emissions (1116.1 Gg OC and 543.9 Gg EC per year) among all studies in 2000, due to inclusion of the emissions from uncontrolled coal-fired boilers, kilns and furnaces in rural industry.

3.1.2.2. Oil combustion. The estimated emission from industrial oil combustion shows a clear growth from 2005, with emissions of 2–3 Gg/yr OC and 3–5 Gg yr^{-1} EC before 2005 which increased to 7–8 Gg/yr OC and 14–15 Gg yr^{-1} EC for the following years (Cui et al., 2015). Cao et al. (2006) estimated much higher emissions from oil combustion in industry for 2000 (25.5 Gg OC and 17 Gg EC), mainly due to inclusion of emissions from rural industry. As shown in Table 4, the emission factor for industrial oil combustion that is approximately 8–11 g/GJ for OC and 25–35 g/GJ for EC, is higher than that from an oil or coal-fired power plant (Lu et al., 2011).

3.1.2.3. Power generation. According to the State Power Corporation of China (2017), electricity was mainly derived from coal combustion (66%) in China in 2016. According to the National Bureau of Statistics of China (NBSC) data, power plants consumed 1845 Tg of coal, which is 44.8% of total coal combustion in 2014. However, the OC and EC emissions are relatively low, only 11 and 21 Gg/yr in 2010, constituting about 0.3 and 1.9% of total national emissions of OC and EC, respectively within China (Cao et al., 2006; Cui et al., 2015; Lu et al., 2011). This is because pulverized coal is the dominant coal used in power plants, and emits lower levels of carbonaceous materials at high temperatures. In addition, the emissions of carbonaceous aerosols from coal-fired power plants are reduced by electrostatic precipitators (ESP)

Table 4
Emission factors of OC and EC from industry in China (g/GJ).

	Fuel type	OC					EC				
		1996	2000	2004	2008	2010	1996	2000	2004	2008	2010
Power plant	coal	1.2	0.8	0.5	0.3	0.3	1.2	0.9	0.7	0.6	0.6
	oil	0.4	0.4	0.4	0.3	0.3	0.8	0.8	0.8	0.6	0.6
Industry	coal	29.6	24.7	17.9	12.7	8.6	29	23.8	17.9	13.3	10.3
	oil	7.9	9.9	9	11	10.9	25.5	31.9	28.8	35.5	35.3

Data from Lu et al. (2011).

and flue-gas desulfurization (FGD) devices. For example, Zhao et al. (2011) estimated the removal efficiencies by ESP for $PM_{2.5}$ to be 92.3% from field measurements, and Zhang et al. (2009) reported that net $PM_{2.5}$ emission factors declined from 2.0 g/kg coal to 1.2 g/kg coal (a reduction of 40%) using FGD. For coal-fired power plants, OC and EC emission rates reduced from 1.2 g/GJ and 0.9 g/GJ in 1998 to 0.3 g/GJ and 0.6 g/GJ in 2010, respectively. These OC and EC emission factors were higher than those for oil combustion power plants, but by 2010 these were equal (Table 4) (Lu et al., 2011). Cui et al. (2015) estimated that the annual EC emission decreased from 11 Gg/yr in 2000 to 6 Gg/yr in 2010. Besides ESP, some other dust collectors have been also used, including fabric filter systems, wet scrubbers and cyclones (Li et al., 2009b; Zhao et al., 2010). However, the coal-fired power plants have resulted in a tremendous rise in greenhouse gas emissions. For instance, Chen et al. (2010) found that the direct CO_2 emissions from electric power and hot water production accounted for 42.8% of the total.

3.1.3. Residential combustion emissions

Residential emissions include those from heating and cooking by coal combustion, natural gas combustion and biofuel burning. In this section, we focus on the emissions from domestic coal combustion.

The emission factors for residential coal combustion varied from 0.014 to 13.71 g/kg for OC and from 0.005 to 10.96 g/kg for EC (shown in Table 5). Higher EF_{OC} and EF_{EC} values are found in the field from combustion of anthracite briquettes rather than from burning under laboratory test conditions. For instance, the EF_{OC} and EF_{EC} of anthracite briquettes burned in a brick stove with a chimney were 0.47 g/kg and 0.028 g/kg, respectively (Zhang et al., 2008c). It is also reported that the EF_{OC} of anthracite burned in an improved stove with a chimney in Shanxi was 0.14 g/kg (Shen et al., 2013). However, the results of an experimental test with anthracite briquettes were 0.014 g/kg and 0.005 g/kg for EF_{OC} and EF_{EC}, respectively (Shen et al., 2010). It is noted that great differences exist in EFs for coals of different maturity. As shown in Table 5, medium-volatile bituminous coal has the highest EF_{OC} (13.71 g/kg) and EF_{EC} (10.96 g/kg), which are 334 and 2192 times higher than those from semi-anthracite respectively (Chen et al., 2006), suggesting that estimation of carbonaceous emissions from residential coal would be very difficult in China, because coals have a wide range of maturity. Other studies also gave similar results that the EF_{OC} and EF_{EC} are 0.014–0.47 g/kg and 0.005–0.028 g/kg respectively for anthracite briquettes and 0.59–13.713 g/kg and 0.2–10.96 g/kg for bituminous coal. More mineral matter and less OC are emitted from anthracite coals due to the higher burning temperature.

The largest OA source in China is coal combustion, which accounts for about 70% of total energy consumption (Huang et al., 2013). According to Fig. 3, coal consumption increased from 1.2×10^9 tonnes in 2001 to 2.75×10^9 tonnes in 2014, contributing 68–72.5% of total energy consumption during this period (NBSC, 2015). Power plants are the largest coal consumer (1.95×10^9 tonnes), followed by industry (1.19×10^9 tonnes) and residential use (3.6×10^8 tonnes). Coal burning is a very common fuel in Northern China for heating in winter. Zhang et al. (2008c) estimated that residential coal consumption emits more than five times more OC than from industry. The large contribution from residential sources is mainly because of the lack of after-treatment in the residential stove. Meanwhile, improved stoves with galvanized flue pipes have been used to reduce the EF of carbonaceous aerosols. For example, Zhi et al. (2009) found that approximately 61% and 98% of OC and EC emissions were reduced in the improved stove.

3.1.4. Biomass burning

Biomass burning emissions in this review include open biomass burning and household biofuel use. The main sources of household biofuel for cooking and heating in the countryside of China include crop wastes (rice straw, maize residue, wheat residue, bean straw, cotton stalk, and kaoliang stalk), and woody fuels (wood and branches). The emission factors (EFs) of organic aerosols are strongly related to the type of fuel burning. For example, a stove-fuel combination test was conducted to compare emissions from crop residue combustion and woody fuel combustion (as in Table 6), indicating that crop waste combustion emitted much higher OC (10.86–14.66 g/kg) but lower EC (2.71–3.53 g/kg) than those emitted from woody fuel combustion (1.97–3.16 g/kg for OC and 2.62–4.91 g/kg for EC, respectively) (Li et al., 2009b). However, the efficiency of biomass burning depends on the temperature of burning, heat intensity, aeration and process of smoldering, which determine the organic compounds emitted from burning (Simoneit, 2002). For instance, the EFs of OC and EC were reported to be 10.53 and 0.49 g/kg dry fuel for rice straw burning in flaming combustion in the laboratory, respectively, which is a little higher than those emitted from smoldering combustion with 8.77 g/kg of OC and 0.37 g/kg of EC (Zhang et al., 2013b).

Biomass combustion is estimated to have emitted about 41–79% of OC (1264–2750 Gg/yr) and 27–50% of EC (398.3–716 Gg/yr) in China during 2000–2012 by different studies (Cui et al., 2015; Lu et al., 2011). Agricultural waste burning emitted about 13% of OC, forest fires contributed 2–11% of OC, and residential biofuel burning accounted for 56% of anthropogenic OC emissions in 2010 in China (Lu et al., 2011). Based on statistical data from NBSC, straw residue combustion has reached about 600 million tonnes currently, accounting for 70% of rural energy. Alternatively, a survey of open burning fires in Beijing found that open fires increased from 2000 locations (in 2005) to 6000 locations (in 2012) except for 2008 (1700 locations) owing to the Olympic games. This suggests an increasing OA emission from biomass

Table 5
Emission factors of OC, EC and PM from residential coal combustion in China (g/kg).

Type of coal	Stove	OC	EC	$PM_{2.5}$	
Anthracite briquettes	A movable metallic stove without flue	0.014	0.005	0.119	Shen et al. (2010)
MVB		0.588	0.380	5.203	
HVB	A metallic outer cover and thermal-insulated ceramic liner	2.66	0.20	4.05	Chen et al. (2006)
HVB		11.52	5.34	23.24	
MVB		13.71	10.96	29.86	
LVB		9.29	6.97	22.96	
LVB		3.85	0.48	6.8	
SA		0.041	0.005	0.795	
Anthracite briquettes[a]	An improved stove with a chimney	0.13–0.14	0.004–0.0041	0.54–0.64	Shen et al. (2013)
Coal cake[a]	A brick stove with and outdoor flue	0.38–0.58	0.022–0.052	3.2–8.5	
Sub-bituminous Briquettes	A metallic outer cover and thermal-insulated ceramic line	4.729	0.096	8.001	Chen et al. (2005)
Bituminous briquettes		7.817	0.283	12.911	
Anthracite briquettes		0.017	0.004	1.329	
Anthracite[a]	Brick stove with a brick chimney	0.47	0.028	1.054	Zhang et al. (2008c)
Bituminous[a]		2.975	2.750	7.373	

HVB: High-volatile bituminous coal; MVB: Medium-volatile bituminous coal; LVB: Low-volatile bituminous coal; SA: semi-anthracite.
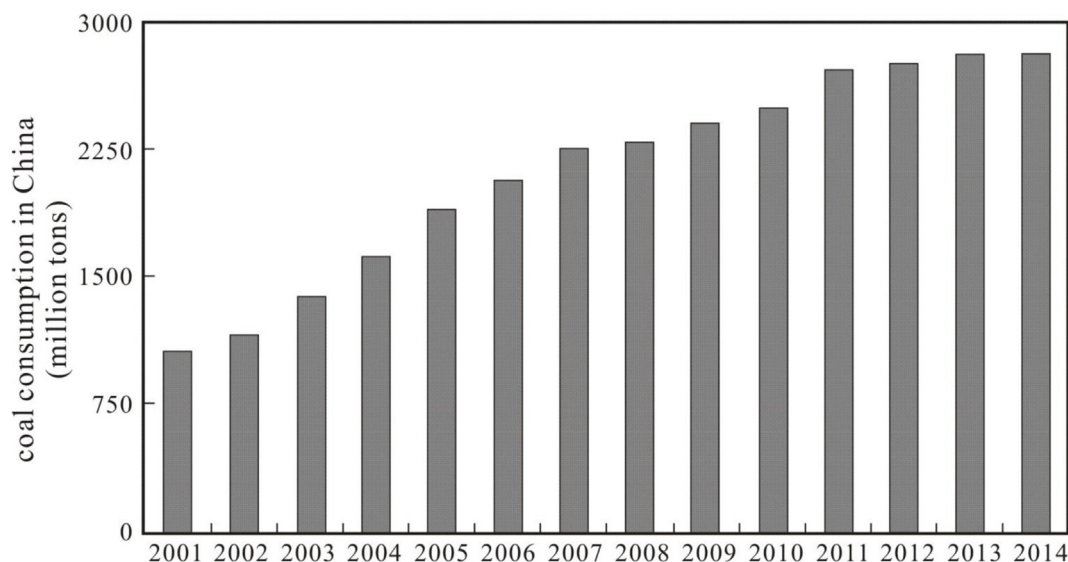
[a] Field coal consumption.

Fig. 3. Diagram showing the annual coal consumption (million tonnes) from 2001 to 2014 in China. Data are sourced from National Bureau of Statistics, China (NBSC, 2015).

Table 6
OC and EC emission factors from household biofuel combustion.

Fuel type	OC(g/kg)	BC(g/kg)	OC/PM$_{2.5}$ (%)	BC/PM$_{2.5}$ (%)
Rice straw	1.06–1.07	0.09–0.11	54.64–64.46	4.64–6.63
Maize residue	0.85–3.21	0.21–0.68	34.69–83.38	8.57–17.66
Bean straw	0.89	0.94	27.74	29.69
Cotton stalk	2.75	0.6	45.27	9.88
Wheat residue	2.01–2.77	0.28–0.44	33.03–35.84	4.99–5.25
Kaoliang stalk	3.3–3.97	0.59–0.76	52.64–55.21	9.41–10.57
Fuel wood	0.41–1.43	1.03–3.26	18.53–31.22	46.55–71.18
Branch	1.56–1.73	1.59–1.65	39.31–58.59	40.06–55.88

Data from Li et al. (2009b).

burning in Beijing (Wang et al., 2015c). The distribution of fire locations indicates that the fires occurred mostly in the plains, such as east of Henan, south of Shandong, north of Anhui and Jiangsu, which is where winter wheat is cultivated.

3.1.5. Source profiles of primary organic aerosols
In the CMB (Chemical Mass Balance) receptor model, it is very important to obtain representative source profiles for emissions. The selected molecular markers should be stable during transportation from the source to receptor. CMB inputs often include OC, EC, n-alkanes, n-alkanoic acids, PAHs, hopanes, levoglucosan and sterols (Fraser et al., 2003; Schauer et al., 1996, 2002). The major source profiles and molecular tracers are summarized in Table 7 and Table 8.

Gasoline and diesel engine source profiles were measured by Cai et al. (2017) in China. This study included several types of gasoline vehicles (light duty and heavy duty with electronic fuel injection and catalyst, heavy duty with carburetor and catalyst, heavy duty carburetor, and motorcycles) and two types of diesel vehicles (light duty and heavy duty). OC contributed respectively 31.7% and 54.9% to PM$_{2.5}$ from light and heavy duty gasoline vehicles. For diesel vehicles, OC accounted for 56.9% of PM$_{2.5}$, while EC was 17.6% and 17.7% of PM$_{2.5}$ for heavy and light duty diesel, and 8% on average for gasoline. These results are consistent with previous work by Zhang (2006), who found that the average content of OC and EC in fine particles is 38% and 4% from gasoline cars and 58% and 16% from diesel cars, respectively. In other studies, Pio et al. (2011) measured the OC and EC at both roadside and urban background sites in Portugal and the UK, and obtained the lowest OC/EC ratio ranging from 0.3 to 0.4 for the road-generated aerosols. The results of Pio et al. (2011) are in agreement

with the findings by Yu et al. (2011), but they are lower than those measured by Hildemann et al. (1991) for particles emitted from gasoline (OC/EC = 2.2) and diesel vehicles (0.8).

Heptadecane (C17) is one of the major tracer compounds for vehicle emissions, and the dominant carbon number of the n-alkanes (C$_{max}$) from PM in vehicle exhaust can range from C17 to C25. The carbon preference index (CPI) of gasoline and diesel exhaust is reported as 0.93 and 1.07, respectively (Cai et al., 2017). The hopane concentrations in gasoline emitted particles is higher than that from diesel vehicles and the predominant hopane is 17α(H),21β(H)-hopane (HP30), which has been used as a tracer for vehicle emissions (Shrivastava et al., 2007). Vehicle emissions are found as a major source of PAHs in Chinese megacities such as Hong Kong, Guangzhou and Beijing (Gao et al., 2012; Guo, 2003; Wu et al., 2014). This is consistent with observations from the western countries. For example, Harrison et al. (1996) identified benzo(ghi)perylene (BGP) and coronene along with phenanthrene (PHE) and benzo[b]naphtha[2,1-d]-thiophene (BNT) as a source fingerprint for vehicle emissions; Miguel et al. (1998) and Masclet et al. (1986) found that the gasoline engine emission was enriched in BGP and coronene and diesel exhaust emitted mainly chrysene (CHR), fluoranthene and pyrene (as in Table 10).

Source profiles of coal combustion were measured from industrial boilers and residential stoves, including anthracite, bituminite and sub-bituminite coal (Zhang et al., 2008c). The contribution of OC and EC to PM$_{2.5}$ is 45% and 12%, respectively, and the POM from coal combustion was predominantly comprised of n-alkanes (20%), PAHs (38%) and aliphatic acids (46–68%). The CPI of n-alkanes is 1.2–1.4 and dominated by C17 to C25. PAHs are by-products of incomplete combustion of carbonaceous fuels with emissions of many individual compounds higher than those from other sources, especially picene, benzo[b]fluoranthene, pyrene and retene (Shen et al., 2012). For example, Wei et al. (2016) observed that naphthalene, fluoranthene, pyrene, phenanthrene, fluorene, chrysene and benzo(a)pyrene were dominant PAHs emitted from a coal-fired power plant. For a heavy oil and natural gas fuelled-boiler, naphthalene, phenanthrene, fluoranthene, pyrene, fluorene and benzo(b)chrysene were found to be the major PAHs. OC/EC ratios for the industrial emissions are 3.5–5, which are higher than those from traffic emissions. A study by Yin et al. (2010) in the UK found that picene is predominantly from coal combustion.

The composition of organic aerosol from biomass burning varies significantly depending on the type of biomass fuel and combustion conditions. In China, there is a large quantity of crop straw produced,

Table 7

Source profiles with organic tracers and EC used in the CMB model (ng/mg PM$_{2.5}$).

	Gasoline	Diesel	Coal combustion	Straw	Wood	Cooking	Vegetative detritus
OC	43.3%	56.9%	45%	52%	30%	84%	32%
EC	8.0%	17.7%	12%	4.6%	16%	1.5%	0.1%
n-tridecane	7.35	16.4	11.4			70.5	
n-tetradecane	77.5	106.0	21.1			155	
n-pentadecane	495.3	388.2	217.1			156	
n-hexadecane	1572	1165.6	1461.8	128		362	
n-heptadecane	5756	3655.9	5422.9	13.7		493	
n-octadecane	1778.5	2975.6	1265.2	9.8		339	
n-nonadecane	2152.6	6803.3	1542.67	17.3		329	
n-eicosan	1960.5	9960.8	1943.2	23		197	
n-heneicosane	1807	11876.6	2159.2	31.9		215	
n-docosane	1893.6	10226.8	2374.7	39.3		163	
n-tricosane	1347	5991.7	2996.8	31.7		54.4	
n-tetracosane	1134.7	2926.2	1979.2	24.1		121	
n-pentacosane	964.8	1500.0	1814.4	29.6		103	
n-hexacosane	996.3	755.6	688.8	16.6	48.8	56.4	109
n-heptacosan	723.3	290.1	474.2	124.1	54.7	121	929
n-octacosane	588.1	197.2	179.4	20.2	16.1	26	282
n-nonacosan	484.4	90.0	135.3	492.3	17.6	276	6290
n-triacontane	334	29.6	77.3	19.4	7.4	59.7	440
n-hentriacontane	245.0	5.8	61.8	441.3	17.1	340	9440
n-dotriacontane	145.0	0.0	17.3	7.8	0	28.7	820
n-tritriacontane	108.8	0.0	184.4	79.1	16.8	39.9	5060
Nonanoic acid	1215.7	118.7	153	31.7		5156	
Decanoic acid	548.6	125.5	196.6	10.9		45.6	
Undecanoic acid	98.7	42.8	94.2	5.7		15.9	
Dodecanoic acid	294.4	91.8	386.4	89.2		281	
Tridecanoic acid	38.2	28.2	112.9	4.6		55.5	
Tetradecanoic acid	269.8	93.8	624.73	185.4		1269	
Pentadecanoic acid	90.1	56.0	199.7	86		419	
n-hexadecanoic acid	1430.6	185.4	1789.6	3782.8	1526	34301	713
n-heptadecanoic acid	42.3	36.8	67.2	84.5	64.9	465	17.4
n-octadecanoic acid	564.7	98.1	258.9	1052.3	335	11993	206
n-eicosanoic acid	27.1	13.6	57.1	309.9	125	977	436
n-docosanoic acid	20.1	3.3	60.1	399.8	780	976	182
9-Hexadecenoic acid(palmitoleic acid)	9.3	0.0	33.3	171.6		739	
9-Octadecenoic acid(oleic acid)	83.1	30.0	64.2	1703.9		14905	
9,12-Octadecanedienoic acid(linoleic acid)	19.5	3.7	9.6	1202.3		15821	
Adipic acid	88.1	36.05	2.3			200	
Pimelic acid	6.74	0	2.1	3.8		360	
Suberic acid	7.12	0	5			819	
Azelaic acid	24.26	11.5	29.4	78.4		4177	
Sebacic acid	3.82	5.6	0	0.9		223	
benzo[e]pyrene	127.18	22.95	848.1	6.9	297	14.5	0
benzo[ghi]perylene	527.64	19.4	522	6.5	334	6.41	0
coronene	236.8	2.6	86.1	1.9	97		0
Fluoranthene	164.9	122	1771	27.9		8.19	
Picene	0.1	0	146.6	0			
Benzo(b)fluoranthene	101.6	28.2	1822.9	13		18.8	
Pyrene	279.2	223	4914.4	27.4		7.8	
Retene	113.8	54.7	2019.6	1.5			
Perylene	19.2	0	170.1	1.4			
Benzo(ghi)fluoranthene	189	64.8	359.6	9.1		3.81	
Benz(a)anthracene	66	37.3	1293.6	10.8		1.72	
Chrysene	79.6	53	1097.8	12.2		6.68	
Benzo(k)fluoranthene	32.5	6.4	423.7	4.3		16.4	
Benzo(a)pyrene	134.4	8.6	1007.5	13.5		9.2	
17β(H),21α(H)-30- norhopane	319.4	80.2	349.3		0		0
17α(H),21β(H)- hopane	422.3	101.6	161.6		0		0
22S-17α(H),21β(H)- homohopane	116	21.5	34.3		0		0
22R-17α(H),21β(H)- homohopane	87.3	11.4	49.3		0		0
22S-17α(H),21β(H)- bishomohopane	72.1	11.8	5		0		0
22R-17α(H),21β(H)- bishomohopane	46.6	5.5	17.5				
levoglucosan	39.6	0	1790.3	45196.6	17350	4473	0
cholesterol	81	3	66.9	50.5	25.6	785	0
campesterol			0	1876.1	41.7	555	0
Arabitol						676	
β-sitosterol			2.7	3271.4		1375	
Malic acid						606	
Glyceric acid						1323	
	Cai et al. (2017)	Cai et al. (2017)	Zhang et al. (2008c)	Zhang et al. (2007b)	Wang et al. (2009a)	Zhao et al. (2015b)	Wang et al. (2009a)

0 in table refers to the value below detection and the blank means that was not analysed.

Table 8

Major source specific tracers for POA compounds used in CMB and PMF source apportioning analysis.

Compounds	Major source	Emission process
EC	urban	Diesel engine exhaust
N-alkanes, C_{29}, C_{30}, C_{31}, C_{32}, C_{33}	Vegetative detritus, road-dust, tire wear, biomass burning	Burning (direct)
n-alkanes,C15-C20	Microbial	Direct/resuspension
C20-C37	Plant waxes	Biomass burning
C15-C37	Urban	Vehicle exhaust
hentriacontane		
Tritriacontane		
Anteiso-triacontane		
Anteiso-dotriacontane, Iso-hentriacontane	Vegetative detritus, cigarette smoke	Burning (direct)
17α(H)-22,29,30-Trisnorhopane; 17α(H),21β(H)-29-norhopane; 17α(H),21β(H)-Hopane; 22R + R-17α(H),21β(H)-30-Homohopane; 22S + R-17α(H),21β(H)-30-Bishomohopane	Petroleum	Smoking engine, Gasoline and diesel vehicle exhaust
Benzo[e]pyrene, indeno[1,2,3-cd]pyrene, benzo[g,h,i]perylene, coronene, benzo[b+j] fluoranthenes	Metallurgical coke-production, soot deposit	Industry
benzo[k]fluoranthene	Natural gas	Combustion
Benzo[ghi]perylene, indeno[1,2,3-cd]pyrene	Petroleum	Gasoline engine
Dibenzothiphene	Asphalt, coke and diesel	Diesel vehicle exhaust
Picene	Coal combustion	Urban (burning/heating)
Benz[de]anthracen-7-one, Benz[a]anthracene-7,12-dione	Natural gas combustion	Home appliances and non-catalyst gasoline powered vehicles
1,3,5-Triphenylbenzene	incineration of refuse	solid waste incinerators and burning of plastics
Benzothiazole	Tire wear	
Levoglucosan	Wood smoke/Biomass with cellulose	Burning
Mannosan, galactosan	Biomass with hemicellulose	Burning
β-sitosterol	vascular plant wax, vegetation	Burning
Syringaldehyde, acetosyringone, syringic acid	Hardwood	Combustion
Pimaric acid, isopimaric acid	Softwood	Burning
Resin acids (dehydroabietic acid, 7-oxodehydroabietic acid)	Softwood (Conifer resin)	Combustion
4-hydroxybenzoic acid	Grasses and other nonwoody vegetation	Burning
Hexacosanoic acid, octacosanoic acid, triacontanoic acid, dotriacontanoic acid	Biomass and primary biogenic	Burning
Cholesterol, palmitoleic acid	Meat cooking	Direct
1,3 Benzenedicarboxylic acid	Vehicle	Urban
Oleic acid	Meat cooking, seed oil cooking, wood and other primary sources	Direct
Phthalates (bis(2-ethylhexyl), diisobutyl, dibutyl)	Plastics	Burning or evaporation
Saccharides	soil dust	resuspend soil dust into the passing aerosols
Arabitol, mannitol	Fungal spores	Adsorbed onto smoke aerosols
Vanillic acid	Softwood and hardwood	Conifer burning

Data source from Simoneit (2002), Yin et al. (2015).

Table 9

Emission factors and emission estimations of SOA precursors in China.

Region	Methods	Time and Type	BVOC emission factor (µgC/g/h)			emission (gC/yr)	BVOC emission flux (g C km^{-2} yr^{-1})	Reference
			isoprene	Total monoterpene	Other BVOCs			
Beijing	GloBEIS	2003, 39 vegetable types	33.1	2.7	1.5	1.6×10^{10}	8.9×10^{5}	Wang et al. (2003)
Hongkong	GloBEIS	2004/2005, 13 tree species	35	17.9	1.5	8.6×10^{9}	7.8×10^{6}	Tsui et al. (2009)
PRD	GloBEIS	2006, tree species	2.2	1.4	1.2	2.2×10^{11}	4.7×10^{6}	Zheng et al. (2010)
China	G95	2000, 12 forest types	11.8	0.2	5.3	2.1×10^{13}	2.2×10^{6}	Klinger et al. (2002)
China	MEGAN	2003, forest and shrub				1.3×10^{13}	1.4×10^{6}	Chi and Xie (2012)
China	MEGAN	1994–1998, forest trees and crops	16.0	1.3		4.6×10^{13}	4.8×10^{6}	Li and Xie (2014)
China	MEGAN	1999–2003				4.9×10^{13}	5.1×10^{6}	
China	MEGAN	2003				4.3×10^{13}	4.5×10^{6}	Li et al. (2013a)
China	MEGAN	2013				5.6×10^{13}	5.8×10^{6}	Li et al. (2016c)

GloBEIS: Global Biosphere Emissions and International System (Guenther et al., 1999); MEGAN: Model of Emissions of Gases and Aerosols from Nature (Guenther, 2006); G95: Global BVOC emission model (Guenther et al., 1995): PRD-Pearl River Delta.

up to about 6×10^8 tonnes per year, and half is combusted as an energy source in rural regions or burned for disposal (Zhang et al., 2007b). Many previous papers have focussed on the composition characteristics of cereal straw and wood burning aerosol as in Table 9. The most abundant species in biomass combustion is levoglucosan, contributing about 4.5% and 1.7% to the mass of fine particulate matter from straw and wood burning, respectively, followed by n-hexadecanoic acid

(0.4% for straw burning and 0.2% for wood burning). Moreover, the methoxyphenols from lignin and dehydroabietic acid from conifer smoke are significant tracers for biomass burning (Simoneit, 2002) as shown in Table 10. Potassium is also well-known as a tracer for biomass burning. The high K^+/OC ratio values (0.19–0.21) in summer in Beijing suggest that biomass burning is active in this period (Duan et al., 2004; Sun et al., 2014). High OC/EC ratios of 3.8–13.2 characterize biomass

Table 10
Comparison of concentrations of SOA tracers (ng m^{-3}) in different studies.

Location		PRD		PRD rural	Shanghai region		HK urban	BJ		BJ		Mt.Tai		Mt. Chang		HN	
Season		rural		F-W 2007	2010/2011		Su 2006	Su 2007		Su 2008		Su 2006		Su 2007		W 2006	
		Su 2008	F-W 2008		urban	suburban		urban	rural	urban	rural	Day	Night	Day	Night	Day	Night
Isoprene Tracers	2-Methylglyceric acid	7.71	4.75	2.04	1.65	1.75	0.97	6.8	8.8	21	29.9	45	40	3	NA	0.66	0.74
	C5-alkenetriols cis-2-Methyl-1,3,4-trihydroxy-1-butene	7.71	1		1.2	1.2	18.59	13[a]	11[a]	NA[a]	NA[a]	18[a]	18[a]	10	1.2[a]	19[a]	17[a]
	3-Methyl-2,3,4-trihydroxy-1-butene	4.96	0.76	1.16	1.7	1.93	8.46										
	trans-2-Methyl-1,3,4-trihydroxy-1-butene	14.2	2.53		3.85	3.35	34.86										
	2-Methyltetrols 2-Methylthreitol	25.6	5.14	9.6	1.78	2.48	8.32	11	16	42.2	63.6	32	42	35	26	17	12
	2-Methylerythritol	65.9	10.9	18	5.15	7	20.28	28	39	77.2	121.5	66	81	96	86	43	38
Monoterpene	3-hydroxyglutaric acid	2.62	3.57	0.43	0.6	0.75	83.77	15	19	51.7	57.5	16	15	16	25	3.1	2.8
	3-hydroxy-4,4-dimethylglutaric acid	1.61	1.59	0.17	1.77	2.33	9.68			9.9	8.3						
	3-methyl-1,2,3-butanetricarboxylic acid	4.95	3.56	1.16	1.57	2.17	73.47	1.9	2.2	4.6	4.3	6.7	4.9	22	16	2.1	
	cis-pinonic acid	1.69	6.73	3.6	1	1.1		8.4	4.9	11.9	21.9	6.8	4.5				
	cis-norpinic							2.7	3.9			0.87	0.7				
	Pinic acid	0.7	0.99	1.25				4.7	5.2	3.2	3.4	2.9	2.3				
	3-Isopropylpentanedioic acid						8.42			8.7	9.6						
	3-Acetyl pentanedioic acid						18.52			6.8	5.3						
	3-Acetyl hexanedioic acid						4.65			8.3	7.7						
β-caryophyllene	β-caryophyllenic acid	2.87	3.25	0.54	0.77	1.1	12.47			5.1	3.6	12	12				
Aromatics	2,3-Dihydroxy-4-oxopentanoic acid	17.8	13.1		1.33	1.33	1.77										
	Phthalic acid							14	15	13.3	11.7						
Reference		Ding et al. (2012)		Ding et al. (2011)	Feng et al. (2013)		Hu et al. (2008)	Yang et al. (2016)		Guo et al. (2012)		Fu et al. (2010)		Wang et al. (2008)			

PRD refers to Pearl River Delta Region; HK refers to HongKong; BJ refers to Beijing; HN refers to Hainan; Su means summer; F means fall; W is winter.

[a] The concentration of C5-alkenetriols.

burning (Zhang et al., 2007b).

A Chinese cooking source profile was measured in the studies of Zhao et al. (2007a) and Zhao et al. (2015b). During these studies, fatty acids (tetradecanoic acid, hexadecanoic acid, octadecanoic acid, oleic acid and linoleic acid) were the major contributor to OC, comprising 75.7% of the total mass of quantified organic compounds and with n-hexadecanoic acid as the predominant compound. They are released by hydrolysis and thermal oxidation of glycerides (Rogge et al., 1991). Sterols, which include cholesterol, campesterol and β-sitosterol, are also found in Chinese cooking emissions (Zhao et al., 2007a). This observation is similar to that reported by He et al. (2004) that fatty acids comprise over 90% of the quantified organic mass emitted from cooking in Shenzhen, and fatty acids comprise 78% of measured compounds from western style fast cooking (Zhao et al., 2007b). However, in some previous studies in other countries, fatty acids emitted from meat cooking have been low (Rogge et al., 1991; Schauer et al., 1999). The composition of organic compounds is different among various cooking styles. For example, Cantonese style cooking emitted 39 μg of fatty acids per mg of POA, and released high amounts of sterols with 2 μg/mg of POA. The typical OC/EC ratios of 4.3–7.7 are used as an alternative indicator of kitchen emissions (See and Balasubramanian, 2008).

3.2. Secondary organic aerosols

Secondary organic aerosols (SOA) are formed from gas to particle conversion of volatile organic compounds (VOC) from both biogenic and anthropogenic sources by oxidation primarily with ozone (O_3) and hydroxyl radicals (OH), forming products of lower volatility that subsequently partition into the particle phase. Biogenic VOCs (BVOC) are released from terrestrial vegetation, grassland, shrublands, peatlands and forest, and include isoprene, monoterpenes, sesquiterpenes, and oxygenated hydrocarbons (Guenther, 2006). Anthropogenic VOC (AVOC) mainly come from biomass burning, fossil fuel combustion, transportation, solvent utilization and industry (Li et al., 2016c).

3.2.1. BVOC

Emission factors of BVOC have been estimated either from direct field measurements, or assigned based on the vegetation class of the plants which have not been measured experimentally. Most studies focus on isoprene, monoterpene and other volatile organic compounds (other VOC) emission factors (Tsui et al., 2009; Wang et al., 2003). In Table 9, the average emission rate of isoprene of 33.1 μg C g^{-1} h^{-1} is calculated from 39 vegetation types in Beijing (Wang et al., 2003), which is comparable to the result by Tsui et al. (2009), who measured the annual average EF of BVOC in Hong Kong from 13 tree species with 35 μg C g^{-1} h^{-1} for isoprene. Overall, these regional EFs of isoprene are higher than the average EF from China (10.3–11.8 μg C g^{-1} h^{-1}) due to the different measurement methods and variable vegetation types present. For monoterpenes, the highest reported value of emission factor is from tree emissions (17.9 μg C g^{-1} h^{-1} in Hong Kong), and the lowest EF is from forest types (0.24 μg C g^{-1} h^{-1}) (Klinger et al., 2002; Tsui et al., 2009). The other VOC emission factors for different plants and forests have been based on a value of 1.5 μg C g^{-1} h^{-1} (Geron et al., 1994; Wang et al., 2003) except for the value of 5.28 μg C g^{-1} h^{-1} from a study by Klinger et al. (2002), who measured the EF from 12 forest types. Estimates of isoprene and monoterpene emission rates from forest types have been calculated from weighted averages based on the species distribution (Li et al., 2013a). Some emission rates from shrub and crop species have been estimated from measurements made in China (Tsui et al., 2009; Wang et al., 2003).

The estimated annual BVOC emissions in China, Beijing, Hong Kong and Pearl River Delta (PRD) from 1994 to 2013 are shown in Table 9. It shows that the BVOC emissions in 2013 in China were 5.6 × 10^{13} g C, including 3.2 × 10^{13} g C isoprene, 0.6 × 10^{13} g C monoterpenes and 1.5 × 10^{13} g C other VOC (Li et al., 2016c). Li et al. (2013a) and Li and

Xie (2014) estimated that the annual emissions during 1999–2003 ranged from 4.3 to 4.9 × 10^{13} g C. This result is two and three times as high as the annual emissions from measurements by Klinger et al. (2002) and Chi and Xie (2012), which are 2.1 and 1.4 × 10^{13} g C, respectively. The isoprene contributes the highest percentage of 55% (2.3 × 10^{13} g C) to the total emission in 2003, followed by other VOC with 31.8% (1.4 × 10^{13} g C) and monoterpenes with a lower emission at 13.1% (0.6 × 10^{13} g C). The discrepancy in the estimates is likely due to the isoprene emissions, which used different emission factors, information on land cover distribution, meteorological parameters and models (Wang et al., 2016c). Moreover, the BVOC emission estimates exhibit varying proportions of isoprene, monoterpene and other VOC between different regions. The highest contribution of total emission in the PRD was other VOC of about 41% and isoprene contributed least with 25% (Zheng et al., 2010). However, the isoprene emission accounted for 48% of total BVOC emission in Beijing, which is higher than that from monoterpene (22%) and other VOC (30%) (Wang et al., 2003). The area average BVOC emission in Hong Kong is higher than that from PRD, Beijing and China, because the vegetation coverage in Hong Kong is higher than that in PRD and Beijing, and there is less forest cover in China as a whole (Klinger et al., 2002; Tsui et al., 2009).

3.2.2. AVOC

Emission factors of AVOC (anthropogenic VOC) have been estimated from different emission sources. Estimates of EF from anthropogenic categories were provided in previous studies (Li et al., 2009a; Wang et al., 2009b, 2013, 2014; Wu et al., 2016c). In general, the highest AVOC emission rates are from solvent utilization in China (pesticide utilization and dry cleaning) with 276–1000 g/kg, followed by the EF for VOC from biomass burning with 2.12–15.7 g/kg. The industrial processes emitted about 0.1–81.4 g VOC per kg original materials, except for the raw chemical medicine (430 g/kg) and polyfoam (770 g/kg). For transportation, the VOC EF of on-road vehicles, dependent on the technology level and type of fuels, ranged from 7.43-9.98 g/km for pre-Euro 1 gasoline to 0.14–0.2 g/km for Euro 5 gasoline in China, but there is less variation around 0.22–0.31 g/kg for the diesel EF. On the other hand, the EFs of off-road vehicles ranged from 6.1 to 91.5 g/kg, including railway engines, marine vessels, construction machinery, agricultural machinery, agricultural tractors and trucks (Wu et al., 2016c).

The total annual AVOC emissions increased from 2.2 × 10^{13} g in 2008 to 3.1 × 10^{13} g C in 2013, dominating in many urban areas and regions (Li et al., 2016c; Wu et al., 2016c). However, the contribution of different AVOC sources to the total emission varied in different studies. For example, Wu et al. (2016c) reported that the industry sector is the largest contributor to the AVOC emissions, accounting for 29–39% of total AVOC during 2008–2012, followed by transportation with 26% and then solvent utilization with 17%. On the contrary, the emissions in 2013 estimated by Li et al. (2016c) are dominated by solvent utilization, transportation and industry, which emitted 1.0 × 10^{13} g (32.8%), 0.8 × 10^{13} g (25.7%) and 7.6 × 10^{12} g C (24.7%), respectively. The discrepancy is probably due to the different classifications between industry and solvent utilization. Generally, it indicates that industry and transportation are the main sector to target to reduce VOC emission, and solvent utilization plays an increasingly important role in the total AVOC emissions in China. Emissions from biomass burning are relatively stable (3 × 10^{12} g-4.2 × 10^{12} g C), but the relative contribution to total AVOC emissions decreased slightly from 17% in 2008 to 10% in 2013, which was due to the rapid growth of industrial emissions.

As discussed above, the annual BVOC emissions are higher than the annual AVOC emissions in China, but the AVOC dominate in urban and some economic regions. For example, Li et al. (2016c) estimated that the emissions of BVOC and AVOC are 5.3 × 10^{13} g and 3.1 × 10^{13} g in China, respectively. However, the AVOC emissions account for more than 80% of total VOC emissions in Beijing, Tianjin, Shanghai, and

Table 11
Mean carbonaceous aerosol mass concentrations in PM$_{2.5}$ observed in the primary megacities of the world cited from the literature (µg/m^3).

cities	Type	Sampling time	OC	EC	PM$_{2.5}$	Protocol	Reference
Delhi, India	Industry, commercial	2011	41.1	13	145.6	IMPROVE-TOR	Pervez et al. (2016)
Pune, India	upcoming city, commercial, institutional	2013	31.3	2.7	104.3	IMPROVE-TOR	
Birmingham, US	urban, commercial	2009–2013	2.7	1.0	11.9	TOT	Hidy et al. (2014)
Gulfport, US	urban, costal	2009–2014	2.0	0.4	8.6	TOT	
Los Angeles[a]	urban	Aug.2014–Feb. 2015	4.3		16.3	TOT	Saffari et al. (2016)
Mid-western, US	urban	Aug.–Nov.2011	2.3	0.2		TOT	Jayarathne et al. (2016)
Toronto[a]	urban	Dec. 2010–Nov. 2011	3.4	0.5	8	IMPROVE-TOR	Sofowote et al. (2014)
Seoul, South Korea	urban	2013	5.1	2.5		TOT	Kim et al. (2016)
Chiayi, Taiwan	urban	2014/2015	3.3	1.7	38.3	IMPROVE-TOR	Tseng et al. (2016)
Po Valley, Italy	urban	Nov.2011–Mar.2015	5.7	1.75	32.4	TOT	Pietrogrande et al. (2015)
Paris, France	region	Sep.2009–Sep.2010	2.7	0.8	13.0	EUSAAR 2	Bressi et al. (2013)
Barcelona, Spain	urban background	2011/2012	3	1.2	18.6	EUSAAR 2	Salameh et al. (2015)
Marseille, France	urban background	2011/2012	6.2	1.8	19.6	EUSAAR 2	
Genoa, Italy	urban background	2011/2012	2.7	1.4	14	EUSAAR 2	
Thessaloniki, Greek	urban background	2011/2012	6.6	1.3	37.2	TOT	
Barcelona, Spain	urban background	Aug.–Sep.2013	6.3	1.3	14.5	EUSAAR 2	Minguillón et al. (2016)
Barcelona, Spain	urban background	2011	3.0	1.12	18.2	EUSAAR 2	Pérez et al. (2016)
Thessaloniki	urban background	Jul.–Sep. 2011	5.7	0.7	23.5	TOT	Samara et al. (2014)
Greece	urban traffic	Feb.–Apr. 2012	8.4	5.3	31.2	TOT	

TOT refers to NIOSH-TOT.
[a] The values here refers to median concentration.

Jiangsu Province (Li et al., 2016c). A similar result was reported for Hong Kong by (Tsui et al., 2009), who estimated that AVOC and BVOC accounted for 79% and 21% of the total annual VOC emissions, respectively, owing to the high population and vehicle density in the megacity.

3.2.3. SOA yield

In previous studies, most parameters used in traditional modeling SOA mass loadings are based on observations from laboratory chambers. The SOA mass yield (Y) is defined as the ratio of aerosol mass concentration formed per mass of hydrocarbon reacted (ΔM, in µg m^{-3}) to the amount of total precursor VOCs reacted (ΔHC, in µg m^{-3}) (Hao et al., 2011; Kroll and Seinfeld, 2008). Odum et al. (1996) have developed a semi-empirical model based on the gas-particle partitioning of semivolatile compounds as follow:

$$Y = \frac{\Delta M}{\Delta HC} = \Delta M \sum \frac{\alpha_i K_{p,i}}{1 + \Delta M K_{p,i}}$$

Where α_i is the mass of gas phase fraction for semi-volatile species i and $K_{p,i}$ is the partitioning coefficient of compound i. For example, Hao et al. (2011) determined that the SOA yield from α-pinene oxidation in O$_3$-initiated chemistry was 28.9%. For aromatics, the SOA yield of 30% was presented by Gordon et al. (2014).

Then, the SOA production from precursors could be estimated by the SOA yield Y and mass of the reacted precursor ΔHC (Deng et al., 2016). However, the calculated SOA abundance is normally less than ambient levels using the current chamber/flow tube yields.

3.3. SOA tracers

Table 10 lists commonly used molecular tracers of biogenic and anthropogenic SOA.

3.3.1. Biogenic SOA tracers

Isoprene, monoterpenes and sesquiterpenes are important biogenic precursor of SOA (Claeys et al., 2004; Hu et al., 2008). The high-volatility precursor isoprene, emitted from vegetation, is oxidised to 2-methylglyceric acid, C5-alkenetriols and 2-methyltetrols (2-methyl-threitol and 2-methylerythritol) (Marais et al., 2016). Nine tracers were identified as monoterpene oxidation products in China (Table 10), which result from the photooxidation of α/β-pinene via reactions with hydroxyl radicals (OH) and ozone (O$_3$) (Guo et al., 2012). However,

more tracers of monoterpene precursors can be found in the studies in other countries, like 2-hydroxy-4-isopropyladipic acid and 3-(2-hydroxy-ethyl)-2,2-dimethylcyclobutane-carboxylic acid (Kleindienst et al., 2007). The lower-volatility sesquiterpenes are emitted from plants, and the most abundant specie is β-caryophyllene (about 66% of sesquiterpenes emissions) that produces β-caryophyllinic acid by photooxidation (Jaoui et al., 2007). Studies have found a positive correlation coefficient (R^2 = 0.52) between β-caryophyllinic acid and levoglucosan, suggesting that it is related to biomass burning (Fu et al., 2010). Hu et al. (2008) also reported that malic acid, citramalic acid, hexadecanoic acid and octadecanoic acid may be photooxidation products of other biogenic SOA precursors.

3.3.2. Anthropogenic SOA tracers

Several anthropogenic SOA tracers were measured in previous studies in China, including phthalic acids (o-, m-, and p-isomers), hydroxybenzoic acids (2-hydroxybenzoic acid, 3-hydroxybenzoic acid and 4-hydroxybenzoic) and 3,4-dihydroxybenzoic acid for SOA derived from aromatic compounds, and 2, 3-dihydroxy-4-oxopentanoic acid for SOA from toluene (Baltensperger et al., 2005; Emanuelsson et al., 2013; Zhao et al., 2004).

4. Spatial and temporal variations of atmospheric organic aerosol

4.1. Atmospheric concentration of carbonaceous aerosols

Table 1 lists annual mean concentrations of OC, OA, EC and PM$_{2.5}$ of major cities in China since 2008 (Lang et al., 2017; Wang et al., 2016b; Wu et al., 2016b). Annual concentrations of OC and EC in Chinese megacities (e.g., Beijing, Shanghai, Guangzhou, Xiamen, Nanjing and Tianjin) range from 3.3 to 27.8 µg/m^3 and 1.3 to 9.3 µg/m^3 respectively. The mean value of OC (14.5 µg/m^3) is five times as high as those typically observed in North America (3 µg/m^3) and three times higher than those in Europe; the mean EC concentration (4.4 µg/m^3) is approximately seven and four times higher than those in North America and Europe respectively (Table 11).

The OC/EC ratio is commonly used to diagnose sources of organic aerosols and for estimation of SOA (Chen et al., 2006; Pio et al., 2011). Reported OC and OC/EC ratios from various functional areas in China are plotted in Fig. 4. Samples collected from near road sites are characterized by low OC/EC ratios ranging from 2.5 to 5.0, similar to that of gasoline vehicle exhaust reported by Schauer et al. (2002). Industrial
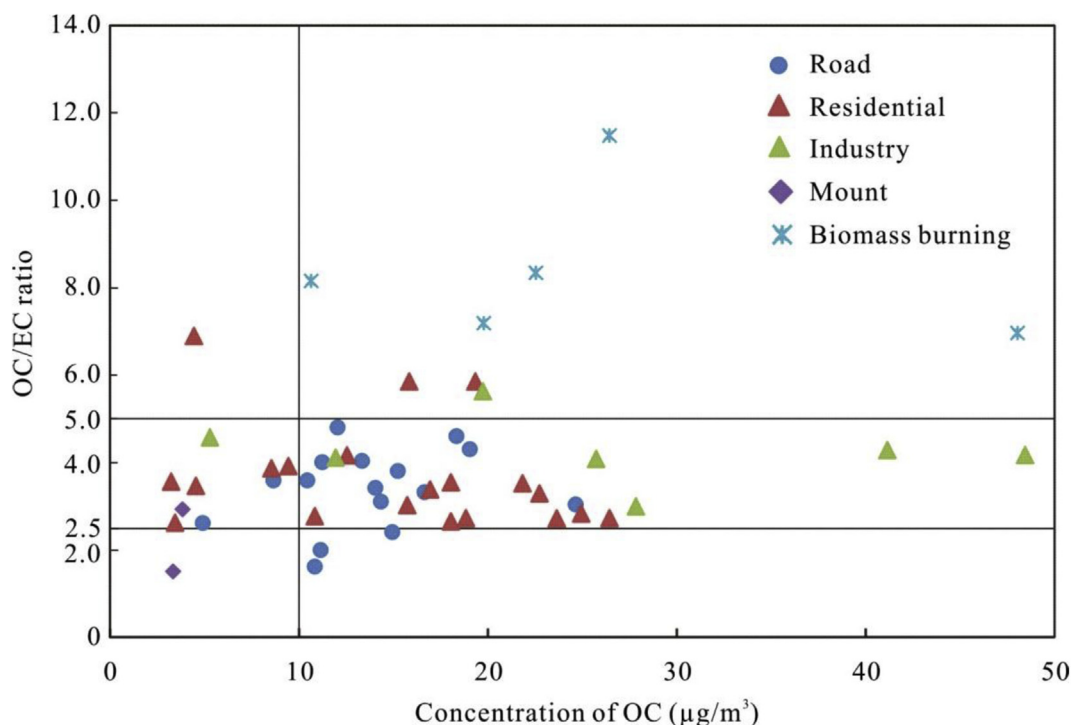
Fig. 4. Scatter plot of OC and OC/EC ratios of different functional areas.

emissions have a slightly higher OC/EC ratio ranging from 3.5 to 5.5, which is comparable with those from coal smoke reported in other studies with a OC/EC ratio of 2.5–10.5 (Chen et al., 2006). Residential and commercial sites exhibit a significantly lower OC/EC ratio (2.5–4.0) relative to the result from See and Balasubramanian (2008), who estimated the OC/EC ratio from typical kitchen emissions was 4.3–7.7. The difference in ambient data from these cooking sources is likely due to the contribution from vehicle exhaust and coal combustion to those sites. It is worth noting that OC/EC ratio at residential sites is relatively high in data collected at residential sites in Xiamen, which is attributed to the fuel used for cooking which changed to natural gas (Zhao et al., 2015a). Very high OC/EC ratios were observed in particles from biomass burning (7–11.5) (Wang et al., 2016a; Sun et al., 2014), consistent with that (4.1–14.5) measured by Watson et al. (2001). In Fig. 4, OC shows a wide range of concentrations from 3.2 to 26.4 μg/m³ in residential areas.

4.2. Temporal variations of OA in China

In China in both urban and suburban areas (with the exception of some rural sites), organic aerosols were generally higher in winter and lower in summer. As shown in Fig. 5, in most of the Chinese cities the average concentrations of OA revealed a winter maximum (urban: 46.4 μg/m³; suburban: 29.7 μg/m³), followed by fall (urban: 29.0 μg/m³; suburban: 20.6 μg/m³) and spring (urban: 20.0 μg/m³; suburban: 16.9 μg/m³), and a summer minimum (urban: 14.7 μg/m³; suburban: 12.8 μg/m³) (Feng et al., 2015; Ji et al., 2016; Li et al., 2015a; Tao et al., 2017b; Zhang et al., 2008b, 2014a; Zhao et al., 2013). Generally, the wintertime OA in urban ambient air is 2–5 times higher than that in summertime, while the values of OA during spring and fall are similar. However, in some suburban sites (e.g., Shanghai), the highest concentrations were found in fall, likely due to biomass burning activities (Feng et al., 2009).

This seasonality is mainly determined by the meteorological conditions and the variability in emission intensities. The low temperature and low boundary layer heights have been shown to affect significantly the accumulation of OA (Zhao et al., 2013). For example, the low

boundary layer height can promote SOA condensation and enhance the accumulation of semi-volatile organic compounds (SVOC) that can be subsequently adsorbed onto the existing aerosol surface (Cao et al., 2007; Zhang et al., 2013a). The low temperature facilitates SVOC condensation, thus increasing the OA concentrations (Pankow and Bidleman, 1992). Biomass burning is an important source of OA in China. Biomass burning activities are most prevalent in fall, leading to very high OA concentrations especially at the suburban sites (Chen et al., 2017; Feng et al., 2009). In northern China, domestic heating, using both coal and biofuels, contributes to a high OA loading in winter (Xu et al., 2015). Moreover, the cold start of vehicles was suggested to have a stronger impact on the OA winter concentrations (Zheng et al., 2005). OA commonly exhibits lower concentrations in summer as a result of the greater boundary layer height that enhances the vertical dispersion of pollutants (Chang et al., 2016), although the strong solar radiation facilitates photochemical reactions leading to formation of oxidised VOCs (Tuet et al., 2017), and the high temperature, shifts the SVOC to the gas phase. In southern China, the organic aerosols can be washed out by the summer rain and are affected by air masses origins (Tao et al., 2017b). For instance, since the Pearl River Delta is in a transitional climate region experiencing both tropical and subtropical air masses, significant variations of air masses are found between different seasons. In summer, the PRD is mainly affected by the air masses from the China South Sea with low pollutant loadings, leading to the lowest concentrations of OA. On the contrary, the air masses in winter predominantly come from the north and northeast of the PRD where numerous pollutant sources exist, causing elevated OA levels (Zheng et al., 2009).

Hong Kong is one of the exceptions. Gao et al. (2016) indicated that the highest concentration of PM₁₀ OA is in fall and summer when taking an average from clean and haze days, not in winter, since the traffic-related OA makes a relatively high contribution to OA in summer, when air masses come from the ocean and bring local emissions from downtown areas to this sampling site. In addition, the OA is likely dominated by SOA in fall.

Distinct seasonal variations in organic aerosols on the haze and non-haze days have been observed in more recent studies (Huang et al.,
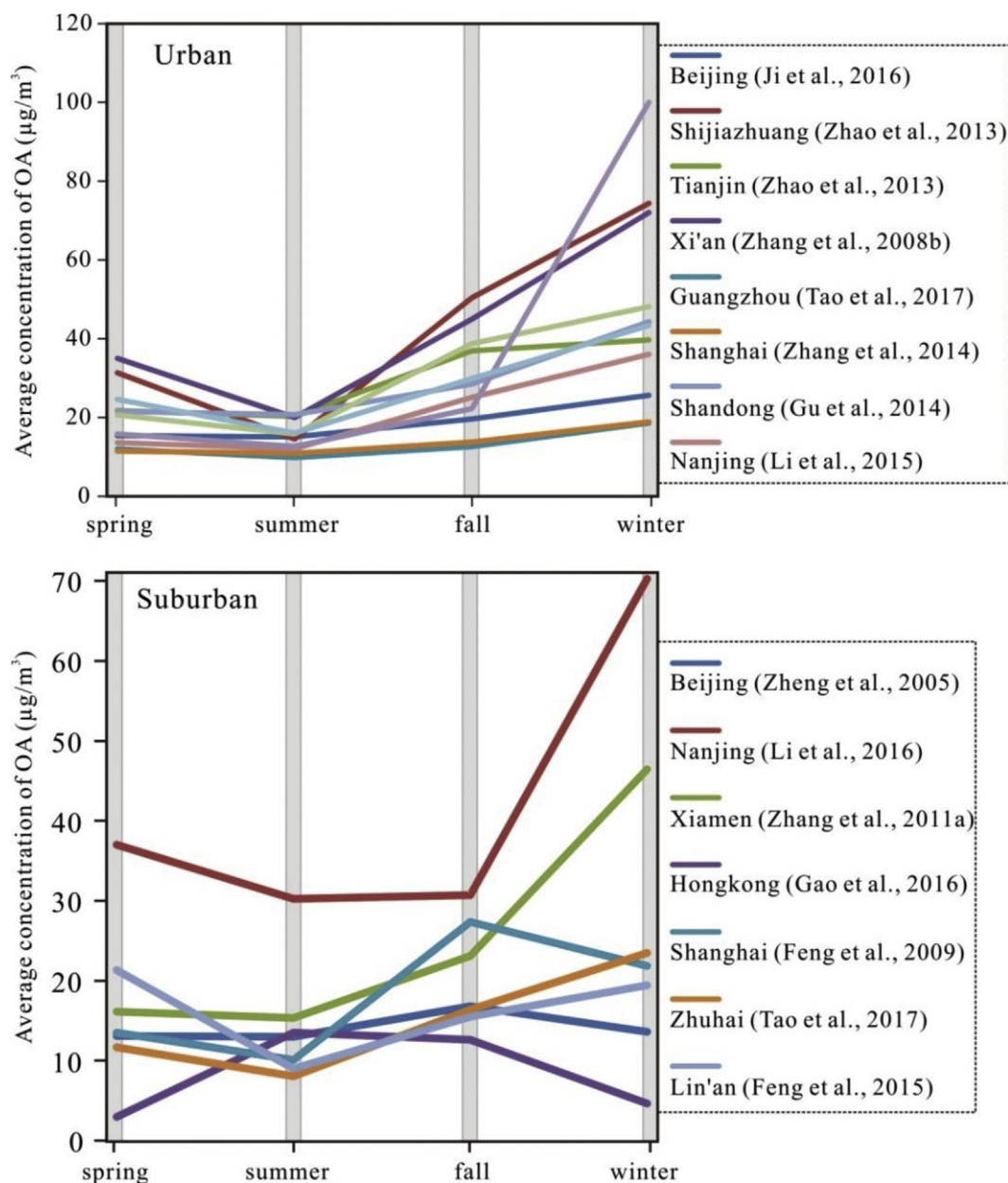
Fig. 5. The average concentration of OA in four seasons in megacities ($\mu g/m^3$).

2014; Zhou et al., 2017). For example, Zhou et al. (2017) reported that the highest OA concentration on a haze day in the North China Plain was in winter (55 $\mu g/m^3$), followed by that in summer (39.3 $\mu g/m^3$), fall (32.5 $\mu g/m^3$), and lowest in spring (22.2 $\mu g/m^3$). These were approximately two times higher than those observed on non-haze days. The higher OC/EC ratio on haze days indicates that SOA is a key contributor to OAs during haze events (Huang et al., 2011).

4.3. Spatial variations of OA in China

In this section, concentrations are annual means, unless stated otherwise. Concentrations reported as OC in the original papers have been converted to OA using factors of 1.4 for Beijing (Song et al., 2007), 1.9 for Hong Kong (Gao et al., 2016) and 1.6 for all other cities (Cao et al., 2007). Table 1 summarizes the OA concentrations measured in different regions in China with at least one year of sampling from 2010 to 2014. Geographical locations of the sampling sites for the compiled data are presented in Fig. 1, which are grouped as the North China Plain

(NCP: Beijing, Tianjin, Tanshan, Jinan, Zhengzhou), the Yangtze River Delta (YZRD: Shanghai, Nanjing, Hangzhou, Lin'an), Pearl River Delta (PRD: Guangzhou, Hong Kong, Zhuhai, Shenzhen), Southeastern coast (Fuzhou, Xiamen, Putian, Quanzhou), Southwest (Chengdu, Chongqing, Neijiang, Wanzhou), and other regions (Northeast and Northwest).

In the NCP, the annual mean concentrations of OA in 2010–2014 range from 17.3 to 42.2 $\mu g/m^3$ with an average of 28.9 $\mu g/m^3$ (Geng et al., 2013; Gu et al., 2014; Ji et al., 2016; Zhao et al., 2013). OA concentrations show a decreasing trend in the NCP. For instance, the annual mean OA level of 28.0–67.5 $\mu g/m^3$ measured in 2006 in some cities of the NCP by Zhang et al. (2008b) exceeds current concentrations. Such a decrease is presumably due to improved implementation of emission control policies, such as a widespread switch from coal and biofuel to natural gas in residential areas (Ge et al., 2004). The concentration of EC in Beijing ranges from 2.1 to 8.6 $\mu g/m^3$ (mean: 4.8 $\mu g/m^3$) and an average OC/EC ratio of 4.58 suggests that a high proportion of SOC is present in OC (Castro et al., 1999). This high level of OA and EC in Beijing is explained not only by the local anthropogenic sources

due to the large population living there, but also by transported pollution from surrounding industries.

In the YZRD, the annual OA and EC concentration range from 12.8–28.8 μg/m^3 and 2.1–9.3 μg/m^3, with mean values of 20.9 μg/m^3 and 4.5 μg/m^3, respectively (Chang et al., 2017; Chen et al., 2010, 2016; Feng et al., 2015; Li et al., 2015a). The OA concentration varied significantly depending on the level of industrialization and urbanization, population density and lifestyles (Feng et al., 2013). For example, the highest OA concentration was measured in downtown Nanjing surrounded by industry, and was relatively steady (22–28.8 μg/m^3) during 2007–2015 (Chen et al., 2016; Li et al., 2016b). Moreover, there was a higher OA concentration (18.3–28 μg/m^3) at a suburban site than in urban Shanghai, suggesting that the organic pollutants were mainly affected by local sources. Highly effective strategies were used to reduce the particles, leading to a sharp decrease in the OA level from 23.5 μg/m^3 to 12.8 μg/m^3 from 2006 to 2014 due to the 2010 Shanghai World Expo (Tao et al., 2017a).

As one of the most economically developed regions with many industries and electric power plants in southern China, the PRD has not suffered from haze episodes as much as northern China. The annual mean OA is 8.6–15 μg/m^3 (Gao et al., 2016; Tao et al., 2017b), which is 30–50% of that in the NCP. Moreover, the average OA in urban Guangzhou decreased by 45.9% and 9% in 2014 when compared to concentrations (24.2 μg/m^3 and 14.4 μg/m^3) measured in 2003 and 2009, respectively (Cao et al., 2004; Tao et al., 2014). However, the EC concentration was reduced by 33% from 2009 to 2014. Tao et al. (2017b) concluded that the dominant source of organic aerosols in Guangzhou is vehicle emissions owing to a good correlation (R^2 = 0.81) of OC and EC with a regression slope of 1.96 found in 2014. Therefore, the decline of OA concentration in recent years may be due to the efficient control measures applied to vehicle emissions (Lai et al., 2016; Tao et al., 2014). For the other coastal cities in the Southeast adjacent to the YRD and PRD (Fig. 1), the annual mean OA concentration was 12.9–19.1 μg/m^3 (Wu et al., 2015), which is lower than that in YRD and slightly higher than the value in PRD. Among these cities, the pollutant concentrations in Xiamen and Putian are influenced by a sea breeze (Zhang et al., 2011a).

Organic aerosol concentrations were high in Southwestern and Northwestern China with an average of 24.3–30.4 μg/m^3 and 29.8–34.9 μg/m^3, respectively (Chen et al., 2014; Wang et al., 2015d; Zhang et al., 2015b). The Sichuan Basin is in the agricultural heartlands of the Southwest, including Chengdu and Chongqing, which are influenced by anthropogenic organic matter sources, like biomass burning, coal combustion, high relative humidity and located in basins surrounded by mountains which inhibit the dispersion of pollutants (Chen et al., 2014). Compared with previous studies, the levels of OA in Chengdu in 2010–2015 were 38% lower than the 53.4 μg/m^3 OA measured in 2006 (Zhang et al., 2008b). The OA level in Chongqing was also 54% lower than 25.1–76.8 μg/m^3 measured in 2003 (Cao et al., 2007). It is clear that the organic aerosols in the Southwest have declined in the last decade.

The downward trends are mainly attributable to the pollution controls implemented to improve air quality including changes in fuels. A similar trend was observed in Xi'an in Northwestern China. The initial higher OA concentrations in Xi'an were mainly attributable to coal combustion emissions and unfavorable meteorological conditions (Cao et al., 2005). The annual concentration of OA there has decreased to 33.8 μg/m^3 in 2013 from 68.5 μg/m^3 in 2005 and 34.9 μg/m^3 in 2010 (Cao et al., 2007; Han et al., 2016a; Wang et al., 2015d), which is probably the consequence of pollution control measures, including the replacement of coal by natural gas. Furthermore, the higher OC/EC ratio (4–5.1) in winter corresponded to elevated residential coal combustion and biofuel for heating, and the mass of OC and EC resided predominantly in the PM$_{2.5}$ fraction (Han et al., 2016a; Wang et al., 2015d). The difference between the OA concentration at the rural (24.5 μg/m^3) and the urban site (30.1 μg/m^3) is not very large,

indicating that the organic component loadings at the rural site are affected by a combination of outflow from urban areas and local emissions (Wang et al., 2015d).

4.4. SOA tracer concentrations

As summarized in Table 10, the SOA tracer concentrations are highly dependent on locations and seasons. For example, the concentrations of 2-methylglyceric acid, C5-alkenetriols and 2-methyltetrols were 45, 18, 98 ng/m^3 at Mt. Tai in eastern central China, respectively (Fu et al., 2010). Their concentrations were higher at nighttime than in daytime owing to reduction of the planetary boundary layer (PBL) depth (Fu et al., 2010). Comparing the concentrations of total isoprene-SOA tracers between urban and rural locations in Beijing, the former site concentration of 73.8 ng/m^3 is lower than that at the latter of 93.8 ng/m^3, presumably due to higher isoprene emissions (Yang et al., 2016). Isoprene-derived SOA is the predominant contributor to BSOA in early June (accounting for 65% of BSOA), which is higher than that in fall-winter owing to the higher emission and reaction rates in the summer (Ding et al., 2011). This result is similar to that in the Canadian High Arctic (Fu et al., 2009). The concentration of monoterpene tracers was 20–306 ng/m^3 in urban Beijing and 28–230 ng/m^3 in the rural Beijing area (Hu et al., 2008; Guo et al., 2012; Yang et al., 2016). Ding et al. (2012) observed that the level of these compounds is slightly higher in the fall-winter (16.4 ng/m^3) than in the summer (11.6 ng/m^3) in PRD. This was attributed to the lower temperature, which results in an increase of tracer levels in the particle phase. On the contrary, Hu et al. (2008) estimated that monoterpenes and sesquiterpenes are the largest contributors to OA in the summer in Hong Kong due to high emissions of these biogenic hydrocarbons, consistent with those found in Hong Kong by Li et al. (2013b). Generally, there is no difference between the contribution of β-caryophyllinic acid in summer and fall-winter, with an average concentration of 3 ng/m^3 in both season (Ding et al., 2012). Moreover, Fu et al. (2010) observed that the sesquiterpene SOA tracers have the same level in daytime (12 ng/m^3) and nighttime (12 ng/m^3).

The contribution of SOA from anthropogenic precursors to total SOA is highly dependent on the location and season. They are the dominant source of SOA in the highly urbanized and industrialized PRD region. For instance, Ding et al. (2012) found that a tracer of precursor toluene (taken to represent all aromatics) ranged from 2.84 to 52 ng/m^3 and 1.7 to 48.9 ng/m^3 with the average of 17.8 and 13.1 ng/m^3 summer and winter-fall (Table 10), accounting for 76% and 79% of estimated SOC in summer and winter-fall, respectively. Recently, Hu et al. (2016) estimated in a modelling study that the country-average level of ASOA is 2 μg/m^3, representing 21% of annual average SOA, 31% in the winter and 14% in summer. This was attributed to lower biogenic emissions of SOA precursors and higher emissions of ASOA in the winter, as well as the effect of cold temperatures and high humidity. These conditions favor the condensation of ASOA compounds. The toluene-derived SOA in the urban atmosphere (1.33 ng/m^3) contributes as much as that in the rural atmosphere (1.33 ng/m^3) in Shanghai, consistent with that in Hong Kong (1.77 ng/m^3) and in Beijing (13.3 ng/m^3 at urban and 11.7 ng/m^3 at rural sites). This suggests that ASOA is formed on a regional scale (Feng et al., 2013; Guo et al., 2012). A possible explanation for the higher ASOA in Beijing than other cities is the high regional SOA background concentration. Wang et al. (2009c) reported that aromatic precursors contributed about 55–65% of the SOA in the PRD.

5. Source apportionment results for OA

The OC/EC ratio, and individual molecular markers such as hopanes, PAHs and levoglucosan are commonly used to estimate the source contribution to POA and SOA (Shrivastava et al., 2007; Simoneit, 2002). Also, the application of chemical mass balance (CMB) and positive matrix factorization (PMF) receptor models has been

widely reported in previous studies. In this section, we begin with a survey of recent laboratory and field observations, and discuss the estimation of POA and SOA concentrations.

5.1. Receptor modeling of OA

The most commonly used receptor models include the Chemical Mass Balance (CMB), isotopic mass balance using ^{14}C and factor analytical methods that include Positive Matrix Factorization (PMF) and Principal Component Analysis-Absolute Principal Component Scores (PCA-APCS), UNMIX, and multi-linear engine (ME) (Cao et al., 2005; Hu et al., 2010; Li et al., 2013c; Sun et al., 2012a, 2013; Zhang et al., 2014a). The application of CMB requires locally determined and quantitative knowledge of the emission source profiles. Given that the source profiles are used as inputs to CMB, it has the potential to separate sources clearly but is unable to identify unknown sources and secondary aerosols. On the contrary, PMF and PCA do not require known source profiles but are based on tracer species, e.g., those listed in Table 8 (Paatero and Tapper, 1994; Viana et al., 2008; Xu et al., 2016). These methods have the disadvantage that the interpretation of sources is often subjective as one tracer probably comes from more than one emission source, and that they are unable to separate the contribution from sources that covary in time. Hopke (2015) suggested that PCA is not really a receptor model, because it cannot provide an apportionment of the pollutants to the source. Absolute principal components analysis (APCA) was used by Thurston and Spengler (1985), which can provide a mass apportionment but the limitation of this model is that it does not consider the uncertainties of values of inputted variables. Mass spectrometric, online techniques, such as AMS, have merit for detecting the chemical processing of OA due to the output data carrying much chemical information and mass sensitivity (Xu et al., 2016). As mentioned above, AMS instruments have been widely used for PM_1 analysis and PMF analysis frequently conducted on the mass spectra (m/z 12–150) measured with AMS instruments to identify major organic components. For example, Sun et al. (2013) and Zhang et al. (2014a) divided the organic aerosol into five components by PMF, including low-volatility and semi-volatile oxygenated organic aerosol (LV-OOA and SV-OOA) that represents SOA, a hydrocarbon-like OA (HOA) that refers to POA related with urban emissions, a coal combustion OA (CCOA), and a cooking-emitted OA (COA). In addition, radiocarbon ^{14}C analysis combined with organic tracers is used to improve the direct differentiation of fossil fuel (FF) sources from modern carbon sources (non-fossil fuel, NF) (Liu et al., 2013; Sun et al., 2012a).

5.2. Source contribution of POA

Results of receptor modelling of OAs in China are summarized in Table 12 and Fig. 6. About 60–80% of total OA was apportioned. Shown in Fig. 6, Feng et al. (2006) and Wang et al. (2009a) used a CMB model to estimate the contributions of seven sources (diesel/gasoline vehicles, coal burning, kitchen emission, vegetative detritus, cigarette smoke, biomass burning and other OC, usually taken to be SOC) to particulate organic matter in $PM_{2.5}$. In Hong Kong, OC was dominated by the primary sources with 74% in locally influenced samples but the secondary sources were dominant in samples deriving from regional air masses with approximately 50–60% of OC (Li et al., 2013c). In Fig. 7, Liu et al. (2017a) have combined ^{14}C analysis with unique molecular organic tracers to apportion winter carbonaceous aerosols in 10 cities of China, resulting in the proportions of different carbon fractions as shown in Fig. 7. It includes EC_{bb} (biomass burning-derived EC), EC_f (fossil fuel combustion derived EC), POC_{bb} (biomass burning-derived primary OC), POC_f (fossil fuel combustion derived POC), SOC_{nf} (non-fossil fuel derived SOC), and SOC_f (fossil fuel-derived SOC). On average, the largest contributor of carbonaceous aerosols was the SOC_{nf}, which represented 46%, followed by SOC_f (16%), POC_{bb} (13%), POC_f (12%), EC_f (7%), and EC_{bb} (6%). Therefore, the SOC (62%) in carbonaceous

aerosols sampled in winter in China was higher than the proportion of POC.

In Beijing, the seasonal trend in traffic-generated organic aerosols obtained by CMB models is unclear, but AMS-PMF showed an obvious diurnal trend with two distinct peaks corresponding to rush hours around 7:00–9:00 a.m. and 7:00–9:00 p.m. (Cheng et al., 2013a; Song et al., 2007; Zheng et al., 2005). For instance, Zheng et al. (2005) estimated that the contribution of vehicle emissions in Beijing is higher in autumn (6.73 $\mu g/m^3$, 26% of OA) but lower in winter (3.11 $\mu g/m^3$, 11.9% of OA) in 2000, which was attributed to reduced outdoor activities under cold synoptic conditions. By contrast, Cheng et al. (2013a) reported a higher level of OA derived from vehicle emissions in spring (18.5%) and lower in winter (9%) in 2012, which was attributed to relatively lower emissions from other sources (e.g., power plants and biomass burning) in spring. On the basis of isotopic and other analyses, Sun et al. (2012a) and Zhang et al. (2010) estimated that vehicular emissions are the most important contributor to the fossil source in the summer, but coal combustion dominates in the winter in Beijing. Traffic-related AMS hydrocarbon-like organic aerosol (HOA) and EC displayed two peaks corresponding to morning and evening traffic rush hours in Beijing, and the highest concentration maintained at midnight due to more heavy-duty vehicles and a lower mixed layer height (Ji et al., 2016; Xu et al., 2016). Feng et al. (2006) reported that the spatial distribution of hopanes is similar to that of engine exhaust. That study also found that the concentration of hopanes at an urban site (16.1 ng/m^3) is higher than that at a rural site (12 ng/m^3) in Shanghai. This is consistent with the results in Beijing, Pearl River Delta Region, Hebei and Tianjin (Cai and Xie, 2007; Cao et al., 2003a; Wang et al., 2009a).

Coal combustion is shown by AMS to be a significant source of $PM_{2.5}$ organic aerosols that contributes 52% of OA during haze periods in Beijing (Elser et al., 2016). As shown in Table 12, coal combustion OA (CCOA) comprised of 33% of OA and 17% of non-refractory submicrometer aerosol (NR-PM_1) in the winter (Sun et al., 2013). In contrast, it contributes little to OA in the summer (10%) in 2011 in Beijing (Sun et al., 2015). This is due to the intensified emissions from coal combustion during the heating season. However, 15% of the OC came from coal combustion in Shanghai outside the heating season, suggesting that coal usage there mainly comes from industry (Fig. 6).

Regarding the diurnal trends in summer, the CCOA showed the highest values at midnight (18 $\mu g/m^3$) and lowest in the morning (approximately 7 $\mu g/m^3$). This trend was explained by the higher humidity at night that promotes transfer of the semi-volatile water-soluble organic aerosols from the gas phase to the particle phase (Sun et al., 2012b). A similar conclusion is drawn by Xu et al. (2016). Liu et al. (2017a) reported that industrial coal combustion and biomass burning are the main contributors to OAs in northern China and vehicle exhaust has a greater impact in south and central China from ^{14}C analysis (Fig. 7).

Biomass burning is a significant primary source of organic particles, accounting for 18–38% of the fine OA (Streets et al., 2003; Wang et al., 2007; Zhang et al., 2008a). In Beijing, biomass burning was an important contributor to OA (26.1%) in the winter, but only accounted for about 10% of OAs in the summer (Fig. 6). Levoglucosan exhibits season-dependent characteristics with highest concentrations (around 806 ng/m^3) in fall and winter, but lowest levels in summer (Zhang et al., 2008b). This conclusion is consistent with the analysis of organic aerosols in Beijing by the ^{14}C technique (Yang et al., 2005). Duan et al. (2004) compared the contribution of biomass burning to OC between background and urban sites, and reported that a nearly double contribution of biomass burning was found in the background area (53%) compared to the urban area (28.3%).

The contribution of cooking emissions to the OA did not vary greatly between seasons. For instance, Wang et al. (2009a) estimated the contributions of cooking emissions to ambient OA in summer and winter in Beijing, were 7.7 $\mu g/m^3$ (accounting for 23.8% of OA) and 8.0 $\mu g/m^3$ (17.3% of OA) in 2007, respectively. There is approximately

Table 12
Results of source apportionment (SA %) with different receptor models in some cities.

Study areas	Sampling time	Method of SA	OC conc. µg/m³	Biomass burning	Coal combustion	Gasoline exhaust	Diesel exhaust	Cooking	SOA	Others	Reference
Beijing	Spring, 2013	PCA	8	62.9[2]			12.6			24.5	Wang et al. (2015a)
Beijing	Summer, 2012	PCA	8.2	14.6	16.6	38.2	24.8			5.8	
Beijing	Fall, 2012	PCA	10	42.5	29.4		25.3				
Beijing	Winter, 2012	PCA	31	64			22.4				
Sanya[1]	Winter, 2012	PMF	3.4	23.2	22.6	37.9				23.2	Wang et al. (2015b)
Sanya[1]	summer, 2013	PCA	3.2	20		59.8		13.8			
Sanya	Winter, 2012	PCA	3.4	9.7		75.6	7.2			1.6	
Guangzhou[1]	winter, 2009	PMF			31	58	11				Gao et al. (2013)
Xi'an	fall, 2003	PCA	45.1	4		73	23				Cao et al. (2005)
Xi'an	winter, 2003	PCA	74.2	9	44	44	3				
Tianjin	2008	PCA	16.9	9.3	14.6	47.6	2.1		61.7		Gu et al. (2010)
Hongkong	Summer-regional day, 2006	PMF	10.4	21.5		9.2			65	3.4	Hu et al. (2010)
Hongkong	Summer-local day, 2007	PMF	2.86	16.1		46.9			25	11.5	
Beijing	winter-haze day, 2013	PMF-AMS	103	13.8	46.8	8.6		5.8	25		Elser et al. (2016)
Beijing	winter-normal day, 2013	PMF-AMS	42	8.9	55.2	8.7%		11.5	15.7		
Xi'an	winter-haze day, 2013	PMF-AMS	216	43.4	5.7	16		3.6	31.3		
Xi'an	winter-normal day, 2013	PMF-AMS	76	42.2	14.1	18.3		9.3	16.2		
Beijng[3]	Winter, 2011	PMF-AMS			33	17		19	31		Sun et al. (2013)
Lanzhou[3]	Winter	PMF-AMS	29.3	10.8	22	9.8		20.2	37.2		Xu et al. (2016)

1. Source apportionment for PAH; 2. Including biomass burning, coal combustion and gasoline; 3. Results from PM$_1$.

14.5% of OA that was accounted for by the organic species in the cooking emissions (Zhao et al., 2015b). Based on the PMF-AMS technique, Sun et al. (2013) have found that its contribution to OA in PM$_1$ is 19% with the highest values of 32% during lunch and dinner time and the lowest of 11% in late afternoon during winter in Beijing. This number is approximately 20% in OA in Lanzhou province during summer with an average concentration of 5.86 µg/m³ (Xu et al., 2016).

In addition, COA on average increased to 36% in clean periods, suggesting that COA plays a significant role as a local emission source of OA (Sun et al., 2012b, 2013).

Natural POA derives from disintegration of bulk plant material, humic acid in soil dust and the presence of viable biological microbes like viruses, bacteria and fungal spores, which have sizes ranging from 1 nm to 300 µm. In rural areas, the concentration of organic aerosols
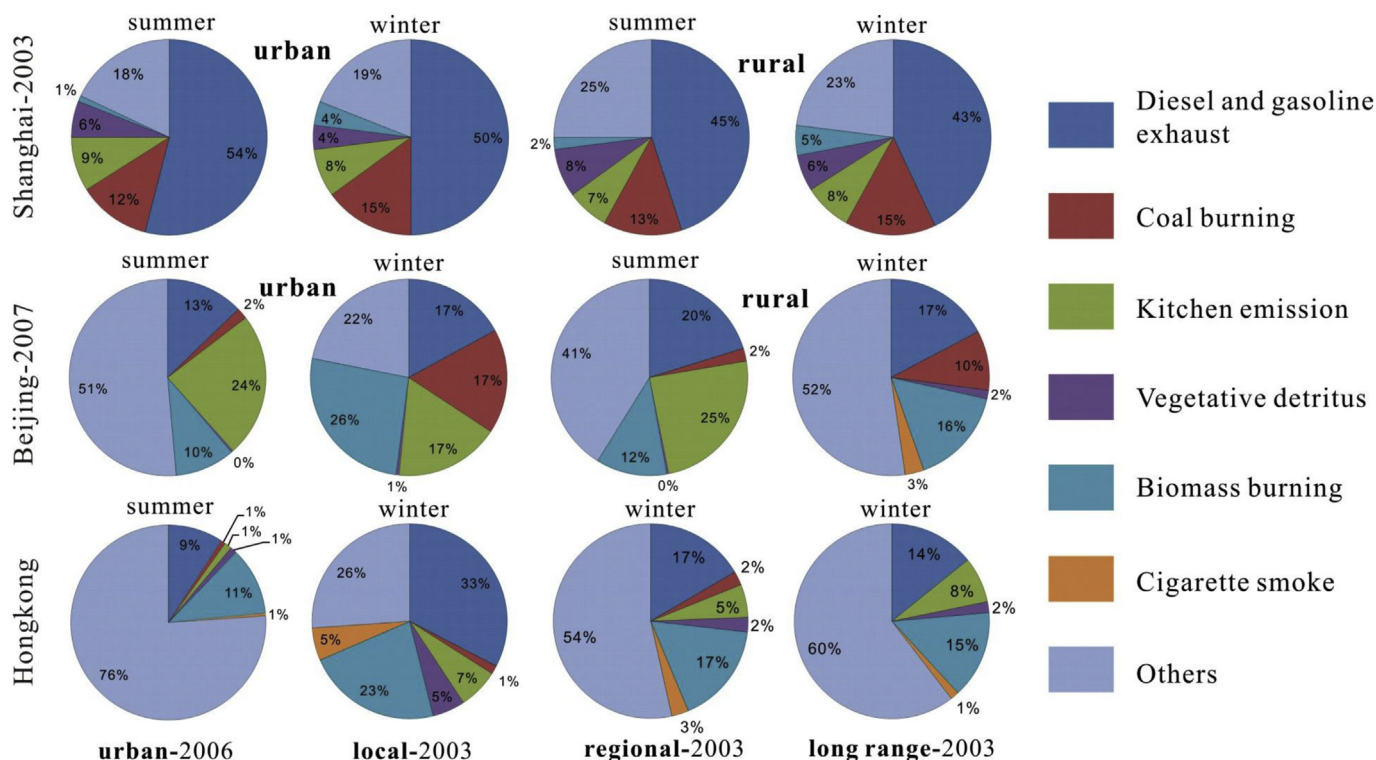

Fig. 6. Summary of CMB apportioned source contributions to OC in PM$_{2.5}$ in Shanghai (Feng et al., 2006), Beijing (Wang et al., 2009a; Zheng et al., 2005), and Hongkong (Hu et al., 2010; Li et al., 2013c).
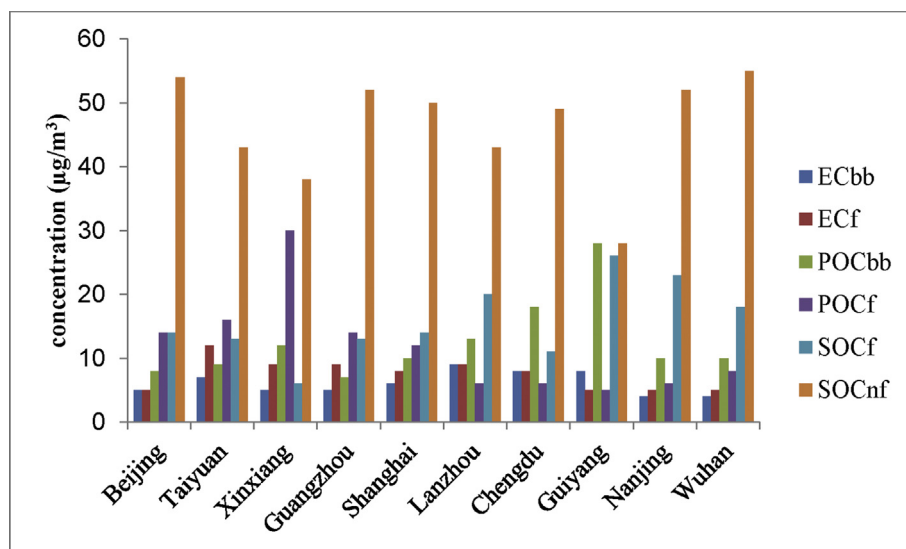
Fig. 7. Proportions of different carbon fractions for 10 urban cities during early winter in 2013 (Liu et al., 2017a): (bb: biomass burning; f: fossil fuels; nf: non-fossil fuel).

was influenced by larger biological particles, whereas in the urban area it shows a higher proportion of smaller particles. The sugar and sugar alcohols are excellent tracers for quantification of microbial activity, including pollen, fungi and bacteria. The total concentration of these is $203 \pm 63 \, \text{ng/m}^3$ at a suburban site and $142 \pm 54 \, \text{ng/m}^3$ at an urban site, indicating an enhanced biological contribution at the suburban site (Fu et al., 2012; Yang et al., 2016). Wang et al. (2009a) found that vegetative detritus is also present in air, contributing 0.3% in summer and 0.5% in winter. Some studies have hypothesized the possibility of marine phytoplankton or sea-salt aerosol as potential source for OA, because marine phytoplankton can emit unsaturated fatty acids into the air while sea-salt aerosols may have an organic component from scavenging of surface active material from seawater (Jacobson et al., 2000; Yang et al., 2016). Fu et al. (2013) studied the organic aerosols over the Arctic Ocean based on a tracer-method and found that primary saccharides were dominant compounds in the marine OA, reaching up to $24.5 \, \text{ng/m}^3$.

5.3. Estimation of SOA

It is impossible to measure the concentration of SOC directly due to its complexity. Therefore, both EC-tracer and SOA-tracer methods are used to estimate the contribution of SOC to the organic aerosols. The EC-tracer method is based on the hypothesis that the EC comes from POA and the POC/EC ratio in POA is relatively constant. Using it, the SOC is calculated as follows:

$$OC_{sec} = OC - \left(\frac{POC}{EC}\right) * EC$$

Where OC_{sec} is the ambient secondary organic carbon and (POC/EC) is the ratio of primary aerosols. The determination of the POC/EC ratio is crucial, because it varies between different sources and can be affected by meteorological conditions. Previous studies have estimated this ratio during periods when SOA is very low, such as during winter, morning traffic periods with low solar radiation, under low ozone concentrations, and without rain and cloud events (Lim and Turpin, 2002). Generally, the OC/EC in the lowest 5–10% of values, or below the threshold of 2.9 was used by Li et al. (2015b).

The SOA tracer based approach to estimation of SOA was first used by Kleindienst et al. (2007), who reported the mass fraction of the SOA (fsoa) on the basis of chamber simulations. It is defined as

$$f_{soa} = \frac{\sum_i [\text{tracers}]}{[\text{SOA}]}$$

Where the $\sum$ [tracers] is the sum of field measured SOA tracers derived from a certain individual or group of precursors, i, and [SOA] is the mass concentration of SOA derived from those precursors. A comparison by Ding et al. (2012) of the EC-tracer and SOA tracer methods showed very poor agreement in fall-winter, but relatively good in summer.

Using a tracer-based method, Fu et al. (2010) found that SOA tracers were formed during long range atmospheric transport due to unclear diurnal variations and estimated that the concentration of biogenic SOA is $2.6 \, \mu\text{g C/m}^3$, accounting for 10% of OA in East China in the summer. It differs between Beijing (4.4%) and Hong Kong (30%) in the same season due to the different geographical locations with different meteorological conditions, local vegetation cover, and oxidant levels (Hu et al., 2008; Yang et al., 2016). For example, the BSOA measured in Hong Kong is affected by regional sources due to the land-sea breeze circulation which advects the pollutants from the PRD. Using an air quality modeling system (WRF/Chem) coupled with an SOA model, Jiang et al. (2012) found that anthropogenic sources accounted for 35% of total SOA over China in 2006, with 41%, 26%, 39% and 59% in spring, summer, autumn and winter, respectively. Subsequently, Hu et al. (2016) studied the distribution of SOA in the whole country in 2013 by a revised Community Multiscale Air Quality model with updated SOA yields, resulting in estimates of the contribution of biogenic SOA of 75% in summer, 50–60% in autumn and spring, and 24% in winter. Some other simulations of SOA over China have found that 65%–85% of SOA in southern China comes from biogenic precursors (Han et al., 2008; Jiang et al., 2012; Li et al., 2013b).

6. Conclusion and recommendations

The main primary sources of organic and elemental carbon aerosols account for 30–50% of $PM_{2.5}$ in China. Motor vehicle emissions contribute 13–50% of OC, especially high in megacities, which is reflected in OC/EC ratios or AMS measurements. Industrial emissions are major contributors in developed regions, like the PRD region, Shanghai and Zhejiang. 70% of rural energy derives from combustion of crop residues, and biomass burning has been considered as a dominant source of OA (accounting for 18–38%). Also, food cooking and coal combustion are reported as significant sources, whose contribution to OA is approximately 20% and 25% respectively. Secondary organic aerosol,

averaged across China, derived from biogenic precursors accounts for 24–75% of total SOA, while estimates of the anthropogenic fraction are from 25-76%.

From the review above, there are some remaining issues that need to be addressed:

1. Further indicative tracers for SOA precursors need to be developed towards a comprehensive characterization of SOA sources in the field due to the complexity of SOA composition;
2. More effort should be given to improving comprehension of SOA formation mechanisms, especially during haze episodes in China;
3. The source profiles available for use in CMB models are limited, and represent some typical emission sources of OA, but do not contain comprehensive information on all relevant sources;
4. The inventory of OA emissions needs refinement of estimates and extension to include all sources. For example, the emissions from cooking are highly variable and influenced by the style and conditions of cooking;
5. Although receptor modeling for source apportionment is an effective method to calculate the contribution of different sources, differences in the results from different models need to be reconciled.

Acknowledgement

Appendix A. Supplementary data

Supplementary data related to this article can be found at http://dx.doi.org/10.1016/j.atmosenv.2018.06.025.

References

Aiken, A.C., Decarlo, P.F., Kroll, J.H., Worsnop, D.R., Huffman, J.A., Docherty, K.S., Ulbrich, I.M., Mohr, C., Kimmel, J.R., Sueper, D., 2008. O/C and OM/OC ratios of primary, secondary, and ambient organic aerosols with high-resolution time-of-flight aerosol mass spectrometry. Environ. Sci. Technol. 42, 4478–4485.

Alam, M.S., Harrison, R.M., 2016. Recent advances in the application of 2-dimensional gas chromatography with soft and hard ionisation time-of-flight mass spectrometry in environmental analysis. Chem. Sci. 7, 3968–3977.

Alam, M.S., Stark, C., Harrison, R.M., 2016. Using variable ionisation energy time-of-flight mass spectrometry with comprehensive GC×GC to identify isomeric species. Anal. Chem. 88, 4211–4220.

Baltensperger, U., Kalberer, M., Dommen, J., Paulsen, D., Alfarra, M.R., Coe, H., Fisseha, R., Gascho, A., Gysel, M., Nyeki, S., Sax, M., Steinbacher, M., Prevot, A.S.H., Sjögren, S., Weingartner, E., Zenobi, R., 2005. Secondary organic aerosols from anthropogenic and biogenic precursors. Faraday Discuss 130, 265–278.

Bautista, A.T., Pabroa, P.C.B., Santos, F.L., Quirit, L.L., Asis, J.L.B., Dy, M.A.K., Martinez, J.P.G., 2015. Intercomparison between NIOSH, IMPROVE_A, and EUSAAR_2 protocols: finding an optimal thermal–optical protocol for Philippines OC/EC samples. Atmos. Pollut. Res. 6, 334–342.

Bi, X., Sheng, G., Peng, P.a, Zhang, Z., Fu, J., 2002. Extractable organic matter in PM_{10} from LiWan district of Guangzhou city, PR China. Sci. Total Environ. 300, 213–228.

Bi, X., Sheng, G., Peng, P.a, Chen, Y., Fu, J., 2005. Size distribution of n-alkanes and polycyclic aromatic hydrocarbons (PAHs) in urban and rural atmospheres of Guangzhou, China. Atmos. Environ. 39, 477–487.

Birch, M., Cary, R., 1996. Elemental carbon-based method for monitoring occupational exposures to particulate diesel exhaust. Aerosol. Sci. Technol. 25, 221–241.

Birch, M.E., 1998. Analysis of carbonaceous aerosols: interlaboratory comparison. Analyst 123, 851–857.

Bond, T.C., Covert, D.S., Kramlich, J.C., Larson, T.V., Charlson, R.J., 2002. Primary particle emissions from residential coal burning: optical properties and size distributions. J. Geophys. Res.: Atmosphere 107, D21,. http://dx.doi.org/10.1029/2001JD000571.

Bressi, M., Sciare, J., Ghersi, V., Bonnaire, N., Nicolas, J., Petit, J.-E., Moukhtar, S., Rosso, A., Mihalopoulos, N., Féron, A., 2013. A one-year comprehensive chemical characterisation of fine aerosol (PM) at urban, suburban and rural background sites in the region of Paris (France). Atmos. Chem. Phys. 13, 7825–7844.

Cai, H., Xie, S., 2007. Estimation of vehicular emission inventories in China from 1980 to 2005. Atmos. Environ. 41, 8963–8979.

Cai, T., Zhang, Y., Fang, D., Shang, J., Zhang, Y., Zhang, Y., 2017. Chinese vehicle emissions characteristic testing with small sample size: results and comparison.

Atmos. Pollut. Res. 8, 154–163.

Canagaratna, M., Jayne, J., Jimenez, J., Allan, J., Alfarra, M., Zhang, Q., Onasch, T., Drewnick, F., Coe, H., Middlebrook, A., 2007. Chemical and microphysical characterization of ambient aerosols with the aerodyne aerosol mass spectrometer. Mass Spectrom. Rev. 26, 185–222.

Cao, J., Lee, S., Ho, K., Zhang, X., Zou, S., Fung, K., Chow, J.C., Watson, J.G., 2003a. Characteristics of carbonaceous aerosol in Pearl River Delta region, China during 2001 winter period. Atmos. Environ. 37, 1451–1460.

Cao, J., Lee, S., Ho, K., Zou, S., Zhang, X., Pan, J., 2003b. Spatial and seasonal variations of isoprene secondary organic aerosol in China: significant impact of biomass burning during winter. China Particuol. 1, 33–37.

Cao, J.J., Lee, S.C., Ho, K.F., Zou, S.C., Fung, K., Li, Y., Watson, J.G., Chow, J.C., 2004. Spatial and seasonal variations of atmospheric organic carbon and elemental carbon in Pearl River Delta Region, China. Atmos. Environ. 38, 4447–4456.

Cao, J., Wu, F., Chow, J., Lee, S., Li, Y., Chen, S., An, Z., Fung, K., Watson, J., Zhu, C., 2005. Characterization and source apportionment of atmospheric organic and elemental carbon during fall and winter of 2003 in Xi'an, China. Atmos. Chem. Phys. 5, 3127–3137.

Cao, G., Zhang, Xiaoye, Zheng, Fangcheng, 2006. Inventory of black carbon and organic carbon emissions from China. Atmos. Environ. 40, 6516–6527.

Cao, J.J., Lee, S.C., Chow, J.C., Watson, J.G., Ho, K.F., Zhang, R.J., Jin, Z.D., Shen, Z.X., Chen, G.C., Kang, Y.M., Zou, S.C., Zhang, L.Z., Qi, S.H., Dai, M.H., Cheng, Y., Hu, K., 2007. Spatial and seasonal distributions of carbonaceous aerosols over China. J. Geophys. Res. 112, D22S11. http://dx.doi.org/10.1029/2006JD008205.

Cao, J.J., Wang, Q.-Y., Chow, J.C., Watson, J.G., Tie, X.-X., Shen, Z.-X., Wang, P., An, Z.-S., 2012. Impacts of aerosol compositions on visibility impairment in Xi'an, China. Atmos. Environ. 59, 559–566.

Cao, J.-J., Zhu, C.-S., Tie, X.-X., Geng, F.-H., Xu, H.-M., Ho, S.S.H., Wang, G.-H., Han, Y.-M., Ho, K.-F., 2013. Characteristics and sources of carbonaceous aerosols from Shanghai, China. Atmos. Chem. Phys. 13, 803–817.

Cao, F., Zhang, Y., Ren, L., Liu, J., Li, J., Zhang, G., Liu, D., Sun, Y., Wang, Z., Shi, Z., 2017. New insights into the sources and formation of carbonaceous aerosols in China: potential applications of dual carbon isotopes. Nat. Sci. Rev. 0, 1–3. http://dx.doi.org/10.1093/nsr/nwx097.

Castro, L., Pio, C., Harrison, R.M., Smith, D., 1999. Carbonaceous aerosol in urban and rural European atmospheres: estimation of secondary organic carbon concentrations. Atmos. Environ. 33, 2771–2781.

Cavalli, F., Viana, M., Yttri, K.E., Genberg, J., Putaud, J.-P., 2010. Toward a standardised thermal-optical protocol for measuring atmospheric organic and elemental carbon: the EUSAAR protocol. Atmos. Meas. Tech 3, 79–89.

Chan, C.K., Yao, X., 2008. Air pollution in mega cities in China. Atmos. Environ. 42, 1–42.

Chang, Y., Zou, Z., Deng, C., Huang, K., Collett Jr., J., Lin, J., Zhuang, G., 2016. The importance of vehicle emissions as a source of atmospheric ammonia in the megacity of Shanghai. Atmos 16, 3577–3594.

Chang, Y., Deng, C., Cao, F., Cao, C., Zou, Z., Liu, S., Lee, X., Li, J., Zhang, G., Zhang, Y., 2017. Assessment of carbonaceous aerosols in Shanghai, China–Part 1: long-term evolution, seasonal variations, and meteorological effects. Atmos. Chem. Phys. 17, 9945.

Chauhan, A., Goyal, M.K., Chauhan, P., 2014. GC-MS technique and its analytical applications in science and technology. J. Anal. Bioanal. Tech. 5 (6). http://dx.doi.org/10.4172/2155-9872.1000222.

Chen, Y., Sheng, G., Bi, X., Feng, Y., Mai, B., Fu, J., 2005. Emission factors for carbonaceous particles and polycyclic aromatic hydrocarbons from residential coal combustion in China. Environ. Sci. Technol. 39, 1861–1867.

Chen, Y., Zhi, G., Feng, Y., Fu, J., Feng, J., Sheng, G., Simoneit, B.R., 2006. Measurements of emission factors for primary carbonaceous particles from residential raw-coal combustion in China. Geophys. Res. Lett. 33, L20815. http://dx.doi.org/10.1029/2006GL026966.

Chen, K., Yin, Y., Wei, Y., Yang, W., 2010. Characteristics of carbonaceous aerosols in $PM_{2.5}$ in Nanjing. China Environ. Sci. 30, 1015–1020.

Chen, Y., Xie, S., Luo, B., Zhai, C., 2014. Characteristics and origins of carbonaceous aerosol in the Sichuan Basin, China. Atmos. Environ. 94, 215–223.

Chen, D., Cui, H., Zhao, Y., Yin, L., Lu, Y., Wang, Q., 2016. A Two-year Study of Carbonaceous Aerosols in Ambient $PM_{2.5}$, at a Regional Background Site for Western Yangtze River Delta. China, vol. 183. pp. 351–361.

Chen, J., Li, C., Ristovski, Z., Milic, A., Gu, Y., Islam, M.S., Wang, S., Hao, J., Zhang, H., He, C., 2017. A review of biomass burning: emissions and impacts on air quality, health and climate in China. Sci. Total Environ. 579, 1000–1034.

Cheng, Y., Lee, S., Ho, K., Chow, J., Watson, J., Louie, P., Cao, J., Hai, X., 2010. Chemically-speciated on-road $PM_{2.5}$ motor vehicle emission factors in Hong Kong. Sci. Total Environ. 408, 1621–1627.

Cheng, Y., Zheng, M., He, K.-b, Chen, Y., Yan, B., Russell, A.G., Shi, W., Jiao, Z., Sheng, G., Fu, J., 2011. Comparison of two thermal-optical methods for the determination of organic carbon and elemental carbon: results from the southeastern United States. Atmos. Environ. 45, 1913–1918.

Cheng, S., Lang, J., Zhou, Y., Han, L., Wang, G., Chen, D., 2013a. A new monitoring-simulation-source apportionment approach for investigating the vehicular emission contribution to the $PM_{2.5}$ pollution in Beijing, China. Atmos. Environ. 79, 308–316.

Cheng, Y., Engling, G., He, K.-B., Duan, F.-K., Ma, Y.-L., Du, Z.-Y., Liu, J.-M., Zheng, M., Weber, R.J., 2013b. Biomass burning contribution to Beijing aerosol. Atmos. Chem. Phys. 13, 7765–7781.

Chesselet, R., Fontugne, M., Buat-Ménard, P., Ezat, U., Lambert, C., 1981. The origin of particulate organic carbon in the marine atmosphere as indicated by its stable carbon isotopic composition. Geophys. Res. Lett. 8, 345–348.

Chi, Y.Q., Xie, S.D., 2012. Spatiotemporal inventory of biogenic volatile organic compound emissions in China based on vegetation volume and production. Adv. Mater.

Res. 356-360, 2579–2582. 10.4028. www.scientific.net/AMR.356-360.2579.

Chow, J.C., Watson, J.G., Pritchett, L.C., Pierson, W.R., Frazier, C.A., Purcell, R.G., 1993. The DRI thermal/optical reflectance carbon analysis system: description, evaluation and applications in US air quality studies. Atmos. Environ. 27, 1185–1201.

Chow, J.C., Watson, J.G., Crow, D., Lowenthal, D.H., Merrifield, T., 2001. Comparison of IMPROVE and NIOSH carbon measurements. Aerosol Sci. Technol. 34, 23–34.

Chow, J.C., Watson, J.G., Chen, L.-W.A., Arnott, W.P., Moosmüller, H., Fung, K., 2004. Equivalence of elemental carbon by thermal/optical reflectance and transmittance with different temperature protocols. Environ. Sci. Technol. 38, 4414–4422.

Claeys, M., Graham, B., Vas, G., Wang, W., Vermeylen, R., Pashynska, V., Cafmeyer, J., Guyon, P., Andreae, M.O., Artaxo, P., 2004. Formation of secondary organic aerosols through photooxidation of isoprene. Science 303, 1173–1176.

Cui, H., Mao, P., Zhao, Y., Nielsen, C.P., Zhang, J., 2015. Patterns in atmospheric carbonaceous aerosols in China: emission estimates and observed concentrations. Atmos. Chem. Phys. 15, 8657–8678.

Cui, M., Chen, Y., Tian, C., Zhang, F., Yan, C., Zheng, M., 2016. Chemical composition of $PM_{2.5}$ from two tunnels with different vehicular fleet characteristics. Sci. Total Environ. 550, 123–132.

Cui, M., Chen, Y., Feng, Y., Li, C., Zheng, J., Tian, C., Yan, C., Zheng, M., 2017. Measurement of PM and its chemical composition in real-world emissions from non-road and on-road diesel vehicles. Atmos. Chem. Phys. 17, 6779–6795.

Dai, S., Bi, X., Chan, L., He, J., Wang, B., Wang, X., Peng, P., Sheng, G., Fu, J., 2015. Chemical and stable carbon isotopic composition of $PM_{2.5}$ from on-road vehicle emissions in the PRD region and implications for vehicle emission control policy. Atmos. Chem. Phys. 15, 3097–3108.

Dan, M., 2004. The characteristics of carbonaceous species and their sources in $PM_{2.5}$ in Beijing. Atmos. Environ. 38, 3443–3452.

de Gouw, J., Jimenez, J.L., 2009. Organic aerosols in the Earth's atmosphere. Environ. Sci. Technol. 43, 7614–7618.

DeCarlo, P.F., Kimmel, J.R., Trimborn, A., Northway, M.J., Jayne, J.T., Aiken, A.C., Gonin, M., Fuhrer, K., Horvath, T., Docherty, K.S., 2006. Field-deployable, high-resolution, time-of-flight aerosol mass spectrometer. Anal. Chem. 78, 8281–8289.

Dentener, F.J., Crutzen, P.J., 1993. Reaction of N_2O_5 on tropospheric aerosols: impact on the global distributions of NO_x, O_3, and OH. J. Geophys. Res.: Atmosphere 98 (D4), 7149–7163.

Ding, X., Wang, X.-M., Zheng, M., 2011. The influence of temperature and aerosol acidity on biogenic secondary organic aerosol tracers: observations at a rural site in the central Pearl River Delta region, South China. Atmos. Environ. 45, 1303–1311.

Ding, X., Wang, X.-M., Gao, B., Fu, X.-X., He, Q.-F., Zhao, X.-Y., Yu, J.-Z., Zheng, M., 2012. Tracer-based estimation of secondary organic carbon in the Pearl River Delta, south China. J. Geophys. Res.: Atmosphere 117, D05313. http://dx.doi.org/10.1029/2011JD016596.

Deng, W., Hu, Q., Liu, T., Wang, X., Zhang, Y., Ding, X., Sun, Y., Ni, X., Yu, J., Yang, W., Huang, X., Zhang, Z., Huang, Z., He, Q., Mellouki, A., George, C., 2016. Chamber simulation on the formation of secondary organic aerosols (SOA) from diesel vehicle exhaust in China. Atmos. Chem. Phys. Discuss. http://dx.doi.org/10.5194/acp-2016-50.

Drewnick, F., Hings, S.S., DeCarlo, P., Jayne, J.T., Gonin, M., Fuhrer, K., Weimer, S., Jimenez, J.L., Demerjian, K.L., Borrmann, S., 2005. A new time-of-flight aerosol mass spectrometer (TOF-AMS)—instrument description and first field deployment. Aerosol Sci. Technol. 39, 637–658.

Du, Z., He, K., Cheng, Y., Duan, F., Ma, Y., Liu, J., Zhang, X., Zheng, M., Weber, R., 2014. A yearlong study of water-soluble organic carbon in Beijing I: sources and its primary vs. secondary nature. Atmos. Environ. 92, 514–521.

Duan, F., Liu, Xiande, Yu, Tong, Cachier, Hélène, 2004. Identification and estimate of biomass burning contribution to the urban aerosol organic carbon concentrations in Beijing. Atmos. Environ. 38, 1275–1282.

Duan, J., Tan, J., Cheng, D., Bi, X., Deng, W., Sheng, G., Fu, J., Wong, M.H., 2007. Sources and characteristics of carbonaceous aerosol in two largest cities in Pearl River Delta Region, China. Atmos. Environ. 41, 2895–2903.

Elser, M., Huang, R.-J., Wolf, R., Slowik, J.G., Wang, Q., Canonaco, F., Li, G., Bozzetti, C., Daellenbach, K.R., Huang, Y., Zhang, R., Li, Z., Cao, J., Baltensperger, U., El-Haddad, I., Prévôt, A.S.H., 2016. New insights into PM2.5 chemical composition and sources in two major cities in China during extreme haze events using aerosol mass spectrometry. Atmos. Chem. Phys. 16, 3207–3225.

Emanuelsson, E.U., Hallquist, M., Kristensen, K., Glasius, M., Bohn, B., Fuchs, H., Kammer, B., Kiendler-Scharr, A., Nehr, S., Rubach, F., Tillmann, R., Wahner, A., Wu, H.C., Mentel, T.F., 2013. Formation of anthropogenic secondary organic aerosol (SOA) and its influence on biogenic SOA properties. Atmos. Chem. Phys. 13, 2837–2855.

Fairbaugh, C., 2015. Methods of Collecting and Separating Atmospheric Organic Aerosols for Analysis Using Two-dimensional Gas and Liquid Chromatography with Mass Spectrometry. BSc thesis. Portland State University.

Feng, J.C., C, K., Fang, M., Hu, M., He, L., Tang, X., 2006. Characteristics of organic matter in $PM_{2.5}$ in Shanghai. Chemosphere 64, 1393–1400.

Feng, Y., Chen, Y., Guo, H., Zhi, G., Xiong, S., Li, J., Sheng, G., Fu, J., 2009. Characteristics of organic and elemental carbon in $PM_{2.5}$ samples in Shanghai, China. Atmos. Res. 92, 434–442.

Feng, J., Li, M., Zhang, P., Gong, S., Zhong, M., Wu, M., Zheng, M., Chen, C., Wang, H., Lou, S., 2013. Investigation of the sources and seasonal variations of secondary organic aerosols in $PM_{2.5}$ in Shanghai with organic tracers. Atmos. Environ. 79, 614–622.

Feng, J., Hu, J., Xu, B., Hu, X., Sun, P., Han, W., Gu, Z., Yu, X., Wu, M., 2015. Characteristics and seasonal variation of organic matter in $PM_{2.5}$ at a regional background site of the Yangtze River Delta region, China. Atmos. Environ. 123, 288–297.

Feng, T., Li, G., Cao, J., Bei, N., Shen, Z., Zhou, W., Liu, S., Zhang, T., Wang, Y., Tie, X., Molina, L.T., 2016. Simulations of organic aerosol concentrations during springtime in the Guanzhong basin, China. Atmos. Chem. Phys. Discuss. 16, 10045–10061.

Fraser, M., Yue, Z., Buzcu, B., 2003. Source apportionment of fine particulate matter in Houston, TX, using organic molecular markers. Atmos. Environ. 37, 2117–2123.

Fu, P., Kawamura, K., Okuzawa, K., Aggarwal, S.G., Wang, G., Kanaya, Y., Wang, Z., 2008. Organic molecular compositions and temporal variations of summertime mountain aerosols over Mt. Tai, North China Plain. J. Geophys. Res. 113, D19107. http://dx.doi.org/10.1029/2008JD009900.

Fu, P., Kawamura, K., Chen, J., Barrie, L.A., 2009. Isoprene, monoterpene, and sesquiterpene oxidation products in the high Arctic aerosols during late winter to early summer. Environ. Sci.Techn 43, 4022–4028.

Fu, P., Kawamura, K., Kanaya, Y., Wang, Z., 2010. Contributions of biogenic volatile organic compounds to the formation of secondary organic aerosols over Mt. Tai, Central East China. Atmos. Environ. 44, 4817–4826.

Fu, P., Kawamura, K., Kobayashi, M., Simoneit, B.R., 2012. Seasonal variations of sugars in atmospheric particulate matter from Gosan, Jeju Island: significant contributions of airborne pollen and Asian dust in spring. Atmos. Environ. 55, 234–239.

Fu, P.Q., Kawamura, K., Chen, J., Charrière, B., Sempéré, R., 2013. Organic molecular composition of marine aerosols over the Arctic Ocean in summer: contributions of primary and secondary aerosol formation. Biogeosciences 10, 653–667.

Fuzzi, S., Andreae, M., Huebert, B., Kulmala, M., Bond, T., Boy, M., Doherty, S., Guenther, A., Kanakidou, M., Kawamura, K., 2006. Critical assessment of the current state of scientific knowledge, terminology, and research needs concerning the role of organic aerosols in the atmosphere, climate, and global change. Atmos. Chem. Phys. 6, 2017–2038.

Gao, B., Guo, H., Wang, X.-M., Zhao, X.-Y., Ling, Z.-H., Zhang, Z., Liu, T.-Y., 2012. Polycyclic aromatic hydrocarbons in $PM_{2.5}$ in Guangzhou, southern China: spatio-temporal patterns and emission sources. J. Hazard Mater. 239, 78–87.

Gao, B., Guo, H., Wang, X.-M., Zhao, X.-Y., Ling, Z.-H., Zhang, Z., Liu, T.-Y., 2013. Tracer-based source apportionment of polycyclic aromatic hydrocarbons in $PM_{2.5}$ in Guangzhou, southern China, using positive matrix factorization (PMF). Environ. Sci. Pollut. Res. 20, 2398–2409.

Gao, Y., Lee, S.-C., Huang, Y., Chow, J.C., Watson, J.G., 2016. Chemical characterization and source apportionment of size-resolved particles in Hong Kong sub-urban area. Atmos. Res. 170, 112–122.

Gautier, T., Carrasco, N., Schmitz-Afonso, I., Touboul, D., Szopa, C., Buch, A., Pernot, P., 2014. Nitrogen incorporation in Titan's tholins inferred by high resolution orbitrap mass spectrometry and gas chromatography–mass spectrometry. Earth Planet Sci. Lett. 404, 33–42.

Ge, S., Xu, X., Chow, J.C., Watson, J., Sheng, Q., Liu, W., Bai, Z., Zhu, T., Zhang, J., 2004. Emissions of air pollutants from household stoves: honeycomb coal versus coal cake. Environ. Sci. Technol. 38, 4612–4618.

Geng, N., Wang, J., Xu, Y., Zhang, W., Chen, C., Zhang, R., 2013. $PM_{2.5}$ in an industrial district of Zhengzhou, China: chemical composition and source apportionment. Particuology 11, 99–109.

Geron, C.D., Guenther, A.B., Pierce, T.E., 1994. An improved model for estimating emissions of volatile organic compounds from forests in the eastern United States. J. Geophys. Res.: Atmosphere 99 (D6), 12,773–12,791.

Gordon, T.D., Presto, A.A., May, A.A., Nguyen, N.T., Lipsky, E.M., Donahue, N.M., Gutierrez, A., Zhang, M., Maddox, C., Rieger, P., Chattopadhyay, S., Maldonado, H., Maricq, M.M., Robinson, A.L., 2014. Secondary organic aerosol formation exceeds primary particulate matter emissions for light-duty gasoline vehicles. Atmos. Chem. Phys. 14, 4661–4678.

Gu, J., Bai, Z., Liu, A., Wu, L., Xie, Y., Li, W., Dong, H., Zhang, X., 2010. Characterization of atmospheric organic carbon and element carbon of $PM_{2.5}$ and PM_{10} at Tianjin, China. Aerosol Air Qual. Res. 10, 167–176.

Gu, J., Du, S., Han, D., Hou, L., Yi, J., Xu, J., Liu, G., Han, B., Yang, G., Bai, Z.-P., 2014. Major chemical compositions, possible sources, and mass closure analysis of $PM_{2.5}$ in Jinan, China. Air Qual. Atmos. Health 7, 251–262.

Guenther, A., Hewitt, C.N., Erickson, D., Fall, R., Geron, C., Graedel, T., Harley, P., Klinger, L., Lerdau, M., McKay, W., 1995. A global model of natural volatile organic compound emissions. J. Geophys. Res.: Atmosphere 100 (D5), 8873–8892.

Guenther, A., Baugh, B., Brasseur, G., Greenberg, J., Harley, P., Klinger, L., Serça, D., Vierling, L., 1999. Isoprene emission estimates and uncertainties for the Central African EXPRESSO study domain. J. Geophys. Res.: Atmosphere 104 (D23), 30625–30639.

Guenther, C., 2006. Estimates of global terrestrial isoprene emissions using MEGAN (model of emissions of Gases and aerosols from nature. Atmos. Chem. Phys. 6, 3181–3210.

Guo, S., 2003. Particle-associated polycyclic aromatic hydrocarbons in urban air of Hong Kong. Atmos. Environ. 37, 5307–5317.

Guo, S., Hu, M., Guo, Q., Zhang, X., Zheng, M., Zheng, J., Chang, C.C., Schauer, J.J., Zhang, R., 2012. Primary sources and secondary formation of organic aerosols in Beijing, China. Environ. Sc.i Techn 46, 9846–9853.

Hahn, J., 1980. Organic Constituents of Natural Aerosols. NYAS. https://nyaspubs.onlinelibrary.wiley.com/doi/pdf/10.1111/j.1749-6632.1980.tb19367.x.

Han, Z., Zhang, R., Wang, Q.g, Wang, W., Cao, J., Xu, J., 2008. Regional modeling of organic aerosols over China in summertime. J. Geophys. Res. 113, D11202. http://dx.doi.org/10.1029/2007JD009436.

Han, Y., Chen, L.-W., Huang, R.-J., Chow, J., Watson, J., Ni, H., Liu, S., Fung, K., Shen, Z., Wei, C., 2016a. Carbonaceous aerosols in megacity Xi'an, China: implications of thermal/optical protocols comparison. Atmos. Environ. 132, 58–68.

Han, Z., Xie, Z., Wang, G., Zhang, R., Tao, J., 2016b. Modeling organic aerosols over east China using a volatility basis-set approach with aging mechanism in a regional air quality model. Atmos. Environ. 124, 186–198.

Hao, L.Q., Romakkaniemi, S., Yli-Pirila, P., Joutsensaari, J., Kortelainen, A., Kroll, J.H., Miettinen, P., Vaattovaara, P., Tiitta, P., Jaatinen, A., Kajos, M.K., Holopainen, J.K., Heijari, J., Rinne, J., Kulmal, M., Worsnop, D.R., Smith, J.N., Laaksonen, A., 2011. Mass yields of secondary organic aerosols from the oxidation of α-pinene and real plant emissions. Atmos. Chem. Phys. 11, 1367–1378.

Harrison, R.M., Smith, D., Luhana, L., 1996. Source apportionment of atmospheric polycyclic aromatic hydrocarbons collected from an urban location in Birmingham, UK. Environ. Sci. Technol. 30, 825–832.

Hart, K.M., Isabelle, L.M., Pankow, J.F., 1992. High-volume air sampler for particle and gas sampling. 1. Design and gas sampling performance. Environ. Sci. Technol. 26, 1048–1052.

He, L.-Y., Hu, M., Huang, X.-F., Yu, B-D., Zhang, Y.-H., Liu, D.-Q., 2004. Measurement of emissions of fine particulate organic matter from Chinese cooking. Atmos. Environ. 38, 6557–6564.

He, L.-Y., Hu, M., Zhang, Y.-H., Huang, X.-F., Yao, T.-T., 2008. Fine particle emissions from on-road vehicles in the Zhujiang Tunnel, China. Environ. Sci. Technol. 42, 4461–4466.

He, L.-Y., Huang, X.-F., Xue, L., Hu, M., Lin, Y., Zheng, J., Zhang, R., Zhang, Y.-H., 2011. Submicron aerosol analysis and organic source apportionment in an urban atmosphere in Pearl River Delta of China using high-resolution aerosol mass spectrometry. J. Geophys. Res. 116, D12304. http://dx.doi.org/10.1029/2010JD014566.

Heal, M.R., Naysmith, P., Cook, G.T., Xu, S., Duran, T.R., Harrison, R.M., 2011. Application of ^{14}C analyses to source apportionment of carbonaceous PM$_{2.5}$ in the UK. Atmos. Environ. 45, 2341–2348.

Hidy, G., Blanchard, C., Baumann, K., Edgerton, E., Tanenbaum, S., Shaw, S., Knipping, E., Tombach, I., Jansen, J., Walters, J., 2014. Chemical climatology of the southeastern United States, 1999–2013. Atmos. Chem. Phys. 14, 11893–11914.

Hildemann, L.M., Markowski, G.R., Cass, G.R., 1991. Chemical composition of emissions from urban sources of fine organic aerosol. Environ. Sci. Technol. 25, 744–759.

Hildemann, L.M., Mazurek, M.A., Cass, G.R., Simoneit, B.R., 1994. Seasonal trends in Los Angeles ambient organic aerosol observed by high-resolution gas chromatography. Aerosol Sci. Technol. 20, 303–317.

Ho, S.S.H., Yu, J.Z., Chow, J.C., Zielinska, B., Watson, J.G., Sit, E.H.L., Schauer, J.J., 2008. Evaluation of an in-injection port thermal desorption-gas chromatography/mass spectrometry method for analysis of non-polar organic compounds in ambient aerosol samples. J. Chromatogr. A 1200, 217–227.

Hopke, P.K., 2015. It is time to drop principal components analysis as a "receptor model". J. Atmos. Chem. 72, 127–128.

Hu, D., Bian, Q., Li, T.W.Y., Lau, A.K.H., Yu, J.Z., 2008. Contributions of isoprene, monoterpenes, β-caryophyllene, and toluene to secondary organic aerosols in Hong Kong during the summer of 2006. J. Geophys. Res. 113, D22206. http://dx.doi.org/10.1029/2008JD010437.

Hu, D., Bian, Q., Lau, A.K.H., Yu, J.Z., 2010. Source apportioning of primary and secondary organic carbon in summer PM$_{2.5}$ in Hong Kong using positive matrix factorization of secondary and primary organic tracer data. J. Geophys. Res. 115, (D16204). http://dx.doi.org/10.1029/2009JD012498.

Hu, J., Wang, P., Ying, Q., Zhang, H., Chen, J., Ge, X., Li, X., Jiang, J., Wang, S., Zhang, J., Zhao, Y., Zhang, Y., 2016. Modeling biogenic and anthropogenic secondary organic aerosol in China. Atmos. Chem. Phys. 17, 77–92.

Huang, L., Yuan, C.-S., Wang, G., Wang, K., 2011. Chemical characteristics and source apportionment of PM$_{10}$ during a brown haze episode in Harbin, China. Particuology 9, 32–38.

Huang, X.-F., Xue, L., Tian, X.-D., Shao, W.-W., Sun, T.-L., Gong, Z.-H., Ju, W.-W., Jiang, B., Hu, M., He, L.-Y., 2013. Highly time-resolved carbonaceous aerosol characterization in Yangtze River Delta of China: composition, mixing state and secondary formation. Atmos. Environ. 64, 200–207.

Huang, R.J., Zhang, Y., Bozzetti, C., Ho, K.F., Cao, J.J., Han, Y., Daellenbach, K.R., Slowik, J.G., Platt, S.M., Canonaco, F., Zotter, P., Wolf, R., Pieber, S.M., Bruns, E.A., Crippa, M., Ciarelli, G., Piazzalunga, A., Schwikowski, M., Abbaszade, G., Schnelle-Kreis, J., Zimmermann, R., An, Z., Szidat, S., Baltensperger, U., El Haddad, I., Prevot, A.S., 2014. High secondary aerosol contribution to particulate pollution during haze events in China. Nature 514, 218–222.

Iavorivska, L., Boyer, E.W., DeWalle, D.R., 2016. Atmospheric deposition of organic carbon via precipitation. Atmos. Environ. 146, 153–163.

Jacobson, M.C., Hansson, H.C., Noone, K.J., Charlson, R.J., 2000. Organic atmospheric aerosols: review and state of the science. Rev. Geophys. 38, 267–294.

Janssen, N.A., Hoek, G., Simic-Lawson, M., Fischer, P., van Bree, L., ten Brink, H., Keuken, M., Atkinson, R.W., Anderson, H.R., Brunekreef, B., Cassee, F.R., 2011. Black carbon as an additional indicator of the adverse health effects of airborne particles compared with PM$_{10}$ and PM$_{2.5}$. Environ. Health Perspect. 119, 1691–1699.

Jaoui, M., Lewandowski, M., Kleindienst, T.E., Offenberg, J.H., Edney, E.O., 2007. β-caryophyllinic acid: an atmospheric tracer for β-caryophyllene secondary organic aerosol. Geophys. Res. Lett. 34, L05816. http://dx.doi.org/10.1029/2006GL028827.

Jayarathne, T., Rathnayake, C.M., Stone, E.A., 2016. Local source impacts on primary and secondary aerosols in the Midwestern United States. Atmos. Environ. 130, 74–83.

Jayne, J.T., Leard, D.C., Zhang, X., Davidovits, P., Smith, K.A., Kolb, C.E., Worsnop, D.R., 2000. Development of an aerosol mass spectrometer for size and composition analysis of submicron particles. Aerosol Sci. Technol. 33, 49–70.

Ji, D., Zhang, J., He, J., Wang, X., Pang, B., Liu, Z., Wang, L., Wang, Y., 2016. Characteristics of atmospheric organic and elemental carbon aerosols in urban Beijing, China. Atmos. Environ. Times 125, 293–306.

Jiang, F., Liu, Q., Huang, X., Wang, T., Zhuang, B., Xie, M., 2012. Regional modeling of secondary organic aerosol over China using WRF/Chem. J. Aerosol Sci. 43, 57–73.

Jiang, B., Kuang, B.Y., Liang, Y., Zhang, J., Huang, X.H., Xu, C., Yu, J.Z., Shi, Q., 2016. Molecular composition of urban organic aerosols on clear and hazy days in Beijing: a comparative study using FT-ICR MS. Environ. Chem. 13, 888–901.

Jimenez, J., Canagaratna, M., Donahue, N., Prevot, A., Zhang, Q., Kroll, J.H., DeCarlo, P.F., Allan, J.D., Coe, H., Ng, N., 2009. Evolution of organic aerosols in the atmosphere. Science 326, 1525–1529.

Kanakidou, M., Seinfeld, J., Pandis, S., Barnes, I., Dentener, F., Facchini, M., Dingenen, R.V., Ervens, B., Nenes, A., Nielsen, C., 2005. Organic aerosol and global climate modelling: a review. Atmos. Chem. Phys. 5, 1053–1123.

Kim, H., Kim, J.Y., Jin, H.C., Lee, J.Y., Lee, S.P., 2016. Seasonal variations in the light-absorbing properties of water-soluble and insoluble organic aerosols in Seoul, Korea. Atmos. Environ. 129, 234–242.

Kleindienst, T.E., Jaoui, M., Lewandowski, M., Offenberg, J.H., Lewis, C.W., Bhave, P.V., Edney, E.O., 2007. Estimates of the contributions of biogenic and anthropogenic hydrocarbons to secondary organic aerosol at a southeastern US location. Atmos. Environ. 41, 8288–8300.

Klinger, L.F., Li, Q.J., Guenther, A., Greenberg, J., Baker, B., Bai, J.H., 2002. Assessment of volatile organic compound emissions from ecosystems of China. J. Geophys. Res.: Atmosphere 107 (D21), 4603. http://dx.doi.org/10.1029/2001JD001076.

Kroll, J.H., Seinfeld, J.H., 2008. Chemistry of secondary organic aerosol: formation and evolution of low-volatility organics in the atmosphere. Atmos. Environ. 42, 3593–3624.

Lai, S., Zhao, Y., Ding, A., Zhang, Y., Song, T., Zheng, J., Ho, K.F., Lee, S.-c, Zhong, L., 2016. Characterization of PM$_{2.5}$ and the major chemical components during a 1-year campaign in rural Guangzhou, southern China. Atmos. Res. 167, 208–215.

Lang, J., Zhang, Y., Zhou, Y., Cheng, S., Chen, D., Guo, X., Chen, S., Li, X., Xing, X., Wang, H., 2017. Trends of PM$_{2.5}$ and chemical composition in Beijing, 2000–2015. Aerosol Air Qual. Res. 17, 412–425.

Li, X., Wang, S., Duan, L., Hao, J., 2009a. Characterization of non-methane hydrocarbons emitted from open burning of wheat straw and corn stover in China. Environ. Res. Lett. 4, 044015.

Li, X., Wang, S., Duan, L., Hao, J., Nie, Y., 2009b. Carbonaceous aerosol emissions from household biofuel combustion in China. Environ. Sci. Technol. 43, 6076–6081.

Li, L., Chen, Y., Xie, S., 2013a. Spatio-temporal variation of biogenic volatile organic compounds emissions in China. Environ. Pollut. 182, 157–168.

Li, N., Fu, T.-M., Cao, J., Lee, S., Huang, X.-F., He, L.-Y., Ho, K.-F., Fu, J.S., Lam, Y.-F., 2013b. Sources of secondary organic aerosols in the Pearl River Delta region in fall: contributions from the aqueous reactive uptake of dicarbonyls. Atmos. Environ. 76, 200–207.

Li, Y.-C., Yu, J.Z., Ho, S.S.H., Schauer, J.J., Yuan, Z., Lau, A.K.H., Louie, P.K.K., 2013c. Chemical characteristics and source apportionment of fine particulate organic carbon in Hong Kong during high particulate matter episodes in winter 2003. Atmos. Res. 120-121, 88–98.

Li, L., Xie, S., 2014. Historical variations of biogenic volatile organic compound emission inventories in China, 1981–2003. Atmos. Environ. 95, 185–196.

Li, X., Xu, Z., Guan, C., Huang, Z., 2014a. Impact of exhaust gas recirculation (EGR) on soot reactivity from a diesel engine operating at high load. Appl. Therm. Eng. 68, 100–106.

Li, X., Xu, Z., Guan, C., Huang, Z., 2014b. Particle size distributions and OC, EC emissions from a diesel engine with the application of in-cylinder emission control strategies. Fuel 121, 20–26.

Li, B., Zhang, J., Zhao, Y., Yuan, S., Zhao, Q., Shen, G., Wu, H., 2015a. Seasonal variation of urban carbonaceous aerosols in a typical city Nanjing in Yangtze River Delta, China. Atmos. Environ. 106, 223–231.

Li, P.H., Wang, Y., Li, T., Sun, L., Yi, X., Guo, L.Q., Su, R.H., 2015b. Characterization of carbonaceous aerosols at Mount Lu in South China: implication for secondary organic carbon formation and long-range transport. Environ. Sci. Pollut. Res. Int. 22, 14189–14199.

Li, C., Chen, P., Kang, S., Yan, F., Hu, Z., Qu, B., Sillanpää, M., 2016a. Concentrations and light absorption characteristics of carbonaceous aerosol in PM2.5 and PM10 of Lhasa city, the Tibetan Plateau. Atmos. Environ. 127, 340–346.

Li, H., Wang, Q.G., Yang, M., Li, F., Wang, J., Sun, Y., Wang, C., Wu, H., Qian, X., 2016b. Chemical characterization and source apportionment of PM$_{2.5}$ aerosols in a megacity of Southeast China. Atmos. Res. 181, 288–299.

Li, J., Li, L., Wu, R., Li, Y., Bo, Y., Xie, S., 2016c. Inventory of highly resolved temporal and spatial volatile organic compounds emission in China. WIT Trans. Ecol. Environ. 207, 79–86.

Li, Y.J., Sun, Y., Zhang, Q., Li, X., Li, M., Zhou, Z., Chan, C.K., 2017. Real-time chemical characterization of atmospheric particulate matter in China: a review. Atmos. Environ. 158, 270–304.

Lim, H.-J., Turpin, B.J., 2002. Origins of primary and secondary organic aerosol in Atlanta: results of time-resolved measurements during the Atlanta supersite experiment. Environ. Sci. Technol. 36, 4489–4496.

Liu, D., Li, J., Zhang, Y., Xu, Y., Liu, X., Ding, P., Shen, C., Chen, Y., Tian, C., Zhang, G., 2013. The use of levoglucosan and radiocarbon for source apportionment of PM$_{2.5}$ carbonaceous aerosols at a background site in East China. Environ. Sci. Technol. 47, 10454–10461.

Liu, Y., Gao, Y., Yu, N., Zhang, C., Wang, S., Ma, L., Zhao, J., Lohmann, R., 2015. Particulate matter, gaseous and particulate polycyclic aromatic hydrocarbons (PAHs) in an urban traffic tunnel of China: emission from on-road vehicles and gas-particle partitioning. Chemosphere 134, 52–59.

Liu, J., Li, J., Liu, D., Ding, P., Shen, C., Mo, Y., Wang, X., Luo, C., Cheng, Z., Szidat, S., 2016. Source apportionment and dynamic changes of carbonaceous aerosols during the haze bloom-decay process in China based on radiocarbon and organic molecular tracers. Atmos. Chem. Phys. 16, 2985–2996.

Liu, J., Li, J., Cheng, Z., Zhong, G., Zhu, S., Ding, P., Shen, C., Zhang, G., 2017a. Sources of non-fossil fuel emissions in carbonaceous aerosols during early winter in Chinese cities. Atmos. Chem. Phys. 17, 11491–11502.

Liu, S., Jia, L., Xu, Y., Tsona, N.T., Ge, S., Du, L., 2017b. Photooxidation of cyclohexene in

the presence of SO₂: SOA yield and chemical composition. Atmos. Chem. Phys. 17, 13329–13343.

Lu, Z., Zhang, Q., Streets, D.G., 2011. Sulfur dioxide and primary carbonaceous aerosol emissions in China and India, 1996–2010. Atmos. Chem. Phys. 11, 9839–9864.

Lu, T., Huang, Z., Cheung, C.S., Ma, J., 2012. Size distribution of EC, OC and particle-phase PAHs emissions from a diesel engine fueled with three fuels. Sci. Total Environ. 438, 33–41.

Marais, E.A., Jacob, D.J., Jimenez, J.L., Campuzano-Jost, P., Day, D.A., Hu, W., Krechmer, J., Zhu, L., Kim, P.S., Miller, C.C., 2016. Aqueous-phase mechanism for secondary organic aerosol formation from isoprene: application to the southeast United States and co-benefit of SO₂ emission controls. Atmos. Chem. Phys. 16, 1603–1618.

Masclet, P., Mouvier, G., Nikolaou, K., 1986. Relative decay index and sources of poly-cyclic aromatic hydrocarbons. Atmos. Environ. 20, 439–446.

Mauderly, J.L., Chow, J.C., 2008. Health effects of organic aerosols. Inhal. Toxicol. 20, 257–288.

Miguel, A.H., Kirchstetter, T.W., Harley, R.A., 1998. On-Road emissions of particulate polycyclic aromatic hydrocarbons and black carbon from gasoline and diesel ve-hicles. Environ. Sci. Technol. 32, 450–455.

Minguillón, M., Pérez, N., Marchand, N., Bertrand, A., Temime-Roussel, B., Agrios, K., Szidat, S., van Drooge, B., Sylvestre, A., Alastuey, A., 2016. Secondary organic aerosol origin in an urban environment: influence of biogenic and fuel combustion precursors. Faraday Discuss 189, 337–359.

Murphy, D.M., Cziczo, D.J., Froyd, K.D., Hudson, P.K., Matthew, B.M., Middlebrook, A.M., Peltier, R.E., Sullivan, A., Thomson, D.S., Weber, R.J., 2006. Single-particle mass spectrometry of tropospheric aerosol particles. J. Geophys. Res.: Atmosphere 111, D23S32. http://dx.doi.org/10.1029/2006JD007340.

National Bureau of Statistics of China (NBSC), 2015. China Statistics Yearbook (2014), Beijing, China.

Odum, J.R., Hoffmann, T., Bowman, F., Collins, D., Flagan, R.C., Seinfeld, J.H., 1996. Gas/particle partitioning and secondary organic aerosol yields. Environ. Sci. Technol. 30, 2580–2585.

Paatero, P., Tapper, U., 1994. Positive matrix factorization: a non-negative factor model with optimal utilization of error estimates of data values. Environmetrics 5, 111–126.

Pankow, J.F., Bidleman, T.F., 1992. Interdependence of the slopes and intercepts from log-log correlations of measured gas-particle paritioning and vapor pressure—I. theory and analysis of available data. Atmos. Environ. 26, 1071–1080.

Penner, J.E., Zhang, S.Y., Chuang, C.C., 2003. Soot and smoke aerosol may not warm climate. J. Geophys. Res.: Atmosphere 108 (D21), 4657. http://dx.doi.org/10.1029/2003JD003409.

Pérez, N., Pey, J., Reche, C., Cortés, J., Alastuey, A., Querol, X., 2016. Impact of harbour emissions on ambient PM₁₀ and PM₂.₅ in Barcelona (Spain): evidences of secondary aerosol formation within the urban area. Sci. Total Environ. 571, 237–250.

Pervez, Y.F., Kushawaha, S.K., Nair, S., Pervez, S., 2016. Status of atmospheric carbo-naceous matter in various locations of India. Asian J. Chem. 28, 1261.

Petzold, A., Ogren, J.A., Fiebig, M., Laj, P., Li, S.M., Baltensperger, U., Holzer-Popp, T., Kinne, S., Pappalordo, G., Sugimoto, N., Wehrli, C., Wiedensohler, A., Zhang, X.-Y., 2013. Recommendations for reporting "black carbon" measurements. Atmos. Chem. Phys. 13, 8365–8379.

Pietrogrande, M.C., Bacco, D., Ferrari, S., Kaipainen, J., Ricciardelli, I., Riekkola, M.-L., Trentini, A., Visentin, M., 2015. Characterization of atmospheric aerosols in the Po valley during the supersito campaigns—Part 3: contribution of wood combustion to wintertime atmospheric aerosols in Emilia Romagna region (Northern Italy). Atmos. Environ. 122, 291–305.

Pio, C., Cerqueira, M., Harrison, R.M., Nunes, T., Mirante, F., Alves, C., Oliveira, C., de la Campa, A.S., Artíñano, B., Matos, M., 2011. OC/EC ratio observations in Europe: Re-thinking the approach for apportionment between primary and secondary organic carbon. Atmos. Environ. 45, 6121–6132.

Reinhardt, A., Emmenegger, C., Gerrits, B., Panse, C., Dommen, J., Baltensperger, U., Zenobi, R., Kalberer, M., 2007. Ultrahigh mass resolution and accurate mass mea-surements as a tool to characterize oligomers in secondary organic aerosols. Anal. Chem. 79, 4074–4082.

Roach, P.J., Laskin, J., Laskin, A., 2010. Molecular characterization of organic aerosols using nanospray-desorption/electrospray ionization-mass spectrometry. Anal. Chem. 82, 7979–7986.

Rogge, W.F., Hildemann, L.M., Mazurek, M.A., Cass, G.R., Simoneit, B.R., 1991. Sources of fine organic aerosol. 1. Charbroilers and meat cooking operations. Environ. Sci. Technol. 25, 1112–1125.

Saffari, A., Hasheminassab, S., Shafer, M.M., Schauer, J.J., Chatila, T.A., Sioutas, C., 2016. Nighttime aqueous-phase secondary organic aerosols in Los Angeles and its implication for fine particulate matter composition and oxidative potential. Atmos. Environ. 133, 112–122.

Salameh, D., Detournay, A., Pey, J., Pérez, N., Liguori, F., Saraga, D., Bove, M.C., Brotto, P., Cassola, F., Massabò, D., 2015. PM 2.5 chemical composition in five European Mediterranean cities: a 1-year study. Atmos. Res. 155, 102–117.

Samara, C., Voutsa, D., Kouras, A., Eleftheriadis, K., Maggos, T., Saraga, D., Petrakakis, M., 2014. Organic and elemental carbon associated to PM₁₀ and PM₂.₅ at urban sites of northern Greece. Environ. Sci. Pollut. Res. 21, 1769–1785.

Sato, K., Takami, A., Kato, Y., Seta, T., Fujitani, Y., Hikida, T., Shimono, A., Imamura, T., 2012. AMS and LC/MS analyses of SOA from the photooxidation of benzene and 1,3,5-trimethylbenzene in the presence of NOₓ: effects of chemical structure on SOA aging. Atmos. Chem. Phys. 12, 4667–4692.

Schauer, J.J., Rogge, W.F., Hildemann, L.M., Mazurek, M.A., Cass, G.R., Simoneit, B.R., 1996. Source apportionment of airborne particulate matter using organic compounds as tracers. Atmos. Environ. 30, 3837–3855.

Schauer, J.J., Kleeman, M.J., Cass, G.R., Simoneit, B.R., 1999. Measurement of emissions

from air pollution sources. 2. C1 through C30 organic compounds from medium duty diesel trucks. Environ. Sci. Technol. 33, 1578–1587.

Schauer, J.J., Kleeman, M.J., Cass, G.R., Simoneit, B.R., 2002. Measurement of emissions from air pollution sources. 5. C1 − C32 organic compounds from gasoline-powered motor vehicles. Environ. Sci. Technol. 36, 1169–1180.

See, S.W., Balasubramanian, R., 2008. Chemical characteristics of fine particles emitted from different gas cooking methods. Atmos. Environ. 42, 8852–8862.

Seinfeld, J.H., Pandis, S.N., 2016. Atmospheric Chemistry and Physics: from Air Pollution to Climate Change, third ed. John Wiley & Sons.

Shen, G., Yang, Y., Wang, W., Tao, S., Zhu, C., Min, Y., Xue, M., Ding, J., Wang, B., Wang, R., 2010. Emission factors of particulate matter and elemental carbon for crop re-sidues and coals burned in typical household stoves in China. Environ. Sci. Technol. 44, 7157–7162.

Shen, G., Tao, S., Wei, S., Zhang, Y., Wang, R., Wang, B., Li, W., Shen, H., Huang, Y., Yang, Y., Wang, W., Wang, X., Massey Simonich, S.L., 2012. Retene emission from residential solid fuels in China and evaluation of retene as a unique marker for soft wood combustion. Environ. Sci. Technol. 46, 4666–46672.

Shen, G., Tao, S., Wei, S., Chen, Y., Zhang, Y., Shen, H., Huang, Y., Zhu, D., Yuan, C., Wang, H., 2013. Field measurement of emission factors of PM, EC, OC, parent, nitro-, and oxy-polycyclic aromatic hydrocarbons for residential briquette, coal cake, and wood in rural Shanxi, China. Environ. Sci. Technol. 47, 2998–3005.

Shrivastava, M.K., Subramanian, R., Rogge, W.F., Robinson, A.L., 2007. Sources of or-ganic aerosol: positive matrix factorization of molecular marker data and comparison of results from different source apportionment models. Atmos. Environ. 41, 9353–9369.

Simoneit, B.R., 2002. Biomass burning—a review of organic tracers for smoke from in-complete combustion. Appl. Geochem. 17, 129–162.

Sofowote, U.M., Rastogi, A.K., Debosz, J., Hopke, P.K., 2014. Advanced receptor mod-eling of near–real–time, ambient PM₂.₅ and its associated components collected at an urban–industrial site in Toronto, Ontario. Atmos. Pollut. Res. 5, 13–23.

Song, Y., Xie, S., Zhang, Y., Zeng, L., Salmon, L.G., Zheng, M., 2006a. Source appor-tionment of PM₂.₅ in Beijing using principal component analysis/absolute principal component scores and UNMIX. Sci. Total Environ. 372, 278–286.

Song, Y., Zhang, Y., Xie, S., Zeng, L., Zheng, M., Salmon, L.G., Shao, M., Slanina, S., 2006b. Source apportionment of PM₂.₅ in Beijing by positive matrix factorization. Atmos. Environ. 40, 1526–1537.

Song, Y., Tang, X., Xie, S., Zhang, Y., Wei, Y., Zhang, M., Zeng, L., Lu, S., 2007. Source apportionment of PM₂.₅ in Beijing in 2004. J. Hazard Mater. 146, 124–130.

Streets, D.G., Yarber, K.F., Woo, J.H., Carmichael, G.R., 2003. Biomass burning in Asia: annual and seasonal estimates and atmospheric emissions. Global Biogeochem. Cycles 17 (4), 1099. http://dx.doi.org/10.1029/2003GB002040.

Sun, X., Hu, M., Guo, S., Liu, K., Zhou, L., 2012a. ¹⁴C-Based source assessment of car-bonaceous aerosols at a rural site. Atmos. Environ. 50, 36–40.

Sun, Y., Wang, Z., Dong, H., Yang, T., Li, J., Pan, X., Chen, P., Jayne, J.T., 2012b. Characterization of summer organic and inorganic aerosols in Beijing, China with an aerosol chemical speciation monitor. Atmos. Environ. 51, 250–259.

Sun, Y.L., Wang, Z.F., Fu, P.Q., Yang, T., Jiang, Q., Dong, H.B., Li, J., Jia, J.J., 2013. Aerosol composition, sources and processes during wintertime in Beijing, China. Atmos. Chem. Phys. 13, 4577–4592.

Sun, K., Qu, Y., Wu, Q., Han, T., Gu, J., Zhao, J., Sun, Y., Jiang, Q., Gao, Z., Hu, M., Zhang, Y., Lu, K., Nordmann, S., Cheng, Y., Hou, L., Ge, H., Furuuchi, M., Hata, M., Liu, X., 2014. Chemical characteristics of size-resolved aerosols in winter in Beijing. J. Environ. Sci. (China) 26, 1641–1650.

Sun, Y., Wang, Z., Du, W., Zhang, Q., Wang, Q., Fu, P., Pan, X., Li, J., Jayne, J., Worsnop, D., 2015. Long-term real-time measurements of aerosol particle composition in Beijing, China: seasonal variations, meteorological effects, and source analysis. Atmos. Chem. Phys. 15, 10149–10165.

Szidat, S., Ruff, M., Perron, N., Wacker, L., Synal, H.-A., Hallquist, M., Shannigrahi, A.S., Yttri, K.E., Dye, C., Simpson, D., 2009. Fossil and non-fossil sources of organic carbon (OC) and elemental carbon (EC) in Göteborg. Sweden. Atmos. Chem. Phys. 9, 1521–1535.

Tao, J., Cheng, T., Zhang, R., Cao, J., Zhu, L., Wang, Q., Luo, L., Zhang, L., 2013. Chemical composition of PM₂.₅ at an urban site of Chengdu in southwestern China. Adv. Atmos. Sci. 30, 1070.

Tao, J., Zhang, L., Ho, K., Zhang, R., Lin, Z., Zhang, Z., Lin, M., Cao, J., Liu, S., Wang, G., 2014. Impact of PM₂.₅ chemical compositions on aerosol light scattering in Guangzhou—the largest megacity in South China. Atmos. Res. 135, 48–58.

Tao, J., Zhang, L., Cao, J., Zhang, R., 2017a. A review of current knowledge concerning PM₂.₅ chemical composition, aerosol optical properties and their relationships across China. Atmos. Chem. Phys. 17, 9485–9518.

Tao, J., Zhang, L., Cao, J., Zhong, L., Chen, D., Yang, Y., Chen, D., Chen, L., Zhang, Z., Wu, Y., 2017b. Source apportionment of PM₂.₅ at urban and suburban areas of the Pearl River Delta region, south China-With emphasis on ship emissions. Sci. Total Environ. 574, 1559–1570.

Thurston, G.D., Spengler, J.D., 1985. A quantitative assessment of source contributions to inhalable particulate matter pollution in metropolitan Boston. Atmos. Environ. 1967 (19), 9–25.

Tong, H., Kourtchev, I., Pant, P., Keyte, I.J., O'Connor, I.P., Wenger, J.C., Pope, F.D., Harrison, R.M., Kalberer, M., 2016. Molecular composition of organic aerosols at urban background and road tunnel sites using ultra-high resolution mass spectro-metry. Faraday Discuss 189, 51–58.

Tseng, C.-Y., Lin, S.-L., Mwangi, J.K., Yuan, C.-S., Wu, Y.-L., 2016. Characteristics of at-mospheric PM₂.₅ in a densely populated city with multi-emission sources. Aerosol Air Qual. Res. 16, 2145–2158.

Tsui, J.K.-Y., Guenther, A., Yip, W.-K., Chen, F., 2009. A biogenic volatile organic com-pound emission inventory for Hong Kong. Atmos. Environ. 43, 6442–6448.

Tuet, W.Y., Chen, Y., Xu, L., Fok, S., Gao, D., Weber, R.J., Ng, N.L., 2017. Chemical oxidative potential of secondary organic aerosol (SOA) generated from the photo-oxidation of biogenic and anthropogenic volatile organic compounds. Atmos. Chem. Phys. 17, 839–853.

Turpin, B.J., Lim, H.-J., 2001. Species contributions to $PM_{2.5}$ mass concentrations: re-visiting common assumptions for estimating organic mass. Aerosol Sci. Technol. 35, 602–610.

Viana, M., Pandolfi, M., Minguillón, M., Querol, X., Alastuey, A., Monfort, E., Celades, I., 2008. Inter-comparison of receptor models for PM source apportionment: case study in an industrial area. Atmos. Environ. 42, 3820–3832.

Wang, Z., Yuhua, B., Shuyu, Z., 2003. A biogenic volatile organic compounds emission inventory for Beijing. Atmos. Environ. 37, 3771–3782.

Wang, Q., Shao, M., Liu, Y., William, K., Paul, G., Li, X., Liu, Y., Lu, S., 2007. Impact of biomass burning on urban air quality estimated by organic tracers: Guangzhou and Beijing as cases. Atmos. Environ. 41, 8380–8390.

Wang, W., Wu, M., Li, L., Zhang, T., Liu, X., Feng, J., Li, H., Wang, Y., Sheng, G., Claeys, M., 2008. Polar organic tracers in $PM_{2.5}$ aerosols from forests in eastern China. Atmos. Chem. Phys. 8, 7507–7518.

Wang, Q., Shao, M., Zhang, Y., Wei, Y., Hu, M., Guo, S., 2009a. Source apportionment of fine organic aerosols in Beijing. Atmos. Chem. Phys. 9, 8573–8585.

Wang, S., Wei, W., Du, L., Li, G., Hao, J., 2009b. Characteristics of gaseous pollutants from biofuel-stoves in rural China. Atmos. Environ. 43, 4148–4154.

Wang, X., Wu, Z., Liang, G., 2009c. WRF/CHEM modeling of impacts of weather condi-tions modified by urban expansion on secondary organic aerosol formation over Pearl River Delta. Particuology 7, 384–391.

Wang, Q., Geng, C., Lu, S., Chen, W., Shao, M., 2013. Emission factors of gaseous car-bonaceous species from residential combustion of coal and crop residue briquettes. Front. Environ. Sci. Eng. 1–11.

Wang, H., Lou, S., Huang, C., Qiao, L., Tang, X., Chen, C., Zeng, L., Wang, Q., Zhou, M., Lu, S., 2014. Source profiles of volatile organic compounds from biomass burning in Yangtze River Delta, China. Aerosol Air Qual. Res 14, 818–828.

Wang, G., Cheng, S., Li, J., Lang, J., Wen, W., Yang, X., Tian, L., 2015a. Source appor-tionment and seasonal variation of $PM_{2.5}$ carbonaceous aerosol in the Beijing-Tianjin-Hebei region of China. Environ. Monit. Assess. 187, 143.

Wang, J., Ho, S.S.H., Cao, J., Huang, R., Zhou, J., Zhao, Y., Xu, H., Liu, S., Wang, G., Shen, Z., 2015b. Characteristics and major sources of carbonaceous aerosols in $PM_{2.5}$ from Sanya, China. Sci. Total Environ. 530, 110–119.

Wang, L., Xin, J., Li, X., Wang, Y., 2015c. The variability of biomass burning and its influence on regional aerosol properties during the wheat harvest season in North China. Atmos. Res. 157, 153–163.

Wang, P., Cao, J.-j, Shen, Z.-x, Han, Y.-m, Lee, S.-c, Huang, Y., Zhu, C.-s, Wang, Q.-y, Xu, H.-m, Huang, R.-j, 2015d. Spatial and seasonal variations of $PM_{2.5}$ mass and species during 2010 in Xi'an, China. Sci. Total Environ. 508, 477–487.

Wang, J., Zhou, M., Liu, B.-s, Wu, J.-h, Peng, X., Zhang, Y.-f, Han, S.-q, Feng, Y.-c, Zhu, T., 2016a. Characterization and source apportionment of size-segregated atmospheric particulate matter collected at ground level and from the urban canopy in Tianjin. Environ. Pollut. 219, 982–992.

Wang, L., Zhou, X., Ma, Y., Cao, Z., Wu, R., Wang, W., 2016b. Carbonaceous aerosols over China—review of observations, emissions, and climate forcing. Environ. Sci. Pollut. Control Ser. 23, 1671–1680.

Wang, X., Situ, S., Chen, W., Zheng, J., Guenther, A., Fan, Q., Chang, M., 2016c. Numerical model to quantify biogenic volatile organic compound emissions: the Pearl River Delta region as a case study. J. Environ. Sci. 46, 72–82.

Wang, X., Hayeck, N., Brüggemann, M., Yao, L., Chen, H., Zhang, C., Emmelin, C., Chen, J., George, C., Wang, L., 2017. Chemical characteristics of organic aerosols in Shanghai: a study by ultrahigh-performance liquid chromatorgraphy coupled with orbitrap mass specgrometry. J. Geophys. Res.: Atmosphere 122, 11703–117011. 722. https://doi.org/10.1002/2017JD026930.

Watson, J.G., Chow, J.C., Houck, J.E., 2001. $PM_{2.5}$ chemical source profiles for vehicle exhaust, vegetative burning, geological material, and coal burning in Northwestern Colorado during 1995. Chemosphere 43, 1141–1151.

Watson, J.G., 2002. Visibility: science and regulation. JAWMA 52, 628–713.

Welthagen, W., Schnelle-Kreis, J., Zimmermann, R., 2003. Search criteria and rules for comprehensive two-dimensional gas chromatography–time-of-flight mass spectro-metry analysis of airborne particulate matter. J. Chromatogr. A 1019, 233–249.

Wei, T.H., Liu, M.C., Hung, P.C., Chang, S.H., Chang, M.B., 2016. PAH emissions from coal combustion and waste incineration. J. Hazard Mater. 318, 32–40.

Wu, Y., Yang, L., Zheng, X., Zhang, S., Song, L., Li, J., Hao, J., 2014. Characterization and source apportionment of particulate PAHs in the roadside environment in Beijing. Sci. Total Environ. 470, 76–83.

Wu, S.-P., Schwab, J., Yang, B.-Y., Zheng, A., Yuan, C.-S., 2015. Two-years $PM_{2.5}$ ob-servations at four urban sites along the coast of southeastern China. Aerosol Air Qual. Res. 15, 1799–1812.

Wu, B., Shen, X., Cao, X., Yao, Z., Wu, Y., 2016a. Characterization of the chemical composition of $PM_{2.5}$ emitted from on-road China III and China IV diesel trucks in Beijing, China. Sci. Total Environ. 551, 579–589.

Wu, J., Xu, C., Wang, Q., Cheng, W., 2016b. Potential sources and formations of the $PM_{2.5}$ pollution in urban Hangzhou. Atmosphere 7, 100,. http://dx.doi.org/10.3390/atmos7080100.

Wu, R., Bo, Y., Li, J., Li, L., Li, Y., Xie, S., 2016c. Method to establish the emission in-ventory of anthropogenic volatile organic compounds in China and its application in the period 2008–2012. Atmos. Environ. 127, 244–254.

Xu, L., Chen, X., Chen, J., Zhang, F., He, C., Zhao, J., Yin, L., 2012. Seasonal variations and chemical compositions of $PM_{2.5}$ aerosol in the urban area of Fuzhou, China. Atmos. Res. 104, 264–272.

Xu, Z., Li, X., Guan, C., Huang, Z., 2013. Characteristics of exhaust diesel particles from

different oxygenated fuels. Energy Fuels 27, 7579–7586.

Xu, Z., Wen, T., Li, X., Wang, J., Wang, Y., 2015. Characteristics of carbonaceous aerosols in Beijing based on two-year observation. Atmos. Pollut. Res. 6, 202–208.

Xu, J., Shi, J., Zhang, Q., Ge, X., Canonaco, F., Prévôt, A.S.H., Vonwiller, M., Szidat, S., Ge, J., Ma, J., An, Y., Kang, S., Qin, D., 2016. Wintertime organic and inorganic aerosols in Lanzhou, China: sources, processes and comparison with the results during summer. Atmos. Chem. Phys. Discuss. 1–52.

Yang, F., He, K., Ye, B., Chen, X., Cha, L., Cadle, S., Chan, T., Mulawa, P., 2005. One-year record of organic and elemental carbon in fine particles in downtown Beijing and Shanghai. Atmos. Chem. Phys. 5, 1449–1457.

Yang, F., Kawamura, K., Chen, J., Ho, K., Lee, S., Gao, Y., Cui, L., Wang, T., Fu, P., 2016. Anthropogenic and biogenic organic compounds in summertime fine aerosols ($PM_{2.5}$) in Beijing, China. Atmos. Environ. 124, 166–175.

Yang, K., Wei, L., Cheung, C., Tang, C., Huang, Z., 2017. The effect of pentanol addition on the particulate emission characteristics of a biodiesel operated diesel engine. Fuel 209, 132–140.

Yin, H., Qiu, C., Ye, Z., Li, S., Liang, J., 2015. Seasonal variation and source apportion-ment of organic tracers in PM10 in Chengdu, China. Environ. Geochem. Health 37, 195–205.

Yin, J., Harrison, R.M., Chen, Q., Rutter, A., Schauer, J.J., 2010. Source apportionment of fine particles at urban background and rural sites in the UK atmosphere. Atmos. Environ. 44, 841–851.

Yu, J.Z., Huang, X.H., Ho, S.S., Bian, Q., 2011. Nonpolar organic compounds in fine particles: quantification by thermal desorption–GC/MS and evidence for their sig-nificant oxidation in ambient aerosols in Hong Kong. Anal. Bioanal. Chem. 401, 3125–3139.

Zhang, Y., 2006. Study on Speciation of Particulate Organic Matter from Combustion Sources. Ph. D thesis. Peking University.

Zhang, Y., Jimenez, J.L., Canagaratna, M.R., Allan, J.D., Coe, H., Ulbrich, I., Alfarra, M.R., Takami, A., Middlebrook, A.M., Sun, Y.L., Dzepina, K., Dunlea, E., Docherty, K., DeCarlo, P.F., Salcedo, D., Onasch, T., Jayne, J.T., Miyoshi, T., Shimono, A., Hatakeyama, S., Takegawa, N., Kondo, Y., Schneider, J., Drewnick, F., Borrmann, S., Weimer, S., Demerjian, K., Williams, P., Bower, K., Bahreini, R., Cottrell, L., Griffin, R.J., Rautiainen, J., Sun, J.Y., Zhang, Y.M., Worsnop, D.R., 2007a. Ubiquity and dominance of oxygenated species in organic aerosols in anthropogenically-influenced Northern Hemisphere midlatitudes. Geophys. Res. Lett. 34, L13801. http://dx.doi.org/10.1029/2007GL029979.

Zhang, Y.-x., Shao, M., Zhang, Y.-h., Zeng, L.-m., He, L.-y., Zhu, B., Wei, Y.-j., Zhu, X.-l., 2007b. Source profiles of particulate organic matters emitted from cereal straw burnings. J. Environ. Sci. 19, 167–175.

Zhang, T., Claeys, M., Cachier, H., Dong, S., Wang, W., Maenhaut, W., Liu, X., 2008a. Identification and estimation of the biomass burning contribution to Beijing aerosol using levoglucosan as a molecular marker. Atmos. Environ. 42, 7013–7021.

Zhang, X., Wang, Y., Zhang, X., Guo, W., Gong, S., 2008b. Carbonaceous aerosol com-position over various regions of China during 2006. J. Geophys. Res.: Atmosphere 113 (D14111). http://dx.doi.org/10.1029/2007JD009525.

Zhang, Y., Schauer, J.J., Zhang, Y., Zeng, L., Wei, Y., Liu, Y., Shao, M., 2008c. Characteristics of particulate carbon emissions from real-world Chinese coal com-bustion. Environ. Sci. Technol. 42, 5068–5073.

Zhang, Q., Streets, D.G., Carmichael, G.R., He, K., Huo, H., Kannari, A., Klimont, Z., Park, I., Reddy, S., Fu, J., 2009. Asian emissions in 2006 for the NASA INTEX-B mission. Atmos. Chem. Phys. 9, 5131–5153.

Zhang, Y.L., Liu, D., Shen, C.D., Ding, P., Zhang, G., 2010. Development of a preparation system for the radiocarbon analysis of organic carbon in carbonaceous aerosols in China. Nucl. Instrum. Meth. Phys. Res. B 268, 2831–2834.

Zhang, F., Zhao, J., Chen, J., Xu, Y., Xu, L., 2011a. Pollution characteristics of organic and elemental carbon in PM 2.5 in Xiamen, China. J. Environ. Sci. 23, 1342–1349.

Zhang, Q., Jimenez, J.L., Canagaratna, M.R., Ulbrich, I.M., Ng, N.L., Worsnop, D.R., Sun, Y., 2011b. Understanding atmospheric organic aerosols via factor analysis of aerosol mass spectrometry: a review. Anal. Bioanal. Chem. 401, 3045–3067.

Zhang, Y.M., Zhang, X.Y., Sun, J.Y., Lin, W.L., Gong, S.L., Shen, X.J., Yang, S., 2011c. Characterization of new particle and secondary aerosol formation during summer-time in Beijing, China. Tellus B 63, 382–394.

Zhang, Y.L., Perron, N., Ciobanu, V.G., Zotter, P., Minguillón, M.C., Wacker, L., Prévôt, A.S.H., Baltensperger, U., Szidat, S., 2012. On the isolation of OC and EC and the optimal strategy of radiocarbon-based source apportionment of carbonaceous aero-sols. Atmos. Chem. Phys. 12, 10841–10856.

Zhang, R., Jing, J., Tao, J., Hsu, S.-C., Wang, G., Cao, J., Lee, C.S.L., Zhu, L., Chen, Z., Zhao, Y., 2013a. Chemical characterization and source apportionment of $PM_{2.5}$ in Beijing: seasonal perspective. Atmos. Chem. Phys. 13, 7053–7074.

Zhang, Y., Shao, M., Lin, Y., Luan, S., Mao, N., Chen, W., Wang, M., 2013b. Emission inventory of carbonaceous pollutants from biomass burning in the Pearl River Delta Region, China. Atmos. Environ. 76, 189–199.

Zhang, J., Sun, Y., Liu, Z., Ji, D., Hu, B., Liu, Q., Wang, Y., 2014a. Characterization of submicron aerosols during a month of serious pollution in Beijing, 2013. Atmos. Chem. Phys. 14, 2887–2903.

Zhang, Y.H., Wang, D.F., Zhao, Q.B., Cui, H.X., Li, J., Duan, Y.S., Fu, Q.Y., 2014b. Characteristics and sources of organic carbon and elemental carbon in $PM_{2.5}$ in Shanghai urban area. Huanjing Kexue 35, 3263–3270.

Zhang, J.K., Ji, D.S., Liu, Z.R., Hu, B., Wang, L.L., Huang, X.J., Wang, Y.S., 2015a. New characteristics of submicron aerosols and factor analysis of combined organic and inorganic aerosol mass spectra during winter in Beijing. Atmos. Chem. Phys. Discuss. 15, 18,537–18,576.

Zhang, L., Huang, Y., Liu, Y., Yang, F., Lan, G., Fu, C., Wang, J., 2015b. Characteristics of carbonaceous species in $PM_{2.5}$ in Wanzhou in the hinterland of the three Gorges reservoir of northeast Chongqing, China. Atmosphere 6, 534–546.

Zhang, Y., Yao, Z., Shen, X., Liu, H., He, K., 2015c. Chemical characterization of PM$_{2.5}$ emitted from on-road heavy-duty diesel trucks in China. Atmos. Environ. 122, 885–891.

Zhang, Z.-H., Balasubramanian, R., 2016. Investigation of particulate emission characteristics of a diesel engine fueled with higher alcohols/biodiesel blends. Appl. Energy 163, 71–80.

Zhao, L., Wang, X., He, Q., Wang, H., Sheng, G., Chan, L.Y., Fu, J., Blake, D.R., 2004. Exposure to hazardous volatile organic compounds, PM$_{10}$ and CO while walking along streets in urban Guangzhou, China. Atmos. Environ. 38, 6177–6184.

Zhao, Y., Hu, M., Slanina, S., Zhang, Y., 2007a. Chemical compositions of fine particulate organic matter emitted from Chinese cooking. Environ. Sci. Technol. 41, 99–105.

Zhao, Y., Hu, M., Slanina, S., Zhang, Y., 2007b. The molecular distribution of fine particulate organic matter emitted from Western-style fast food cooking. Atmos. Environ. 41, 8163–8171.

Zhao, Y., Wang, S., Nielsen, C.P., Li, X., Hao, J., 2010. Establishment of a database of emission factors for atmospheric pollutants from Chinese coal-fired power plants. Atmos. Environ. 44, 1515–1523.

Zhao, Y., Nielsen, C., Lei, Y., McElroy, M., Hao, J., 2011. Quantifying the uncertainties of a bottom-up emission inventory of anthropogenic atmospheric pollutants in China. Atmos. Chem. Phys. 11, 2295–2308.

Zhao, B., Wang, P., Ma, J.Z., Zhu, S., Pozzer, A., Li, W., 2012. A high-resolution emission inventory of primary pollutants for the Huabei region, China. Atmos. Chem. Phys. 12, 481–501.

Zhao, P., Dong, F., Yang, Y., He, D., Zhao, X., Zhang, W., Yao, Q., Liu, H., 2013. Characteristics of carbonaceous aerosol in the region of Beijing, Tianjin, and Hebei, China. Atmos. Environ. 71, 389–398.

Zhao, S., Chen, L., Li, Y., Xing, Z., Du, K., 2015a. Summertime spatial variations in atmospheric particulate matter and its chemical components in different functional areas of Xiamen, China. Atmosphere 6, 234–254.

Zhao, X., Hu, Q., Wang, X., Ding, X., He, Q., Zhang, Z., Shen, R., Lü, S., Liu, T., Fu, X., 2015b. Composition profiles of organic aerosols from Chinese residential cooking: case study in urban Guangzhou, south China. J. Atmos. Chem. 72, 1–18.

Zheng, M., Fang, M., Wang, F., To, K., 2000. Characterization of the solvent extractable organic compounds in PM$_{2.5}$ aerosols in Hong Kong. Atmos. Environ. 34, 2691–2702.

Zheng, M., Salmon, L.G., Schauer, J.J., Zeng, L., Kiang, C.S., Zhang, Y., Cass, G.R., 2005. Seasonal trends in PM$_{2.5}$ source contributions in Beijing, China. Atmos. Environ. 39, 3967–3976.

Zheng, J., Zhang, L., Che, W., Zheng, Z., Yin, S., 2009. A highly resolved temporal and spatial air pollutant emission inventory for the Pearl River Delta region, China and its uncertainty assessment. Atmos. Environ. 43, 5112–5122.

Zheng, J., Zheng, Z., Yu, Y., Zhong, L., 2010. Temporal, spatial characteristics and uncertainty of biogenic VOC emissions in the Pearl River Delta region, China. Atmos. Environ. 44, 1960–1969.

Zhi, G., Peng, C., Chen, Y., Liu, D., Sheng, G., Fu, J., 2009. Deployment of coal briquettes and improved stoves: possibly an option for both environment and climate. Environ. Sci. Technol. 2009 (43), 5586–5591.

Zhou, S., Yang, L., Gao, R., Wang, X., Gao, X., Nie, W., Xu, P., Zhang, Q., Wang, W., 2017. A comparison study of carbonaceous aerosols in a typical North China Plain urban atmosphere: seasonal variability, sources and implications to haze formation. Atmos. Environ. 149, 95–103.